

The Role of Epithelial Transcription Factor Elf3 in Mediating Transcriptional Programs in Zebrafish

by

Briana R. Davis

Department of Molecular Genetics and Microbiology  
Duke University

Defense Date: March 26, 2025

Approved:

John F. Rawls, Advisor

Clare M. Smith

David M. Tobin

Douglas A. Marchuk

Michel Bagnat

Dissertation submitted in partial fulfillment of the requirements for the degree  
of Doctor of Philosophy in the Department of Molecular Genetics and Microbiology in  
The Graduate School of  
Duke University  
2025

ABSTRACT

The Role of Epithelial Transcription Factor Elf3 in Mediating Transcriptional Programs in Zebrafish

by

Briana R. Davis

Department of Molecular Genetics and Microbiology  
Duke University

Defense Date: March 26, 2025

Approved:

John F. Rawls, Advisor

Clare M. Smith

David M. Tobin

Douglas A. Marchuk

Michel Bagnat

An abstract of a dissertation submitted in partial fulfillment of the requirements for the degree of Doctor of Philosophy in the Department of Molecular Genetics and Microbiology in The Graduate School of Duke University  
2025

Copyright by  
Briana Davis  
2025

## Abstract

Animals interact constantly with microorganisms in the external environment that have significant consequences for their development, physiology, and behavior. Microbes can have both positive and negative effects on host health; however, host tissues typically employ mechanisms to physically contain microbial communities to prevent infection and limit microbial interaction. Animal tissues like epithelial cells that line exposed body surfaces are crucial for mediating these interactions that protect the host from infection, inflammation, and other diseases. Epithelial and other animal cell types can adapt to microbial stimuli through regulation of gene expression programs that inform cellular identity and function. While our understanding of microbially regulated transcriptional programs continues to progress, our knowledge of the specific transcription factors (TFs) that mediate these transcriptional responses is of particular interest. In Chapter 1, I provide a historical review of approaches used to evaluate microbiota function in animal hosts as well as functional genomic approaches that allow researchers to decipher host-microbiota interactions in distinct tissues. In Chapter 2, I describe how we identified the epithelial specific transcription factor E-74 like ETS transcription factor 3 (Elf3) as a candidate mediator of host responses to microbiota. We found that it is commonly upregulated in the digestive tissues of zebrafish and mice that are colonized with a microbiome (CV) compared to germ-free animals (GF). Next, I generated *elf3* mutant zebrafish alleles to test the role of Elf3 in larval physiology as well as mediating microbial interactions. Compared to wildtype larvae, *elf3* mutants failed to mount an appropriate host immune response to microbes. Furthermore, *elf3* mutant adults exhibited worse survival outcomes compared to wildtype animals and sporadically displayed signs of disease that included abnormal swimming behavior, ulcer development, and erythema. Histopathological evaluation of moribund *elf3* mutants demonstrated the association between these clinical signs of poor health and swim bladder inflammation (aerocystitis). Based on these data, I conclude that Elf3 is a microbially responsive transcription factor that mediates host responses to microbes in larval

zebrafish and protects against the development of swim bladder inflammation and other pathologies in adults. In the final chapter, I address the limitation of this work and propose future experiments that could further our understanding of the role of Elf3 in mediating host-microbiota interactions. Together this work adds an important new node to the gene regulatory network mediating host responses to microbiota and provides a new animal model of Elf3 deficiency as a resource for the field.

## **Dedication**

I thank my grandparents Dr. Wiley M. Davis Sr., Mrs. Mary E. Davis, Mr. John M. Ray, and Mrs. Winnie W. Carter for showing me the value of pursuing knowledge and dedicate this dissertation in their honor.

# Table of Contents

Abstract .....	iv
List of Tables .....	ix
List of Figures .....	x
Acknowledgements.....	xii
1. Introduction: The importance of investigating host-microbiota interactions.....	1
1.1 Defining the microbial status of animals .....	1
1.2 Zebrafish as a model system for studying host-microbiota interactions .....	3
1.3 Strategies for mutagenesis in zebrafish .....	5
1.4 Genomic approaches for identifying host adaptation to microbes .....	10
1.5 Key tissues for investigating host-microbiota interactions.....	12
1.5.1 Intestine .....	12
1.5.2 Swim bladder.....	16
1.5.3 Blood .....	20
1.6 Biological roles of the epithelial transcription factor Elf3 .....	26
1.6.1 Host-microbiota interactions and inflammation.....	26
1.6.2 Tissue development and differentiation .....	28
1.6.3 EMT in cancer.....	30
1.7 Summary and proposal for future research .....	33
2. Epithelial transcription factor Elf3 mediates host immune responses to microbiota and protects against aerocystitis in zebrafish.....	36
2.1 Introduction .....	36
2.2 Results .....	38

2.2.1 Identification of Elf3, a candidate TF mediating conserved host responses to the microbiota.....	38
2.2.2 Generation of <i>elf3</i> mutant alleles.....	43
2.2.3 Experimental design of larval bulk RNA-seq .....	46
2.2.4 <i>elf3</i> mediates host responses to the microbiota in larval zebrafish.....	49
2.2.5 <i>elf3</i> regulates gene expression in larval zebrafish independent of microbial status .....	84
2.2.6 Interaction genes integrate microbial status and <i>elf3</i> -genotype.....	88
2.2.7 Mapping differentially expressed genes in larval zebrafish to cell-type specificity ....	99
2.2.8 <i>elf3</i> mutation reduces adult survival in zebrafish .....	104
2.2.9 <i>elf3</i> moribund mutants exhibit swim bladder inflammation.....	107
2.2.10 Discussion .....	111
2.3 Methods .....	116
2.3.1 Ethics Statement.....	116
2.3.2 Zebrafish husbandry .....	116
2.3.3 Key resources .....	117
2.3.4 Generation of mutant zebrafish lines.....	117
2.3.5 Cell isolation and RNA extraction for total RNA sequencing .....	118
2.3.6 Bulk RNA-seq analysis .....	118
2.3.7 Brightfield and color camera images of zebrafish.....	119
2.3.8 Longitudinal assessment of <i>elf3</i> <sup>rdu103</sup> survival.....	119
2.3.9 Longitudinal assessment of <i>elf3</i> <sup>rdu103</sup> survival.....	120
2.3.10 Larval zebrafish infections with <i>Mycobacterium marinum</i> .....	121
2.3.11 Isolation and identification of swim bladder bacteria .....	121
3. Conclusions.....	122

3.1 Limitations and future work .....	122
3.1.1 Characterizing Elf3 protein function and protein-protein interactions.....	122
3.1.2 Generation of <i>elf3</i> transgenic reporters .....	125
3.1.3 <i>elf3</i> infections models.....	129
3.2 Concluding remarks .....	131
References.....	132

## List of Tables

Table 1: Isolated causative swim bladder infections in physostomous fishes. ....	19
Table 2: Roles of ELF3 in EMT in cancer.....	32
Table 3: List of mouse and zebrafish studies used to compare CV/GF expression .....	43
Table 4: Metascape (Zhou et al., 2019) enrichment for all significant genes upregulated in CVWT/GFWT .....	51
Table 5: Metascape (Zhou et al., 2019) enrichment for all significant genes downregulated in CVWT/GFWT .....	57
Table 6: Metascape (Zhou et al., 2019) shared upregulated microbial response .....	62
Table 7: Metascape (Zhou et al., 2019) shared downregulated microbial response .....	68
Table 8: Metascape (Zhou et al., 2019) enrichment for all significant genes upregulated in CVMut/GFMut .....	70
Table 9: Metascape (Zhou et al., 2019) enrichment for significant genes downregulated in CVMut/GFMut .....	78
Table 10: Metascape (Zhou et al., 2019) enrichment upregulated genotypic response .....	85
Table 11: Metascape (Zhou et al., 2019) enrichment for downregulated genotypic response .....	88
Table 12: Metascape (Zhou et al., 2019) negative log <sub>2</sub> FC interaction.....	92
Table 13: Metascape (Zhou et al., 2019) positive log <sub>2</sub> FC Interaction Genes .....	96
Table 14: Identification of Interaction Immune Genes .....	98
Table 15: Biological reagents .....	117
Table 16: Primers.....	117

## List of Figures

Figure 1: Identifying a candidate TF mediating conserved host responses to the microbiota. ....	41
Figure 2: <i>elf3</i> is expressed in diverse tissues in adult and larval zebrafish. ....	42
Figure 3: Generation of <i>elf3</i> mutant alleles. ....	45
Figure 4: <i>elf3</i> genotype and microbial status have effect the larval zebrafish transcriptome. ....	47
Figure 5: <i>elf3</i> mutant larvae are not developmentally delayed. ....	48
Figure 6: Identification of interaction genes that integrate <i>elf3</i> genotype and microbial status. ...	91
Figure 7: Differentially expressed genes in larval RNA-seq exhibit cell-type specificity. ....	101
Figure 8: Identification of putative cell-type specific responses among differentially expressed genes in larval RNA-seq (part 1) .....	102
Figure 9: Identification of putative cell-type specific responses among differentially expressed genes in larval RNA-seq (part 2). ....	103
Figure 10: <i>elf3</i> <sup>-/-</sup> adults present immune-related pathologies and exhibit poor survival. ....	105
Figure 11: <i>elf3</i> <sup>-/-</sup> adults of both alleles exhibit premature death. ....	106
Figure 12: moribund <i>elf3</i> <sup>-/-</sup> adults develop aerocystitis. ....	109
Figure 13: Healthy appearing <i>elf3</i> <sup>-/-</sup> adults present normal histopathology. ....	110
Figure 14: Summary model indicating putative roles for <i>elf3</i> in zebrafish. ....	115

## **Acknowledgements**

First, I thank God for this opportunity to explore my passion for science at Duke University and his continued grace during my research years. Thank you to Dr. John Rawls for taking a chance on me joining the lab in 2018. Despite not having any microbiology or genomic experience, you offered me a position in your lab, and I will always be grateful for all that I have learned on this journey. Thank you to the amazing Rawls lab crew that have provided numerous laughs over the years as well as pushed me to pursue this research to the best of my ability. Thank you to the members of my awesome thesis committee, Dr. David Tobin, Dr. Clare Smith, Dr. Doug Marchuk, and Dr. Michel Bagnat, who challenged me to think bigger every time I presented my work. Thank you to my amazing BioCoRE cohort girls Dr. Dilara Anbarci, Dr. Ashleigh Rawls, and Dr. Janai Williams-Doria for being such amazing friends and providing all kinds of life and scientific advice. Thank you to my parents, Dr. Wiley M. Davis Jr. and Mrs. Felicia R. Davis for all that you have done to support all that I do. I know that I would not be where I am today without your love and guidance. And finally, thank you to my future husband Dylan Foley. I appreciate all the times you gave a listening ear and brought comfort food after lab, and I am forever grateful for the memories that we made during this period of my life.

# **1. Introduction: The importance of investigating host-microbiota interactions**

Animals encounter a plethora of microbes throughout their life cycle by engaging with the external environment (natural and artificial surfaces, water, air, etc) and other animals. It is estimated that there are upwards of  $\sim 1.2 \times 10^{30}$  bacterial and archaeal cells inhabiting various marine and terrestrial habitats on Earth (Flemming & Wuertz, 2019). To what extent are development and physiological systems in animals sensitive and responsive to this constant microbial stimulation? In this chapter, I will review techniques and approaches used to address host-microbiota interactions in animals and our knowledge of putative transcription factors mediating those responses.

## ***1.1 Defining the microbial status of animals***

In the late 19<sup>th</sup> century, scientists like Louis Pasteur and Marcell Nencki, who appreciated the omnipresence of microbes, started to ask more questions about what life might look like if there were no microbes (Al-Asmakh & Zadjali, 2015; Basic & Bleich, 2019; Gordon, 1960; Pham et al., 2008). Would animals be able to survive in a germ-free world? George Nuttall and Hans Thierfelder were the first to experimentally test this question in 1895 by sterilely delivering guinea pigs via Caesarean section and rearing them germ-free (GF) for up to 13 days (Basic & Bleich, 2019; Gordon, 1960). Although the sample size was small, their finding that the cecum appeared more enlarged is consistent with our current knowledge that the cecum of other GF rodents like mice is larger than microbially reared controls (Al-Asmakh & Zadjali, 2015; Chai et al., 2024; Gordon, 1960; Savage & Dubos, 1968).

Once scientists learned that germ-free animals could survive, the next questions addressed whether there were significant differences in animal physiology. These questions required scientists to manipulate the microbial status of the host to compare the physiology of germ-free animals to more conventional controls (Basic & Bleich, 2019; Gordon, 1960). Today,

we refer to these types of experiments as gnotobiotic, which is a term originating from ancient Greek terminology for “gnosis” or knowledge and “bios” meaning life (Al-Asmakh & Zadjali, 2015; Pham et al., 2008). Thus, all life forms, including the microbiome, are known in gnotobiotic experiments.

Gnotobiotic conditions typically compare GF animals to those that are (1) conventionally-reared, (2) conventionalized or (3) monoassociated. Conventionally-reared (CR) animals are born and maintained in the presence of microbes (Al-Asmakh & Zadjali, 2015; Pham et al., 2008). Due to the potential for confounding affects, many murine studies will include CR animals that have a complex microbiota but are certified to be free of specific pathogens (Dobson et al., 2019). Gnotobiotic experiments can also compare GF animals to ex-GF animals that are derived germ-free and then subsequently exposed to microbes (Bates et al., 2006; Pham et al., 2008; Rawls et al., 2004). These ex-GF animals are colonized by microbes through immersion or gavage methods in a process called conventionalization (CONVD or CV) (Bates et al., 2007; Pham et al., 2008; Rawls et al., 2004). To test the effects of specific bacteria or bacterial consortium on animal physiology, ex-GF animals can also be colonized with one (monoassociated) or more microbial strains (defined) (Hooper et al., 2001; Pham et al., 2008; Rawls et al., 2004; Ye et al., 2021).

Generation and maintenance of GF animals like mice can be costly, labor intensive, as well as time consuming (Kennedy et al., 2018). Therefore, treatment of CR animals with antibiotic cocktails is sometimes a more accessible method for testing the effect of microbes on host biology (Kennedy et al., 2018). Various combinations of broad-spectrum antibiotics like metronidazole and vancomycin are used to generate microbiota depleted mice that are compared to non-treated controls (Ge et al., 2017; Theriot et al., 2014; Zarrinpar et al., 2018). While antibiotic treatment is a useful tool, it is important to remain cautious when interpreting the data from these experiments. Antibiotic treatment can affect host tissues independent of the

microbiota, and the treatment itself may indirectly affect host physiology by disrupting microbial ecology (Morgun et al., 2015). Pathogen infection models in which GF or CR animals are exposed to known viral, bacterial, fungal pathogens is another way to investigate host responses to microbiota (Cronan & Tobin, 2014; Rosowski et al., 2018; Torraca & Mostowy, 2018). These studies help to further our understanding of how pathogens disrupt normal host physiology as well as the impact of the resident microbiota on exacerbation or protection from disease (Caballero-Flores et al., 2023). Taken together, all the described host microbial statuses (germ-free, gnotobiotic, antibiotic treatment, and infection) provide context for how the host responds to microbes. Importantly, in all the previously discussed contexts, researchers can manipulate the genetic background of the host through chemical or targeted mutagenesis. This introduces the variable of genotype into the experimental design, which is important for identifying host factors that mediate responses to microbes and their effects on infection susceptibility.

## ***1.2 Zebrafish as a model system for studying host-microbiota interactions***

Zebrafish (*Danio rerio*) are a tropical fish averaging 4 to 5 centimeters in length with origins tracing back to freshwater rivers in northern India, Nepal, and Bangladesh (Parichy, 2015). Its potential as a model system in laboratory research was harnessed in the 1960s with early work led by George Streisinger and others to transform what was commonly viewed as household pet into a powerful genetic tool (Grunwald & Eisen, 2002). Today, there are many aspects of zebrafish biology that facilitate investigation of host-microbiota interactions. Because zebrafish are genetically tractable, there are several approaches, such as chemical and targeted mutagenesis, that can be used to probe genetic requirements for host responses (see section “1.3 Strategies for mutagenesis in zebrafish” for more details) (Kanter & Rawls, 2010; Milligan-McClellan et al., 2011; Murdoch & Rawls, 2019). Zebrafish embryos and early larvae are also optically transparent, which facilitates live visualization of fluorescently labeled host cells in transgenic animals (Kanter & Rawls, 2010; Milligan-McClellan et al., 2011; Murdoch & Rawls,

2019). When these transgenic reporter lines are exposed to fluorescent bacterial (Hou et al., 2016) and fungal (Knox et al., 2014) strains, it is possible to visualize dynamic host responses like macrophage phagocytosis in real time. These tools also enable live imaging of the effects of host processes like gut motility on interspecies bacterial competition (Wiles et al., 2016; Wiles et al., 2020). Importantly, epithelial tissues like the intestine that interface with high bacterial burdens are highly conserved in their development, function, and transcriptional landscape to mammals (Flores et al., 2020; Lickwar et al., 2017; Ng et al., 2005; Wallace et al., 2005; Wang et al., 2010) (see section “1.5 Key tissues for investigating host-microbiota interactions” for more details).

Another prominent advantage of zebrafish is the accessibility of reliable and rigorous gnotobiotic protocols that enable researchers to manipulate and define the microbial community associated with animals (Bates et al., 2006; Melancon et al., 2017; Pham et al., 2008; Rawls et al., 2004). These protocols leverage the fact that fertilized zebrafish embryos remain in a protective, axenic chorion until hatching approximately 3 days post-fertilization (dpf) (Murdoch & Rawls, 2019; Pham et al., 2008). With the use of sterilizing agents like iodine and bleach at conservative concentrations, it is thus possible to derive embryos GF and either maintain them in a sterile environment until endpoint or expose them to diverse bacterial communities (conventionalize) or individual bacterial strains (monoassociate) (Pham et al., 2008). The larvae can then be used for downstream applications at endpoint that include imaging, bulk or single cell RNA sequencing, and functional assays (e.g., nutrient uptake, gut motility, behavior, etc.). The majority of gnotobiotic zebrafish experiments have endpoints at larval stages due to challenges with maintaining GF juveniles and adults (e.g., provision of nutritious sterile diets, upkeep of high-water quality, etc.); however, the field is continuing to develop strategies to make long-term rearing of GF animals more convenient (Melancon et al., 2017).

### ***1.3 Strategies for mutagenesis in zebrafish***

To investigate the role of specific host factors in mediating microbial interactions and host physiology in zebrafish, mutagenesis tools are needed. While zebrafish are highly amenable to forward genetic chemical screens, this section will focus on historical and current strategies for targeted mutagenesis in zebrafish.

Morpholinos (MOs) are synthesized oligomers of approximately 25 base pairs that target and bind to specific mRNA transcripts to prevent their translation (Eisen & Smith, 2008; Stainier et al., 2017). These antisense oligomers are typically injected into recently fertilized embryos to induce transient knockdown of the targeted gene (Eisen & Smith, 2008; Stainier et al., 2017). Morpholinos are characterized as either translation blocking, splice inhibiting, or microRNA blocking depending upon the target strategy (Eisen & Smith, 2008). For example, translation blocking morpholinos directly target the translation start site sequence and stall the translation initiation complex from progressing along the target mRNA (Eisen & Smith, 2008). While this strategy is effective, limitations include the inhibition of maternally deposited mRNAs that might be crucial for embryogenesis and thus might render the observed phenotype more severe compared to other mutagenesis strategies (Eisen & Smith, 2008; Stainier et al., 2017). Splice inhibiting morpholinos are typically designed to target exon-intron and intron-exon boundaries to induce exon skipping or intron retention that result in an altered mRNA transcript presented for translation (Eisen & Smith, 2008; Morcos, 2007; Nasevicius & Ekker, 2000). Unlike translation blocking MOs, splice inhibiting MOs do not target maternally deposited transcripts (Eisen & Smith, 2008). Lastly, microRNA-blocking morpholinos inhibit microRNAs from performing biological roles that block translation and promote the degradation of mRNA transcripts (Eisen & Smith, 2008). In practice, target morpholinos designed for two of the different strategies mentioned as well as control morpholinos are injected into embryos to assess gene function (Eisen & Smith, 2008). Additional control measures to assess the specificity of the morpholino

induced phenotype include injecting the same morpholino into closely related species and performing rescue experiments with the wild-type mRNA transcript (Eisen & Smith, 2008). Taken together, the use of morpholinos to investigate gene function has advanced our understanding of many aspects of zebrafish physiology. Its use as a genetic tool is not as common today with the popularity of newer CRISPR/Cas9 technology; however, there are zebrafish labs that use morpholinos in combination with mutant alleles to characterize and validate interesting phenotypes. Some of the limitations of morpholinos that may have contributed to its decreased usage in the field include the potential for decreased and variable efficacy during development and off-target effects (Eisen & Smith, 2008).

In addition to morpholinos, zinc finger nucleases (ZFNs) and transcription activator-like nucleases (TALENs) became useful for mutagenesis in zebrafish (Li et al., 2016). ZFNs are engineered such that chains of zinc finger binding proteins that recognize specific DNA sequences are linked to an endonuclease like FokI (Bibikova et al., 2001; Isalan, 2011; Kim et al., 1996; Klug, 2010; Segal et al., 1999). Two ZFNs are generated per gene (Gupta & Musunuru, 2014). The linked zinc finger binding proteins of one ZFN are designed to target the forward DNA strand, and the zinc finger binding proteins of the second ZFN target the reverse DNA strand (Gupta & Musunuru, 2014). Thus, when both ZFNs bind to their targeted DNA sequences, the dimerization of the accompanying FokI endonucleases introduces a double stranded break in the DNA (Gupta & Musunuru, 2014). While zinc finger nucleases have been successful for mutagenesis in zebrafish (Doyon et al., 2008), limitations include restrictions in DNA target sequences recognized by zinc finger binding proteins and challenges with successful design strategies (Li et al., 2016). Mutagenesis via TALENs is quite similar to the use of ZFNs. Transcription activator-like effector (TALEs) proteins are designed with ~33-35 amino acid repeats that bind to singular nucleotides (Christian et al., 2010; Joung & Sander, 2013; Moscou & Bogdanove, 2009). Like zinc finger binding proteins, TAL effector proteins are linked to FokI

endonucleases. One of the major disadvantages of TALENs and ZFNs for mutagenesis is the need to generate two DNA targeting proteins per gene (Li et al., 2016). This exact design limitation has been addressed in the CRISPR/Cas9 strategies that rely on the design of a singular guide targeting RNA molecule (Li et al., 2016). Therefore, while the technology for ZFNs and TALENs is available, Cas9 is the preferred endonuclease system by most researchers for genome editing.

In recent years, the CRISPR/Cas9 genome editing tool has become one of the most widely used approaches for mutagenesis in diverse species (Jinek et al., 2012; Ran et al., 2013). Its roots are found in early investigations of the protective measures employed by bacteria and archaea to limit the deleterious effects of viruses, plasmids, and other sources of exogenous genetic material (Bhaya et al., 2011; Jinek et al., 2012; Wiedenheft et al., 2012). Bacteria, such as *Streptococcus pyogenes*, that encounter a new virus will integrate fragments of the foreign genetic material into its genome as unique spacers at the ends of “clustered regularly interspaced short palindromic repeats” (CRISPR) arrays during adaptation (Jinek et al., 2012; Wiedenheft et al., 2012). These bacterial loci, which include the recently integrated spacers, are then transcribed to generate pre-CRISPR RNA (cRNA) that is further modified by trans-activating CRISPR RNA (tracrRNA), and other CRISPR associated (Cas) proteins to generate mature cRNA (Jinek et al., 2012; Wiedenheft et al., 2012). The cRNA is hybridized to the tracrRNA and then complexed with the appropriate Cas endonuclease protein (Jinek et al., 2012; Wiedenheft et al., 2012). During interference, the cRNA-tracrRNA hybrid helps to guide the associated Cas protein to the complementary viral photospacer (Jinek et al., 2012; Wiedenheft et al., 2012). The targeted Cas protein is then able to cleave the DNA sequence at the respective photospacer adjacent motif (PAM) to help silence its expression (Jinek et al., 2012; Wiedenheft et al., 2012). When the bacteria encounter the same exogenous DNA again, this defense response is even more rapid

because the spacers needed for targeting the Cas proteins are already integrated into the genome (Jinek et al., 2012; Wiedenheft et al., 2012).

CRISPR/Cas9 genome editing tools leverage the sequence specificity of the bacterial defense response to target animal genomes for mutagenesis. Single guide RNAs reflective of the crRNA-tracrRNA hybrid are injected into animal cells so that the Cas9 protein appropriately targets and introduces a double stranded DNA break at a chosen PAM site (Patsali et al., 2019; Xu & Li, 2020). These double stranded breaks are destined for repair by non-homology end joining (NHEJ) or homology-directed repair (HDR) like the breaks introduced by ZFN and TALEN endonuclease systems (Patsali et al., 2019; Xu & Li, 2020). Mutagenesis strategies directed by NHEJ repair leverage its error prone nature to introduce small deletions and insertions at the cleavage site (Xu & Li, 2020). If the length of the indel is not a multiple of 3, the indel is a frameshift mutation that disrupts the open reading frame when the mRNA transcript is translated (Kervestin & Jacobson, 2012). Frameshift mutations result in an altered codon sequence that is often associated with a premature stop codon (Kervestin & Jacobson, 2012). It is anticipated that many mRNAs that contain premature stop codons are targeted for degradation through nonsense-mediated decay mechanisms (El-Brolosy & Stainier, 2017). Curiously, the triggering of nonsense mediated decay by premature stop codons can sometimes trigger the upregulation of mRNA transcripts for related genes in a process called transcriptional adaptation (El-Brolosy et al., 2019). During transcriptional adaptation, the upregulation of genes closely related to the gene targeted for mutagenesis can mask the expected phenotype and lead to misleading conclusions about gene function (El-Brolosy et al., 2019). Many researchers are responding to these data by developing CRISPR/Cas9 strategies that will specifically avoid this phenomenon.

Recommendations include the generation of full-locus and promoter-less mutations that will altogether prevent the targeted gene from being transcribed as well as the generation of in-frame deletions in highly conserved and predicted functional domains that are unlikely to trigger non-

sense mediated decay (Sztal & Stainier, 2020). While these recommendations help to facilitate the generation of stable mutant lines, there is emerging evidence that injecting pools of single guide RNAs (~3 guides per target gene) into embryos can lead to reliable phenotyping in F0 “crispant” embryos (Bek et al., 2021; Debaenst et al., 2025; Kroll et al., 2021). In these CRISPR pool experiments, F0 crispants are compared to non-injected controls or embryos that are injected with a control CRISPR pool (i.e.- pool targets genes like pigmentation gene *tyr* in which there are clear phenotypic expectations) (Debaenst et al., 2025; Kroll et al., 2021). This strategy is particularly useful for generating early insights to gene function while waiting for the generation of stable mutant lines; however, it can be difficult to phenotype crispants when there are unclear hypotheses, or an exploratory lens applied to questions asking about gene function.

Compared to NHEJ, homology-directed repair (HDR) is a much more precise but less efficient method of DNA repair (Xu & Li, 2020). Mutagenesis strategies informed by HDR include injecting a donor template along with the CRISPR/Cas9 machinery into cells (Xu & Li, 2020). When the double strand break is initiated at the target site, the donor template, which has 5’ and 3’ arms that are homologous to sequence framing the break site, can be inserted and integrated into the host genome (Rein et al., 2018; Xu & Li, 2020). The precision of this repair mechanism is particularly useful for investigating how specific mutated sequences inform gene function (Liao et al., 2024). For example, it is possible to introduce mutations in the donor template outside of the homology arms that recapitulate variants relevant to human disease (Liao et al., 2024).

Disadvantages of the CRISPR/Cas9 system include the tolerance of mismatches between the guide sequence and the intended DNA mutagenesis site (Guo et al., 2023; Uddin et al., 2020). This tolerance enables permissive Cas9 cutting at other locations in the genome, a process that potentially generates off-target effects that can confound the observed phenotype (Uddin et al., 2020). Tools are being developed to limit this mismatch tolerance (Kim et al., 2020); however,

there is a risk that these changes will reduce the efficiency of the desired on-target cleavage (Liu et al., 2020). In the zebrafish community, it is common to see researchers publish two mutant alleles with similar phenotypes to minimize the likelihood that the reported phenotype is attributable to off-target effects. Another disadvantage of the CRISPR/Cas9 system is the limited target site selection due to requirements for a specific adjacent PAM (NGG) sequence (Uddin et al., 2020). Despite these limitations, CRISPR/Cas9 is a useful tool for mutagenesis in zebrafish and is thus the method that was employed for my doctoral work.

#### ***1.4 Genomic approaches for identifying host adaptation to microbes***

Some of the earliest phenotypic characterizations of GF animals included collections of organ weight and histological descriptions of lymphoid tissue in guinea pigs (Gordon, 1960). Since these studies, our ability to use histology, immunology, physiology, high resolution microscopy, advanced cell sorting methods, and behavioral assays has continuously improved our understanding of microbial contributions to host physiology (Wang et al., 2024).

Genetic information encoded within the animal genome is relevant for defining how tissues adapt to microbes. Genomic approaches designed to identify mediators of microbial response leverage the organization of genetic information at interconnected levels. In eukaryotic cells, genetic material or chromatin must be tightly packaged and condensed to fit within the nucleus. It is estimated that if you stretched the coiled and compressed DNA of a human cell, the end-to-end length would reach up to approximately 2 meters (Piovesan et al., 2019). This is in comparison to the estimated 10  $\mu\text{m}$  diameter of the nucleus (Sun et al., 2000). Thus, the genetic material within the cell must be packaged in an organized fashion that respects the confines of the nucleus while remaining interpretable for encoding cellular identity and function. DNA wrapped around histone octamers form nucleosomes that act as the most simplistic structural component of chromatin (Heppert et al., 2021; Klemm et al., 2019). The positioning of nucleosomes relative to neighboring nucleosomes as well as their organization into formal structures such as

heterochromatin has significant effects on the openness or accessibility of chromatin at specific genomic locations (Heppert et al., 2021; Klemm et al., 2019). The more accessible the chromatin, then the more permissive the site for chromatin binding (Klemm et al., 2019). This includes binding by transcription factor (TF) proteins at cis-regulatory regions (CRRs) throughout the genome (Heppert et al., 2021; Klemm et al., 2019). Transcription factor binding at CRRs can then activate or suppress gene transcription to regulate transcriptional programs in response to diverse stimuli such as nutrients, microbes, growth factors, among others (Heppert et al., 2021).

The structure of genetic material at these interconnected levels has informed the development of several genetic tools that can assess how cells adapt to microbially derived signals. This includes tools such as ATAC-seq, FAIRE-seq, and DNase-seq to probe chromatin accessibility across the genome (Heppert et al., 2021). These tools take advantage of the fact that more accessible chromatin is more permissive to binding and cutting by endonucleases like DNaseI or more permissive to transposon insertion compared to closed regions (Klemm et al., 2019). The cut or transposon inserted DNA is then used to construct libraries for sequencing (Klemm et al., 2019). Compiling genome wide accessibility data for specific tissues provides a landscape view of how cells respond to different treatments. Once regions of accessible chromatin have been identified, software like Hypergeometric Optimization of Motif EnRichment (HOMER) is used to uncover enriched transcription factor binding motifs (TFBM) within the sequenced DNA sites to generate hypotheses about putative transcription factor binding (Heinz et al., 2010). Many transcription factors within the same transcription factor family can recognize and bind to similar recognition sequences, so it is often necessary for this data to be combined with gene expression data generated from transcriptomic analyses to generate a more prioritized list of candidates. ChIP-seq leverages the fact that transcription factors bind to specific cis-regulatory regions to regulate target genes (Heppert et al., 2021; Park, 2009). Crosslinking of the transcription factor to its bound DNA and pulling down TF-antibody complexes enables

sequencing of the sites at which the transcription factor interacts (Park, 2009). Lastly, we can think about the fact that transcription factors help to regulate gene expression levels.

Transcriptomic tools such as microarrays and bulk RNA-sequencing facilitate comparisons of differentially expressed genes between different experimental groups. With the advent of scRNA-sequencing (scRNA-seq), we can now observe changes in gene expression within subpopulations of cells within a given tissue (Hwang et al., 2018; Jovic et al., 2022; Li & Wang, 2021). Overall, these tools make it possible to interrogate genomic adaptations to microbes.

### ***1.5 Key tissues for investigating host-microbiota interactions***

In animals, numerous tissues are microbially responsive or influenced by microbial metabolites signaling from other parts of the body. Microbial dysbiosis defined by alterations in microbial composition has been associated with conditions such as depression and anxiety (Liu et al., 2022; Marin et al., 2017), cardiovascular disease (Rosenfeld & Campbell, 2011), and eczema (Byrd et al., 2018; Kong et al., 2012). These data suggest that tissues like the brain, heart, skin and others are useful for investigating host-microbiota interactions; however, we will focus specifically on the intestine, swim bladder, and blood in this introduction.

#### **1.5.1 Intestine**

The intestine is one of the most microbial dense tissues of the human body (Sender et al., 2016). The colon for example is home to upwards of  $10^{14}$  bacteria (number/mL content) (Sender et al., 2016). The plethora of resident microbes provides plenty of opportunity to investigate its interactions with host tissues and its influence on host physiology.

Many aspects of digestive physiology are conserved between zebrafish and mammals. In mammals, ingested material, partially broken down by saliva and gastric acid in the stomach, travels along the gastrointestinal tract to the nutrient-absorbing small intestine (Collins et al., 2025; Ogobuiro et al., 2025). Within the small intestine, the ingested material is further chemically digested in the duodenum before being absorbed in either the jejunum (most nutrients)

or ileum (bile salts and vitamin B12) (Collins et al., 2025; Ogobuiro et al., 2025). The contents of the small intestine are emptied into the colon or large intestine that absorbs water, salts, and any remaining non-absorbed nutrients, before finally being excreted as waste (Collins et al., 2025; Ogobuiro et al., 2025). This efficient digestive process is largely maintained with the regionalization of intestinal functions. Comparatively, the zebrafish intestine has three histologically defined regions such as the (1) anterior or intestinal bulb, (2) mid intestine, and (3) posterior or caudal intestine that possess unique morphological characteristics (Lickwar et al., 2017; Ng et al., 2005; Wallace et al., 2005; Wang et al., 2010). Recent datasets exploring gene expression across ordered adult intestinal sections in zebrafish and mice revealed that there is conservation of transcriptional programs underlying this regionalization (Lickwar et al., 2017; Wang et al., 2010). When genes were ordered from high expression in duodenum and onwards in mice, it was revealed that many of these same genes are similarly ordered along the anterior-posterior gastrointestinal axis in zebrafish (Lickwar et al., 2017; Wang et al., 2010). For example, many lipid metabolism genes that inform nutrient absorption in the small intestine like diacylglycerol acyltransferase 2 (*Dgat2*) were also highly expressed in the more anterior portions of the zebrafish intestine (Lickwar et al., 2017; Wang et al., 2010). Other examples include duodenal marker gene adenosine deaminase (*Ada*) (Dusing et al., 2000) and jejunal associated genes like fatty acid binding protein 2 (*Fabp2*) (Lickwar et al., 2017; Wang et al., 2010). The ileal-like region of the adult zebrafish intestine is highly reminiscent of the bile acid metabolism program within the mammalian ileum (Lickwar et al., 2017; Wang et al., 2010). As scRNA-seq technology and other transcriptomic analysis tools advance, our ability to resolve conserved regional programs along the length of the intestine will also continue to advance. This includes a recent comparative scRNA-seq study of 30 equally cut sections from mouse and human small intestine that proposes five conserved domains or zones with distinct roles in nutrient absorption that goes beyond our traditional understanding of duodenal, jejunal, and ileal regionalization

(Zwick et al., 2024). While our understanding of regionalization will continue to be refined, the data so far suggest that there are conserved transcriptional programs between mouse and zebrafish that support the use of zebrafish to investigate intestinal physiology and host-microbiota interactions.

The microbiota influences the development and function of intestinal epithelial cells (IECs), and many of these host responses are similarly observed in both zebrafish and mammals (Milligan-McClellan et al., 2011). Many of these conserved host responses have previously been reviewed (Burns & Guillemin, 2017; Kanther & Rawls, 2010; Milligan-McClellan et al., 2011). For example, microbial colonization induces IEC proliferation (Milligan-McClellan et al., 2011). GF larvae have fewer proliferating cells as measured via nucleotide analog incorporation compared to CV larvae (Cheesman et al., 2011; Rawls et al., 2004). A similar finding was reported in mice injected with [3H] thymidine where it was revealed that the absence of microbes significantly reduced IEC proliferation within crypts found in the small intestine (Savage et al., 1981). Other conserved host responses include differentiation of secretory cell populations. GF zebrafish larvae have fewer intestinal goblet cells and serotonin-producing enteroendocrine cells (Bates et al., 2006), while the number and size of goblet cells found in the cecum of GF mice are reduced compared to the cecum of CR mice (Kandori et al., 1996). There is also evidence that the microbiota influences gut motility (Milligan-McClellan et al., 2011). Recording and analysis of the peristaltic contractions of GF and CV larvae suggest that the microbiota can stimulate intestinal contractions (Bates et al., 2006). Recent monoassociation studies investigating gut motility in response to specific bacterial strains suggest that this effect might be microbe specific. Microgavage of *Edwardsiella tarda* into the intestinal bulb significantly induced peristaltic motility compared to PBS or other bacteria like *Aeromonas sp.* or *Bacillus sp.*, which is a host adaption mediated by secretion of tryptophan metabolites (Ye et al., 2021). Interestingly, motile bacteria such as *Vibrio cholera* (strain ZWU0020) can take advantage of motility dynamics

within the intestine to persist and outcompete other bacterial strains (Wiles et al., 2016; Wiles et al., 2020). In rats, the frequency of myoelectrical activity within the small intestine is decreased in GF animals, further supporting that the microbiota influences motility (Husebye et al., 1994). The microbiota also has roles in mediating protein absorption within specialized enterocytes known as lysosome rich enterocytes (LREs) in the more posterior region of the zebrafish intestine (Bates et al., 2006; Childers et al., 2024; Rawls et al., 2004). The lysosomes of these cells in GF larvae are largely void of electron-dense material (Rawls et al., 2004), and there is less accumulation of horseradish peroxidase protein within the intestinal LRE region of GF larvae following immersion (Bates et al., 2006). A recent study suggests the microbiota informs LRE activity by reducing protein uptake and degradation (Childers et al., 2024), which is one possible explanation for the reduced horseradish protein accumulation previously visualized in GF larvae (Bates et al., 2006). Different microbes have varying potential for suppressing protein degradation in LREs (Childers et al., 2024). Curiously, monoassociation of larvae with the same *Vibrio cholera* (strain ZWU0020) strain that uses gut motility dynamics to outcompete other bacteria, significantly suppresses protein degradation (Childers et al., 2024).

To understand the underlying mechanisms that facilitate these host responses, the field has generated several transcriptomic analyses identifying differentially expressed genes between GF and CV digestive tissues. The microbiota has conserved effects on host transcriptional programs like lipid metabolism as well as innate immune response in zebrafish and mice (Davison et al., 2017; El Aidy et al., 2013; Milligan-McClellan et al., 2011; Rawls et al., 2004). Genes involved in lipid metabolism like angiopoietin-like 4 (*Angptl4*) (Backhed et al., 2004; Camp et al., 2012), carnitine palmitoyltransferase 1B (*Cpt1b*) (Davison et al., 2017; Rawls et al., 2004), and peroxisome proliferator-activated receptor alpha (*Ppara*) (Hooper et al., 2001; Rawls et al., 2004) are more highly expressed in the intestines of germ-free animals. It is suggested that this increased nutrient and lipid metabolic profile is reminiscent of a fasted state and that GF

animals exhibit a reduced capacity to efficiently metabolize dietary nutrients (Rawls et al., 2004). In support of this perspective, our lab has previously demonstrated that the microbiota enhances IEC uptake of dietary fatty acid and promotes its storage in lipid droplets in the intestine and liver of zebrafish (Semova et al., 2012). Similarly, a study of GF and SPF mice indicated that GF animals had significant deficits in the absorption of lipid and cholesterol and that this impairment was associated with reduced risk of high-fat diet induced obesity (Martinez-Guryn et al., 2018). Conversely, expression of immune response genes like serum amyloid A (*Saa*) (Davison et al., 2017; Rawls et al., 2004), C-reactive protein (*Crp*) (Davison et al., 2017; Rawls et al., 2004), and suppressor of cytokine signaling 3 (*Socs3*) (Davison et al., 2017; Rawls et al., 2004), as well innate immune cell markers like myeloid-specific peroxidase (*mpx*) (Davison et al., 2017; Rawls et al., 2004) (see “1.5.3 Blood” section for more details) is increased in response to colonization. Furthermore, scRNA-seq has improved our ability to understand cell-type specific and regional responses to microbes in the intestine and other tissues (Jones et al., 2023; Massaquoi et al., 2023; Willms et al., 2022). This includes downregulation of immune gene expression like interferon-stimulated genes in specific goblet cell and enterocyte subpopulations (Willms et al., 2022). While these transcriptomic studies are useful for identifying microbially suppressed and microbially induced programs, our understanding of the transcription factors regulating these host responses remains limited.

### **1.5.2 Swim bladder**

Beyond the intestine, epithelial cells lining respiratory organs like the lungs protect internal surfaces from the external environment. The lung epithelium facilitates host-microbiota interactions and provides an additional line of defense against pathogenic colonization (Dumas et al., 2018; Jordan & Clarke, 2024). Microbiota dysbiosis in lung tissue has been associated with the progression of several respiratory diseases like chronic obstructive pulmonary disease (Pragman et al., 2012; Sze et al., 2012) and idiopathic pulmonary fibrosis (Han et al., 2014;

Molyneaux et al., 2017; Molyneaux et al., 2014). Additionally, there are murine models that suggest the microbiota reduces susceptibility to infections like *Pseudomonas aeruginosa* (Brown et al., 2017). While the zebrafish do not possess lungs, there is increasing evidence that there are shared transcriptional programs and morphological architecture between the mammalian lung and the swim bladder of fishes (Bi et al., 2021; Cass et al., 2013; Longo et al., 2013; Zheng et al., 2011). The gas-filled swim bladder, which directs buoyancy (Dumbarton et al., 2010; Robertson et al., 2008), is a highly relevant organ for investigating the water-to-land vertebrate transition that required adaptive changes such as limb development and efficient air respiration (Bi et al., 2021). Transcriptomic comparisons of diverse tissues (swim bladder, lung, liver, heart, brain, etc.) isolated from air-breathing (mouse, African clawed frog, lungfish, bichir, and alligator gar) or non-air breathing vertebrates (zebrafish, snakehead, and American paddlefish) indicate that the transcriptional program of the lung is most similar to that of the swim bladder more than any other tissue (Bi et al., 2021). Recent studies investigating the phylogenetic relationships between the lungs and swim bladders of ancestral and more modern vertebrates propose that the swim bladders of teleost fish, like zebrafish, evolved from the primitive lung of a common bony fish ancestor (Bi et al., 2021; Sagai et al., 2017). This primitive lung is also proposed to be the origin of the more modern tetrapod lung, although additional research is needed to test these hypotheses.

The transcriptional similarities between the swim bladder and lung are supported by embryologic and anatomical data that suggest the swim bladder originates from endodermal foregut (Field et al., 2003; Ng et al., 2005) in a manner reminiscent to the development of the mammalian lung (Faure & de Santa Barbara, 2011; Rawlins, 2011; Zorn & Wells, 2009). In zebrafish larvae, the swim bladder forms as an evagination of the anterior foregut by 2 dpf and continues to elongate to form a sac-like structure that remains connected to the esophagus via a pneumatic duct (Field et al., 2003; Winata et al., 2009). This early swim bladder is maintained as a singular inflated chamber until approximately 21 dpf, at which point the previously uninflated

secondary (anterior) chamber is inflated to produce a fully functioning, two-chamber organ (Winata et al., 2009). The swim bladder has 3 layers: (1) innermost epithelial, (2) mesenchymal, and (3) outermost mesothelial layers (Winata et al., 2009). Striking, the early lung bud described at embryonic day 9.5 in mice also exhibits epithelial, mesenchymal, and mesothelial layers (Rawlins, 2011). It has been demonstrated that the adult swim bladder is lined with surfactant-secreting epithelium (Robertson et al., 2014), which is an important characteristic of mammalian lung tissue for maintaining homeostasis at the air-water interface and preventing adhesiveness between epithelial tissues upon the expiration of air (Daniels & Orgeig, 2001; Whitsett et al., 2010). Taken together, these studies suggest that there is homology between the lung and swim bladder and support the use of the swim bladder in zebrafish to model lung diseases and infection. The swim bladder of larval zebrafish has been used to model acute lung injury (Zhang et al., 2016) and mucosal infections like candidiasis (Gratacap et al., 2014; Gratacap et al., 2013; Gratacap et al., 2017).

The pneumatic duct is often proposed as a potential route of entry for pathogens that infect the swim bladder of fishes (Dykova et al., 2021; Sirri et al., 2020). Its direct connection to the gastrointestinal tract leaves the swim bladder vulnerable to environmental microbes migrating through the esophagus as well as opportunistic microbes originating in the intestine. Despite our anatomic (Field et al., 2003) and functional (Dumbarton et al., 2010) knowledge of the pneumatic duct, there is limited mechanistic insight for how this tissue contributes to swim bladder infections. Recent scRNA-sequencing data in zebrafish has identified new markers of the pneumatic duct, such as surfactant protein ba (*sftpba*) and SIM bHLH transcription factor 1b (*sim1b*), that might facilitate the generation of new tools for further investigation (Sur et al., 2023). While swim bladder infections do occur in zebrafish facilities, there is surprisingly little information about the swim bladder microbiome under homeostatic conditions (Kent et al., 2020). However, the swim bladder microbiota of a larger physostomous fish like rainbow trout

(*Oncorhynchus tshawytscha*) has been reported (Villasante et al., 2019). Comparisons of the microbiota in the swim bladder and distal intestine revealed that there are shared and as well as tissue specific aspects of the microbiota (Villasante et al., 2019). For example, bacterial genera such as *Pseudomonas*, *Acinetobacter*, and *Staphylococcus* among 14 others were identified in both tissues while genera like *Mycoplasma*, *Sphingomonas*, and *Yersinia* were unique to the swim bladder (Villasante et al., 2019). While this suggests that there might be microbes that are more suited for the intestinal environment compared to the swim bladder and vice versa, future work is needed to address whether opportunistic microbes can truly migrate between tissues via pneumatic duct and what microbial factors might facilitate this migration and colonization persistence. In Table 1 below, we review fungal, bacterial and viral swim bladder infections observed in physostomous fishes that have a pneumatic duct.

**Table 1: Isolated causative swim bladder infections in physostomous fishes.**

Fish species(s)	Isolated Microbe(s)	Clinical and histological presentations	Reference
<i>Cyprinus carpio</i> <i>Carassius gibelio</i> * <i>Lebistes Reticulatus</i> * *Not a physostomous fish but was included in infection experiments	Rhabdovirus (thought to be closely related to <i>Rhabdovirus carpio</i> that causes spring viremia of carp)	Sick fish presented with: <ul style="list-style-type: none"> <li>• Apathy</li> <li>• Reduced reflexes (including loss of balance)</li> <li>• Abdominal/anal swelling</li> <li>• Ascitic fluid in abdominal cavity</li> <li>• Severe inflammation of the swim bladder walls and liver</li> </ul> Intraperitoneal injections with isolated virus reproducibly caused swim bladder inflammation in <i>Cyprinus carpio</i> and <i>Lebistes Reticulatus</i> fish. <i>Carassius gibelio</i> were not susceptible.	(Bachmann & Ahne, 1974)
<i>Oncorhynchus mykiss</i>	<i>Phoma herbarum</i> (fungi)	Fish presented infected swim bladders without observable clinical signs during routine health checks of the commercial farm. However, histological analysis of the swim bladders revealed that the bladder walls were infiltrated by fungal hyphae  Intraperitoneal injections with <i>Phoma herbarum</i> resulted in swim bladders filled with recruited immune cells and thickening of the swim bladder wall of the posterior chamber. The fungus also disseminated to other tissues like the liver and spleen.	(Rehulka et al., 2020)

<i>Hemigrammus pulcher</i>	<i>Exophiala pisciphila</i>  <i>Phaeophleospora hymenocallidicola</i>  (both fungi)	Both fungi were isolated from the swim bladder and coelomic cavity of a sick fish with abnormal swimming behavior found in an aquarium. Histopathologic evaluation indicated that the swim bladder walls were thickened and infiltrated by fungal hyphae.  Experimental IP injection of the isolated <i>Exophiala pisciphila</i> fungal strain in <i>Oncorhynchus mykiss</i> and <i>Cyprinus carpio</i> leads to lethal swim bladder infection.  Experimental IP injection of the isolated <i>Phaeophleospora hymenocallidicola</i> fungal strain into <i>Tinca tinca</i> and <i>Pseudorasbora parva</i> did not result in overt infection phenotypes.	(Rehulka et al., 2018)
----------------------------	---	--	------------------------

### 1.5.3 Blood

In all vertebrates, the hematopoietic system produces diverse cell types including multiple professional immune cells that facilitate microbial interactions. There are several aspects of hematopoiesis in zebrafish that are conserved with mammals and other vertebrates (Galloway & Zon, 2003). Hematopoiesis in zebrafish, like all other vertebrates, is characterized by the emergence of two waves that produce distinct cell populations (Galloway & Zon, 2003). The first or primitive wave occurs approximately 12 hours post fertilization (hpf) within either the intermediate cell mass or the more anterior rostral blood island (de Jong & Zon, 2005). While this phase is heavily characterized by the production of erythroid precursors and erythrocytes, the primitive wave also generates limited myeloid precursors (de Jong & Zon, 2005; Jagannathan-Bogdan & Zon, 2013). This early phase includes the expression of transcription factors such as GATA binding protein a (*gata1a*) (Detrich et al., 1995; Long et al., 1997) or Spi-1 proto-oncogene b (*spi1b*) (Lieschke et al., 2002) that help differentiate between erythrocyte and myeloid populations respectively (de Jong & Zon, 2005; Gore et al., 2018; Stosik et al., 2022). The antagonistic nature of these TFs is observed during early embryonic development, in which *gata1a* expression inhibits the development and differentiation of myeloid lineages (Galloway et

al., 2005; Gore et al., 2018). By 24 hpf, nucleated erythrocytes expressing embryonic hemoglobin (*hbae1.1*, *hbae3*, *hbbe1.1*, etc) are in circulation (Brownlie et al., 2003; Ganis et al., 2012; Gore et al., 2018; Long et al., 1997; Tiedke et al., 2011). Conversely, primitive myeloid cells are predominately derived from the rostral blood island (de Jong & Zon, 2005). These cells initially express l-plastin (*lcp1*) as a pan-leukocyte marker prior to more cell-type specific differentiation directed by TFs like interferon regulatory factor 8 (*irf8*) and CCAAT/enhancer binding protein (C/EBP) 1 (*cebpl*) for respective macrophage and neutrophil specification (Gore et al., 2018; Jin et al., 2016; Li et al., 2011). Early macrophages also express markers genes like macrophage-expressed 1 (*mpeg1*) and microfibrillar-associated protein 4 (*mfap4*) while neutrophils express markers like myeloid-specific peroxidase (*mpx*) (Bennett et al., 2001; Ellett et al., 2011; Lieschke et al., 2001; Ong et al., 2020; Zakrzewska et al., 2010). As early as 30 hpf, macrophages can phagocytosis Gram positive and negative bacteria that have been intravenously injected in the axial vein (Herbomel et al., 1999). Thus, the larval zebrafish is equipped with cells during this early wave that accommodate for oxygen requirements within developing tissues as well as immunity (Song et al., 2024).

During the definitive wave of hematopoiesis at approximately 30 hpf, larval zebrafish start production of self-propagating hematopoietic stem cells (HSCs) (Jagannathan-Bogdan & Zon, 2013). These stem cells originate in the aorta-gonad-mesonephros region (Jagannathan-Bogdan & Zon, 2013). Transcription factors such as RUNX family transcription factor 1 (*runx1*) and v-myb avian myeloblastosis viral oncogene homolog (*myb*) are highly expressed in the dorsal aorta found within this region (Burns et al., 2002; Paik & Zon, 2010; Zhang et al., 2011) and are important for generating HSCs that can separate from the aortal wall and enter circulation via endothelial-hematopoietic transition (Kissa & Herbomel, 2010). Around 2 dpf, freed HSCs migrate posteriorly to the caudal hematopoietic tissue (CHT) (Jin et al., 2007; Murayama et al., 2006). This migration is subsequently followed by seeding of the thymus and continues until

reaching the terminal kidney site (Jagannathan-Bogdan & Zon, 2013; Paik & Zon, 2010). Adult zebrafish produce erythrocytes, myeloid cells, and B lymphocytes in the kidney and T lymphocytes in the thymus (Gore et al., 2018). Although there is evidence of circulating lymphocytes at 3 weeks post-fertilization, mature lymphocytes with the capacity to mount humoral responses to formalin killed *Aeromonas hydrophilia* or human gamma globulin are not found until approximately 4-6 weeks post-fertilization (Willett et al., 1999) (Lam et al., 2004).

While there are certain aspects of hematopoiesis in zebrafish that are differential to the mammalian process (i.e., the primitive wave is initiated in two anatomical locations in zebrafish compared to the singular extraembryonic yolk sac in mammals (de Jong & Zon, 2005)), the transcriptional pathways that facilitate development and differentiation are highly conserved (Davidson & Zon, 2004). This includes the roles of transcription factors like *Gata1* (Belele et al., 2009; Pevny et al., 1991), *Spi1* (Lieschke et al., 2002; Scott et al., 1994), *Fli* (Liu et al., 2008; Spyropoulos et al., 2000), *Myb* (Mucenski et al., 1991; Soza-Ried et al., 2010), *Runx1* (Bertrand et al., 2010; Boisset et al., 2010; Bresciani et al., 2014; Kissa & Herbomel, 2010) among others that are essential at varying points of primitive and definitive hematopoiesis (Jagannathan-Bogdan & Zon, 2013). These conserved hematopoietic transcriptional programs contribute to zebrafish being an attractive model for investigating the role of blood in mediating how the host responds to microbes.

The microbiota informs the development function of immune cells (Jordan & Clarke, 2024). Gnotobiotic and antibiotic-treatment of zebrafish and rodents is continuing to expand our knowledge of how the microbiota influences hematopoiesis and primes immune cells for protection against pathogens. Transgenic zebrafish reporter lines allow us to visualize the localization, migration, and phagocytic behavior of neutrophils and macrophages in larvae in real time (Choe et al., 2021; Harvie & Huttenlocher, 2015). Our lab previously demonstrated that conventionalization of zebrafish larvae increased the transcript levels of neutrophil marker genes

like myeloid-specific peroxidase (*mpx*), matrix metalloproteinase 13a (*mmp13a*), and nephrosin (*npsn*) in whole larvae and systemically increased the total number of circulating neutrophils compared to GF (Kanter et al., 2011; Kanter et al., 2014). Neutrophils in CV larvae also demonstrated differences in velocity and meandering metrics suggestive of elevated migratory behavior (Kanter et al., 2014). In addition to the observation of systemic increases in neutrophil number in zebrafish larvae, there are reports of the microbiota regulating neutrophil number in specific epithelial tissues like the intestine. GF zebrafish larvae have fewer neutrophils in the whole (Rolig et al., 2015) and distal intestine (Bates et al., 2007; Koch et al., 2018) compared to CV larvae.

Germ-free rodent models provide additional evidence that the microbiota informs the development and function of immune cells. GF rats not only have fewer neutrophils in circulation, but these neutrophils have significant reductions in the production of superoxide used for killing microbes and impaired phagocytic behavior (Ohkubo et al., 1999; Ohkubo et al., 1990). Peritoneal macrophages isolated from GF mice produce less superoxide compared to those from CV animals at various developmental timepoints from 1 to 8 weeks post birth (Mitsuyama et al., 1986) and exhibit an attenuated lysosomal enzymatic and phagocytic response to *Escherichia coli* endotoxin (Morland et al., 1979). There is also evidence that peritoneal macrophages isolated from GF rats have impaired migratory behavior towards chemoattractants derived from rat serum (Jungi & McGregor, 1978). Comparatively, there is limited knowledge of microbial influences on the development, function, and localization of macrophages in zebrafish, and future studies in this area are needed.

Acting through the immune cell development and function, the microbiota can promote resistance to pathogens (Jordan & Clarke, 2024). Studies have shown that neonatal mice treated with antibiotics *in utero* and post birth do not exhibit the classical expansion of circulating neutrophils during early development and have fewer neutrophils and granulocyte progenitors in

bone marrow (Deshmukh et al., 2014). Furthermore, these antibiotic-treated neonates demonstrated increased susceptibility to both *E. coli serotype* K1 and *Klebsiella pneumoniae* infection compared to neonates that received no antibiotic treatment (Deshmukh et al., 2014), suggesting that microbiota driven hematopoiesis is important for host survival to pathogen exposure. This finding was further supported by a previous study indicating that GF mice have altered myeloid cell profiles in relevant immune tissues like the spleen and bone marrow (Khosravi et al., 2014). In this model, GF mice had a significantly reduced proportion and total number of splenic neutrophils, macrophages, and monocytes compared to SPF control mice (Khosravi et al., 2014). This reduction in myeloid cell populations was similarly observed in the neutrophil and monocytes of the bone marrow and liver macrophages (Khosravi et al., 2014). Furthermore, granulocyte and/or monocyte progenitors (GMPs) isolated from these GF mice had a reduced capacity to form colonies in cell culture (Khosravi et al., 2014), suggesting that these progenitors have impaired hematopoietic function. Not only did GF mice exhibit a systemic reduction in myeloid cell populations, but these mice were more susceptible to *Listeria monocytogenes* infection, an infection model dependent on innate immunity for infection control (Khosravi et al., 2014).

Pulmonary infection models of *Klebsiella pneumoniae* and *Streptococcus pneumoniae* provide evidence that the microbiota primes macrophages for bacterial killing (Brown et al., 2017). Antibiotic mice infected intranasally with either *K. pneumoniae* or *S. pneumoniae* exhibited higher lung burdens, heightened cytokine production, and ultimately worse survival outcomes (Brown et al., 2017). The enhanced ability of non-antibiotic treated mice to clear and survive infection was associated with a GM-CSF (granulocyte-macrophage colony stimulating factor) mediated alveolar macrophage killing (Brown et al., 2017). The microbiota also informs bacterial killing by neutrophils. Neutrophils derived from the murine bone marrow of non-

antibiotic treated mice are more efficient at killing *S. pneumoniae* or *S. aureus*, which is driven by enhanced recognition of bacterial peptidoglycan by the receptor NOD1 (Clarke et al., 2010).

In addition to bacterial infection, the microbiota is implicated in health outcomes resulting from parasitic or viral infection. GF mice infected subcutaneously with *Leishmania major* in the footpad healed more slowly compared to conventionally reared mice in one gnotobiotic model of parasitic infection (Oliveira et al., 2005). The GF mice had larger lesions and parasitic burdens throughout the 13-week observation period compared to CR mice (Oliveira et al., 2005). These poor health outcomes were associated with the reduced ability of IFN- $\gamma$  stimulated GF macrophages to efficiently kill parasitic cells (Oliveira et al., 2005). The microbiota also primes macrophages in response to viral infection. Antibiotic treatment can have significant effects on the clearance of lymphocytic choriomeningitis virus and the severity of health outcomes from influenza (PR8-GP33) infection (Abt et al., 2012). Antibiotic-treated mice infected intranasally with influenza had higher viral titers in the lung, increased degeneration and necrosis of bronchial epithelium, and ultimately reduced survival compared to conventionally reared controls (Abt et al., 2012). This increased susceptibility to infection was associated with macrophages that exhibited reduced sensitivity to interferon stimulation and an attenuated antiviral transcriptional response to virus (Abt et al., 2012). Interestingly, administration of poly I:C, immunostimulatory double-stranded RNA, was able to rescue the poor health outcomes resulting from infection of antibiotic-treated mice with influenza (Abt et al., 2012). Other examples of the microbiota mediating the response of immune cells to viral infections include West Nile virus (Thackray et al., 2018) and Chikungunya virus (Winkler et al., 2020). Taken together, these studies suggest that the microbiota informs the development and function of immune cell populations in zebrafish as well as mammals and has important implications for resistance to pathogens.

## ***1.6 Biological roles of the epithelial transcription factor Elf3***

Epithelial tissues like the skin, lung, and intestine, are known to be important sites for facilitating communication between the external microbial environment and internal organ systems. Many researchers are curious to know if transcription factors enriched specifically in epithelial tissues are putative mediators of host-microbiota interactions. The ETS transcription factor family, which is unique to metazoans, is a family of interest (Degnan et al., 1993; Laudet et al., 1993). ETS transcription factors are known for their characteristic ~85 amino acid ETS DNA binding domain (Karim et al., 1990); however, these TFs are further subdivided into 11 to 12 subfamilies based on conservation of functional protein domains (e.g., Pointed domain that facilitates protein-protein interactions) and preferred binding motifs (Gutierrez-Hartmann et al., 2007; Laudet et al., 1993; Oikawa & Yamada, 2003; Sharrocks, 2001). Curiously, the ETS TF family includes a subfamily of transcription factors with enriched expression in epithelial tissues known as the “epithelium specific” ETS TFs (Hollenhorst et al., 2011; Kas et al., 2000; Oettgen et al., 1997; Oettgen et al., 1999; Sharrocks, 2001). This subfamily consists of ESE-1 (Elf3), ESE-2 (Elf5), and ESE-3 (Ehf) that have diverse biological roles including epithelial tissue development (Zhou et al., 2005), differentiation (Albino et al., 2012; Fossum et al., 2017; Song et al., 2023; Stephens et al., 2013), and homeostasis (Reehorst et al., 2021). I will review the biological roles and general perspective of Elf3, the founding member of the ESE subfamily (Oettgen et al., 1997), in this section.

### **1.6.1 Host-microbiota interactions and inflammation**

The microbial responsiveness of Elf3 to symbiotic and pathogenic microbes is conserved in many vertebrates. Elf3 transcript levels are induced in the epithelial light organ of squid (*Euprymna scolopes*) after acquisition of its bioluminescent bacterial symbiont *Vibrio fishcheri* (Chun et al., 2008) and are upregulated by colonization in the digestive tissue of CV zebrafish (Davison et al., 2017) and mice (Fu et al., 2017) compared to GF animals. Furthermore, scRNA-

sequencing studies enabling cell-type specific resolution in zebrafish revealed that *elf3* is upregulated by microbiota in IECs like absorptive enterocytes (Willms et al., 2022) and secretory goblet cells (Massaquoi et al., 2023). Interestingly, zebrafish *elf3* is also induced in infection models of conventionally reared mice and zebrafish, suggesting that Elf3 retains the ability to be microbially induced even in the presence of microbes. For example, larval zebrafish injected with *Edwardsiella tarda* and *Salmonella typhimurium* exhibit *myd88*-dependent upregulation of *elf3* mRNA transcript levels in whole larval extracts compared to controls (van der Vaart et al., 2013; van Soest et al., 2011). There is also evidence that Elf3 mRNA levels are increased specifically in enterocytes three days following *Heligmosomoides polygyrus* helminth infection in mice (Haber et al., 2017). Despite these observations that microbiota can induce Elf3 expression in diverse contexts, there is a need to elucidate the specific transcriptional program regulated by Elf3 in response to microbes and investigate the functional consequences of perturbations in this program for host survival.

In addition to being microbially responsive, Elf3 is responsive to inflammatory stimuli. Across diverse cell types, *ELF3* expression can be induced by stimulating cells with pro-inflammatory cytokines like IL-1 $\beta$ , IL-17A, and TNF- $\alpha$  as well as bacterial components like lipopolysaccharide (Brown et al., 2004; Grall et al., 2003; Grall et al., 2005; Kouri et al., 2023; Longoni et al., 2013; Otero et al., 2012; Rudders et al., 2001; Wu et al., 2008; Zhang et al., 2024). This induction is often mediated by NF- $\kappa$ B signaling and can occur in non-epithelial cells. For example, a rat model of neuroinflammation that showed that injection of lipopolysaccharide into the cerebral cortex induced ELF3 protein levels in neurons (Feng et al., 2016). In inflamed settings, ELF3 mediates the upregulation of genes with known inflammatory roles like inducible nitric-oxide synthase (NOS2) (Rudders et al., 2001), interleukin-6 (IL-6) (Wu et al., 2008), and even close ETS TF family member, ETS homologous factor (EHF) (Wu et al., 2008). Induction of ELF3 protein in inflamed tissue has also been observed in clinical practice in patients with

ulcerative colitis (chronic inflammation of the colon) (Li et al., 2015) and osteoarthritis (chronic degradation of articular cartilage) (Otero et al., 2012). These studies demonstrated that protein levels of ELF3 were increased in inflamed mucosal biopsies isolated from patients with ulcerative colitis compared to uninflamed tissue or tissue from healthy controls (Li et al., 2015) and were increased in articular cartilage isolated from knee replacement candidates (Otero et al., 2012). Furthermore, murine models of acute and chronic DSS-induced colitis show upregulation of ELF3 in IECs in response to DSS treatment (Li et al., 2015), and conditional knockout of *Elf3* specifically in articular cartilage can protect against more severe osteoarthritis following surgical induction in mice (Wondimu et al., 2018). There is also a murine model of ovalbumin lung sensitization in which *Elf3* mediates inflammation through impairments in Th17 helper T cell differentiation (Kushwah et al., 2011), suggesting that *Elf3* might facilitate crosstalk between epithelial and immune cell populations in response to inflammatory stimuli. While these studies support Elf3 as TF responsive to inflammatory stimuli, there are limited genome-wide transcriptome studies assessing the transcriptional program regulated by Elf3 in response to these inflammatory cues and its subsequent impact on either the progression or resolution of inflammation.

### **1.6.2 Tissue development and differentiation**

Murine models of *Elf3* mutation indicate that this TF has a role in epithelial development and differentiation. The earliest published model revealed that whole animal mutation of *Elf3* leads to variable lethality, as fewer than expected homozygous mutant mice were recovered in litters produced from heterozygous incrosses (Ng et al., 2002). It was estimated that 30% of all *Elf3*<sup>-/-</sup> mice died in utero and that greater than 50% of those that survived to term died within the first 21 days of life (Ng et al., 2002). This reduced survival in pups was associated with clinical signs of health deterioration such as diarrhea, lethargy, and a general malnourished appearance (Ng et al., 2002). Furthermore, assessment of gastrointestinal development revealed that the *Elf3*<sup>-/-</sup>

mice had severe abnormalities in the small intestine that included disorganization of villus architecture and the apical brush border, reduced number and length of microvilli protruding from intestinal epithelial cells, and fewer sialomucin-mucin producing goblet cells (Ng et al., 2002). The uterine epithelium was also disorganized in *Elf3*<sup>-/-</sup> mice (Ng et al., 2002). Interestingly, later work demonstrated that transgenic *Elf3*<sup>-/-</sup> mice expressing transforming growth factor beta receptor 2 (TGFBR-II) specifically in IECs rescued the reduced TGFBR-II protein levels observed in the small intestine of mutants (Flentjar et al., 2007). Restoration of intestinal TGFBR-II expression significantly improved overall survival and reversed the impairments in intestinal architecture associated with *Elf3* mutation (Flentjar et al., 2007). These data supported previous work suggesting that ELF3 regulates TGFBR-II expression *in vitro* (Choi et al., 1998; Lee et al., 2003). Curiously, there are no genome wide transcriptional studies to-date in mouse IECs that provide additional context to the genes regulated by Elf3 beyond TGFBR-II. Furthermore, explanations for the variable penetrance in lethality resulting from *Elf3* mutation are limited. The spontaneous nature of the death in postnatal *Elf3*<sup>-/-</sup> mice suggests environmental factors in addition to genetics might have a role on host survival, and it would be interesting to formally test whether the intestinal microbiota is associated with better or worse health outcomes.

The intestinal phenotypes reported in whole animal *Elf3* mutant mice are strikingly similar to those observed with conditional knockout of *Crif1* (CR6-interacting factor 1) in IECs (Kwon et al., 2009). *Crif1* mutant mice exhibit significant alterations in intestinal organization and IEC differentiation, and *in vitro* data suggests that *Crif1* co-localizes with *Elf3* in the nucleus and enhances its DNA binding activity (Kwon et al., 2009). While these studies support roles for *Elf3* in the differentiation of intestinal epithelium, there is also data indicating that *Elf3* mediates the differentiation of corneal epithelial cells (Yoshida et al., 2000). Cells transfected with an ELF3 antisense expression vector have fewer keratinous differentiation structures compared to

controls, and ELF3 expression increases the activity of a luciferase reporter for a known keratin differentiation marker (Yoshida et al., 2000).

The function of *elf3* in tissue development and differentiation has also been explored using zebrafish as a model system. Morpholino knockdown of *elf3* expression in zebrafish embryos was reported to have significant consequences for development (Sarmah et al., 2022). This was demonstrated by the overall shorter body length with severe tail and notochord defects, alterations in jaw development and craniofacial cartilage, and brain abnormalities, such as a disrupted midbrain-hindbrain boundary, observed in *elf3* morphants (Sarmah et al., 2022). These effects on development varied from moderate to severe in injected embryos and were further validated via CRISPR-mediated knockdown of *elf3* in F0 crispants (Sarmah et al., 2022). Knockdown of *elf3* also resulted in increased expression of genes with roles in the organization and structure of extracellular matrix like matrix metalloproteinases (*mmp2*, *mmp9*, and *mmp13*) and collagen (*col2a1*) (Sarmah et al., 2022). These data suggest that *elf3* is indispensable for normal larval development, but many questions remain about the specific mechanisms underlying these phenotypes. As described in Chapter 2, our *elf3* mutant zebrafish analysis suggest Elf3 is not required for normal embryogenesis, suggesting that there may be other contributing factors to this phenotype.

### **1.6.3 EMT in cancer**

Epithelial-mesenchymal transition (EMT) is defined by the fact that epithelial and mesenchymal cells have distinct biological and morphological properties that inform their function. Epithelial cells highly express tight and adherens junction proteins and desmosomes to associate with neighboring cells and form barriers that protect internal organs from environmental insults (Dongre & Weinberg, 2019). They additionally express hemidesmosomes and other anchor junction proteins that attach to the underlying scaffold of the basement membrane (Dongre & Weinberg, 2019). Together, the expression of proteins facilitating cell-cell junctions

and cell-extracellular matrix connections help to establish the characteristic apical-basal polarity of epithelial sheets (Dongre & Weinberg, 2019). Conversely, mesenchymal cells, which are maintained in the three-dimensional extracellular matrix, do not highly express junction proteins that establish apical-basal polarity or facilitate close cellular contexts (Dongre & Weinberg, 2019; Sart et al., 2014). Mesenchymal cells display front-back polarity and often contain actin stress fibers that help to facilitate cell migration (Dongre & Weinberg, 2019). EMT thus describes the process through which epithelial cells lose expression of cell-cell junction genes like E-cadherin and their apical-basal polarity while gaining a more elongated cell shape and increased expression of mesenchymal cell markers like vimentin, fibronectin, and N-cadherin (Dongre & Weinberg, 2019; Ribatti et al., 2020). These transitioned cells can exhibit enhanced invasive and migratory properties that are associated with metastasis in certain cancers (Dongre & Weinberg, 2019; Lee et al., 2006; Ribatti et al., 2020; Roth et al., 2017). EMT is also associated with cancer cell resistance to chemotherapeutics (Fischer et al., 2015; Zheng et al., 2015). Therefore, EMT is a biological process with important implications for the progression and prognosis of cancer.

The epithelial nature of TF ELF3 has generated a lot of interest in understanding how it informs epithelial identity and putatively inhibits or promotes EMT transcriptional programs in cancer cells. While the impact of ELF3 expression on EMT programs can vary depending on cell type, there are several examples of ELF3 suppressing EMT and fostering maintenance of genes associated with epithelial identity (Table 2). These findings align with previous *in vivo* work suggesting that Elf3 drives epithelial differentiation of diverse cell types (see “1.6.2 Tissue development and differentiation”). By investigating the role of Elf3 in EMT, we can further our understanding of how this TF contributes to the maintenance of epithelial identity and the consequences of disruptions in this maintenance program for host biology, including interactions with microbes. Table 2 below provides a review of studies that investigate the roles for ELF3 in maintaining epithelial identity as it relates to EMT progression in cancer.

**Table 2: Roles of ELF3 in EMT in cancer**

Cancer model Cell Line	Promotes or Inhibits EMT	Key Findings	Reference
Ovarian cancer OVCA429, SKOV3ipluc (overexpression) CaOV3, OVCA33 (siRNA knockdown)	Inhibits EMT	High Elf3 expression in tumor samples is associated with more favorable prognosis.  ELF3 overexpression inhibits EMT by promoting expression of epithelial markers like E-cadherin and inhibiting the expression of mesenchymal markers (N-cadherin, Slug, Vimentin).	(Yeung et al., 2017)
Pancreatic ductal adenocarcinoma (PDAC)  L3.6 cells	Inhibits EMT	TFGβ-induced EMT downregulates the expression of ELF3.  ELF3 inhibits cell migration, mesenchymal morphology, and expression of mesenchymal markers (Vimentin, N-cadherin) during TFGβ-induced EMT.	(Xu et al., 2023)
Heptaocellular carcinoma  MHCC-LM3  Huh7	Promotes EMT	High ELF3 expression is inversely correlated with E-cadherin expression and is associated with reduced overall patient survival and disease-free survival.  ELF3 expression promotes the induction of EMT-promoting TF ZEB1 and other mesenchymal markers. Knockdown of ELF3 expression upregulates E-cadherin.	(Zheng et al., 2018)
Lung  A549 cells	Inhibits EMT	Down-regulation of ELF3 induces a TGFβ-signaling transcriptional program (including mesenchymal markers) while decreasing the expression of markers for epithelial identity.  ELF3 inhibits expression of mesenchymal markers and characteristics (i.e.- enhanced motility) during TGFβ-induced EMT.	(Lin et al., 2024)
Non-small cell lung cancer  A549, H358, H1299, H1703	N/A- doesn't directly test the effects of ELF3 knockdown or overexpression on EMT genes	ELF3 overexpression restricts the invasive and migratory behaviors of H1299 and H1703 cells.  TGFβ-induced EMT suppresses expression of ELF3 in A549 and H358 cells.	(Lou et al., 2018)
Ampullary carcinoma  HBDEC2-3H10	Inhibits EMT	ELF3 expression inhibits EMT in HBDEC2-3H10 cells as evidenced by the increased expression of EMT TFs (ZEB1, ZEB2, TWIST1) and EMT marker genes (Vimentin) in knockdown cells.  ELF3 knockdown cells had enhanced invasive and migratory characteristics.	(Yachida et al., 2016)

Biliary Tract Cancer HBDEC2-3H10	Inhibits EMT	ELF3 knockout cells had increased expression of vimentin and EMT-promoting TFs (ZEB1, ZEB2, TWIST1). Similar effects were seen in conditional knockout cells.  Reduced ELF3 expression increased migratory and invasive behaviors of HBDEC2-3H10 cells.	(Suzuki et al., 2021)
Breast cancer (basal and luminal subtypes) MDA-MB-231, MCF7, T47D	Inhibits EMT	ELF3 expression suppresses EMT-promoting TFs (ZEB1 and ZEB2) by suppressing the expression of ETS TF Ets1.	(Sinh et al., 2017)
Colorectal cancer HCT116, HKe3, HKh2	Inhibits EMT	Low ELF3 expression in colorectal adenocarcinoma is associated with reduced patient survival.  Mutations in beta-catenin in HCT116 cells induces an EMT transcriptional program that includes downregulation of ELF3 and other epithelial marker genes.  Knockdown of ELF3 enhances Ras-signaling activation of ZEB1 through the Wnt/ $\beta$ -catenin signaling pathway.	(Liu et al., 2019)
Esophageal squamous cell carcinoma Kyse150	Promotes EMT	ELF3 expression promotes an EMT transcriptional program through the repression of miR-144.	(Dong et al., 2022)
Gastric cancer MKN45, HGC27	Inhibits EMT	ELF3 acts downstream of FZD5 to inhibit an EMT transcriptional program (ZEB1, ZEB2) and alterations in cell morphology.	(Dong et al., 2021)
NMuMG (murine cell line)	*Role of ELF3 in MET*  ELF3 can promote MET	ELF3 is required for MET induced by TGF $\beta$ withdrawal in NMuMG cells. Ghrl3 is a downstream target of ELF3 during MET.	(Sengez et al., 2019)

## ***1.7 Summary and proposal for future research***

Animals must constantly adapt to host-microbiota interactions that facilitate their normal development, physiology, and behavior. While many tissues within the animal are directly or indirectly influenced by the microbiome, epithelial tissues that line internal organs like the intestine and lung are often at the first line of the defense for limiting harmful adaptations that confer damaging health consequences and promoting beneficial adaptation (Hooper, 2015; Kim et

al., 2010; Whitsett & Alenghat, 2015). The development of gnotobiotic experimentation allows researchers to ask questions about how the microbiome affects animal hosts through comparisons of GF and CV animals and identify microbe-dependent phenotypes. TFs that mediate transcriptional programs in epithelial and other host tissues have an important role in the development of microbe-dependent phenotypes. Researchers leverage several genomic approaches such as RNA-sequencing, chromatin accessibility assays, and ChIP-seq to identify transcription factors that putatively mediate these host responses to the microbiota. The ETS transcription factor family is a family of interest for mediating host responses to microbes due to several of its members being key differentiators of tissues thought to directly interact with high microbial burdens like the blood (e.g., Spi1, Fli1, Erg, etc.) (Lieschke et al., 2002; Liu et al., 2008; Loughran et al., 2008; Scott et al., 1994), and intestine (e.g., Ehf, Elf3, Spdef, etc.) (Flentjar et al., 2007; Gregorieff et al., 2009; Ng et al., 2002; Reehorst et al., 2021). The larger ETS TF family includes the epithelial specific sub-family that was first described with the identification of Elf3 and is strongly enriched in epithelial tissues (Kas et al., 2000; Oettgen et al., 1997; Oettgen et al., 1999). Previous studies suggest roles for Elf3 in directing epithelial identity and differentiation (Flentjar et al., 2007; Ng et al., 2002), and there are several studies indicating that this transcription factor is responsive to pro-inflammatory signaling molecules (Brown et al., 2004; Grall et al., 2003; Grall et al., 2005; Otero et al., 2012; Rudders et al., 2001; Wu et al., 2008; Zhang et al., 2024) and microbially derived products (Feng et al., 2016). However, our understanding of whether Elf3 mediates host responses to the microbiota in animals is limited. Zebrafish are a powerful model for investigating host-microbiota interactions, and thus in Chapter 2, I will discuss the mutagenesis approaches as well as the comparative transcriptomic analyses performed in this model system to address (1) whether *elf3* transcriptionally mediates host responses to the microbiota and (2) describe the consequences of *elf3* on zebrafish biology. The findings from this investigation are important for furthering our understanding of the

transcriptional networks that allow animals to sustain interactions with the external microbial environment.

## **2. Epithelial transcription factor Elf3 mediates host immune responses to microbiota and protects against aerocystitis in zebrafish**

Chapter 2 was modified from a manuscript of the same title that includes the following co-authors: Colin R. Lickwar, Christiane V. Löhr, Jia Wen, Margaret Morash, Mollie I. Sweeney, Elizabeth L. Reich, David M. Tobin, and John F. Rawls. Briana R. Davis is the first author of this manuscript and as such made substantial contributions to the design, execution, and analysis of reported scientific experiments as well as manuscript preparation. Colin R. Lickwar contributed to experimental design in addition to bioinformatic analyses. Christiane V. Löhr contributed to experimental design and histopathologic evaluation of animal slides. Jia Wen and Margaret Morash contributed to experimental design and preparation of animals for histopathologic assessment. Elizabeth Reich and John F. Rawls contributed to experimental design as well as the isolation and identification of swim bladder bacteria. John F. Rawls additionally provided strong mentorship and guidance that influenced the experimental design, execution, and analyses presented in this body of work. All co-authors contributed to the manuscript preparation.

For access to the raw RNA-sequencing files and raw count data used for the bulk RNA-seq analysis presented in this chapter, please download the files deposited in NCBI's Genome Expression Omnibus through GEO Series accession number GSE293676.

### ***2.1 Introduction***

Beginning at birth, animals are exposed to diverse microorganisms that significantly influence their physiology while also posing a constant risk of infection. To manage these complex microbial relationships, animals evolved to deploy epithelial barriers and immune cells at the interfaces between their bodies and the microbial world beyond (Hooper, 2015; Whitsett & Alenghat, 2015). Homeostasis in these exposed epithelial tissues relies on the capacity of the host

cells to adapt their physiology in accordance with the microbial and inflammatory signals they receive. These adaptive changes in epithelia and associated immune cell populations are achieved largely through their ability to adapt their programs of gene transcription. Identification of the mechanisms underlying epithelial and immune cell transcriptional responses to microbiota is therefore an important research goal.

Zebrafish (*Danio rerio*) are useful for investigating the mechanisms of host-microbe interactions due to the conservation of their developmental biology and physiology with mammals (Lickwar et al., 2017; Ng et al., 2005; Wallace et al., 2005), genetic tractability, and facile gnotobiotic methods (Milligan-McClellan et al., 2011; Stream & Madigan, 2022; Xia et al., 2022). Emerging evidence indicates substantial conservation between zebrafish and mice in their patterns of microbially-responsive gene expression in the digestive tract and underlying host transcription factors (TFs). For example, we previously uncovered conserved microbial suppression of the epithelial TF Hepatocyte nuclear factor 4 alpha (Hnf4a) and the epithelial and metabolic gene expression programs it mediates in both zebrafish and mice (Davison et al., 2017; Lickwar et al., 2022). However, we still have an incomplete understanding of the larger network of TFs used by epithelia and their supporting immune systems to coordinate appropriate responses to microbes.

Elf3 along with ESE-2 (Elf5), and ESE-3 (Ehf) belong to a subclass of epithelial-specific (ESE) ETS TFs that have diverse biological roles including epithelial tissue development (Zhou et al., 2005), differentiation (Albino et al., 2012; Fossum et al., 2017; Song et al., 2023; Stephens et al., 2013) and homeostasis (Reehorst et al., 2021). Elf3 expression is enriched in epithelial-rich tissues in mammals, including the intestine, lung, kidney, and uterus (Fung et al., 2024; Oettgen et al., 1997; Tymms et al., 1997). Whole animal mutation of *Elf3* in mice leads to variable lethality, with the surviving animals showing altered villus architecture in the small intestine and impaired intestinal epithelial cell differentiation (Flentjar et al., 2007; Ng et al., 2002; Yoshida et al., 2000). In zebrafish, morpholino and CRISPR knockdowns of *elf3* have suggested roles in

embryogenesis and extracellular matrix assembly and organization (Sarmah et al., 2022). Gene expression studies in zebrafish indicate that *elf3* is upregulated by microbiota colonization in intestinal enterocytes (Willms et al., 2022) and goblet cells (Massaquoi et al., 2023), and is also upregulated in response to pathogenic infections (Haber et al., 2017; van der Vaart et al., 2013; van Soest et al., 2011). In accord, mammalian studies have shown that expression of *Elf3* homologs is responsive to pro-inflammatory stimuli (Brown et al., 2004; Feng et al., 2016; Grall et al., 2005; Otero et al., 2012; Zhang et al., 2024) and can be mediated by key immunomodulatory TFs like NF- $\kappa$ B in diverse cell types (Grall et al., 2003; Kouri et al., 2023; Longoni et al., 2013; Rudders et al., 2001; Wu et al., 2008). While these studies suggest expression of *Elf3* homologs can be induced by microbial and inflammatory signals, the specific roles of *Elf3* in host response to microbiota remains untested in any animal system.

## **2.2 Results**

### **2.2.1 Identification of *Elf3*, a candidate TF mediating conserved host responses to the microbiota**

We performed a computational screen of intestinal genomic datasets from zebrafish and mouse to identify conserved transcriptional regulatory mechanisms that mediate host responses to microbiota. The intestine was selected because it harbors the largest microbial community in the body (Sender et al., 2016) and has been the subject of numerous functional genomic studies of host-microbiota interactions (Davison et al., 2017; Jones et al., 2023; Massaquoi et al., 2023; Rawls et al., 2004). We first identified TF binding motif (TFBM) enrichment from intestinal accessible chromatin regulatory regions neighboring genes that were induced or suppressed by colonization of a normal microbiota into germ-free (GF) mice and zebrafish (Lickwar et al., 2017). We found that in addition to TFBMs for well characterized inflammatory regulators like NF- $\kappa$ B, IRF and STAT, the regions near genes upregulated by microbiota showed conserved TFBM enrichment for members of the ETS TF family (Fig. 1A). ETS family members can share highly similar motifs, so

we further characterized expression levels of ETS family members in IECs from adult zebrafish and mice. We observed that Elf3 was the most highly expressed ETS TF factor in IECs in both animals (Fig.1B). This is consistent with findings that *elf3* is expressed in diverse epithelia-rich tissues like the intestine and kidney in adult and larval zebrafish (Fig.2A-D). Next, we leveraged the availability of numerous existing transcriptomic datasets comparing mice and zebrafish reared GF or colonized with microbiota (conventionalized, CV) to identify TFs that were up- or down-regulated by microbiota colonization in the intestine (Table 3). This again revealed that in addition to well-known inflammatory TFs like IRF and STAT family members, Elf3 was consistently induced by microbiota in both species (Fig.1C). Taken together, these findings strongly implicate Elf3 as the leading ETS TF candidate and suggest it may be capable of initiating a unique microbial response specifically in epithelial tissues.

We reasoned that conserved tissue-specific expression of Elf3 and induction by microbiota may be driven by conserved regulatory mechanisms. While DNA sequence conservation levels from teleosts to mammals was low in the Elf3 proximal promoter, we searched for common modular TFBMs in zebrafish, mouse, and human (Lickwar et al., 2017; Villar et al., 2015). We only identified proximal NF-kB and more distal Egr1 motifs as in common, consistent with known NF-kB sites in the human *ELF3* promoter (Longoni et al., 2013; Wu et al., 2008) (Fig.1D). Remarkably, this exact order of motifs relative to the Elf3 transcriptional start site was conserved in a broad range of vertebrate genomes (Fig.1E). To determine if this motif structure related to chromatin architecture, we queried accessible chromatin from multiple tissues in zebrafish (Yang et al., 2020), mouse (Camp et al., 2014), and human (Lickwar et al., 2017) and observed two distinct accessible chromatin peaks each overlapping a different NF-kB or Egr1 motif. Importantly, these peaks frequently showed opposite accessibility across tissues with the NF-kB motif being accessible in epithelial-rich tissues such as intestine and kidney (Fig.1D). This implies conserved

Elf3 function across vertebrate species and suggests a plausible conserved mechanism by which signaling through NF- $\kappa$ B to Elf3 is tissue specific.

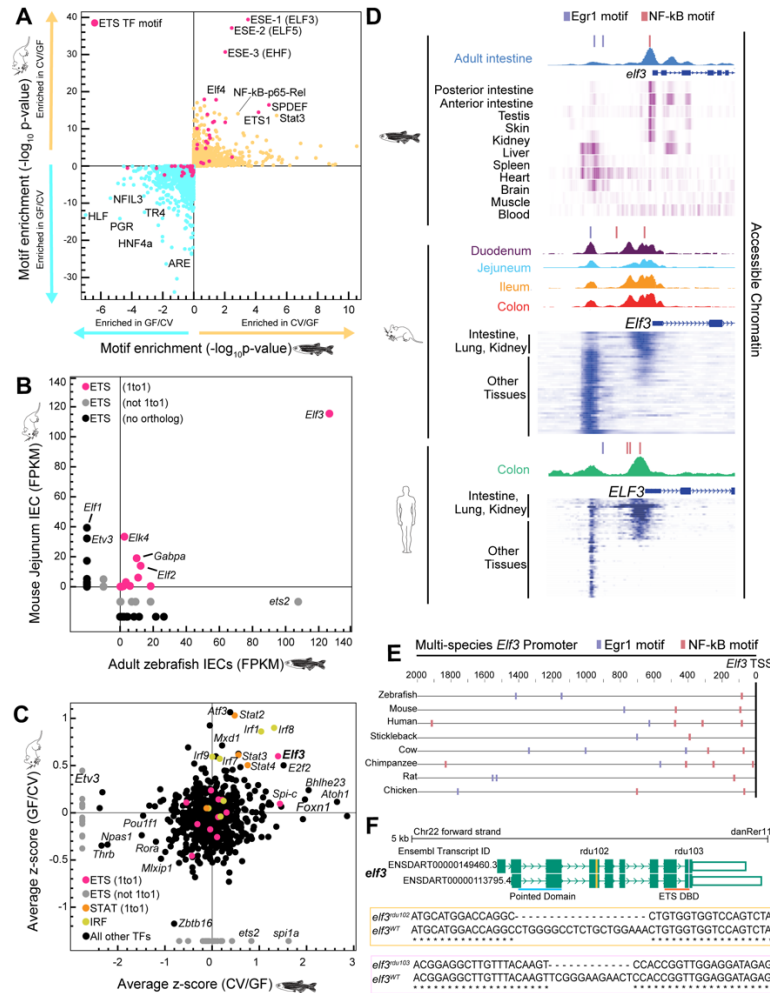


**Figure 1: Identifying a candidate TF mediating conserved host responses to the microbiota.**

(A) Transcription factor binding motif (TFBM) enrichment as assessed by HOMER (Heinz et al., 2010) near genes microbially responsive in mouse (y-axis) and zebrafish (x-axis) digestive tissue (B) mRNA expression of ETS transcription factors in mouse and zebrafish IECs represented as fragments per kilobase of transcript per million (FPKM) mapped reads. The orthologous relationships between each ETS TF in zebrafish and mice are indicated by the pink (1 to 1), gray (1 to many) and black (no ortholog) colored data points. (C) Average z-scored mRNA levels of genes significantly differential in CV/GF comparisons across multiple mouse (15) and zebrafish (2) studies. (D) Visualization of accessible chromatin peaks within the *elf3* promoter of zebrafish (Lickwar et al., 2017), mouse (Camp et al., 2014), and human (Lickwar et al., 2017) IECs. Below the accessible chromatin peaks for each species are heatmaps (visualized via the WashU genome browser, <http://genome.ucsc.edu>) of ATAC-seq performed in diverse tissue types (Consortium, 2012; Davis et al., 2018; Yang et al., 2020). For the mouse and human datasets, more epithelial tissues like the intestine and lung are group compared to other tissue types. (E) Comparison of the *elf3* promoter across diverse vertebrate species with the location of the conserved Egr1 and NF-κB motifs depicted by the blue and pink boxes respectively. The vertebrates featured in this analysis include zebrafish (*Danio rerio*), mouse (*Mus musculus*), human (*Homo sapiens*), stickleback (*Gasterosteus aculeatus*), cow (*Bos taurus*), chimpanzee (*Pan troglodytes*), rat (*Rattus norvegicus*), and chicken (*Gallus gallus*). (F) Schematic of the protein coding *elf3* isoforms in zebrafish with the exons colored green and introns depicted as green arrows. The yellow and pink vertical lines indicate the location of the rdu102 and rdu103 CRISPR lesions respectively. The horizontal lines at the bottom of the schematic indicate the location of the SMART predicted functional domains (Letunic & Bork, 2018; Letunic et al., 2021) pointed (blue) and ETS DNA binding (orange).

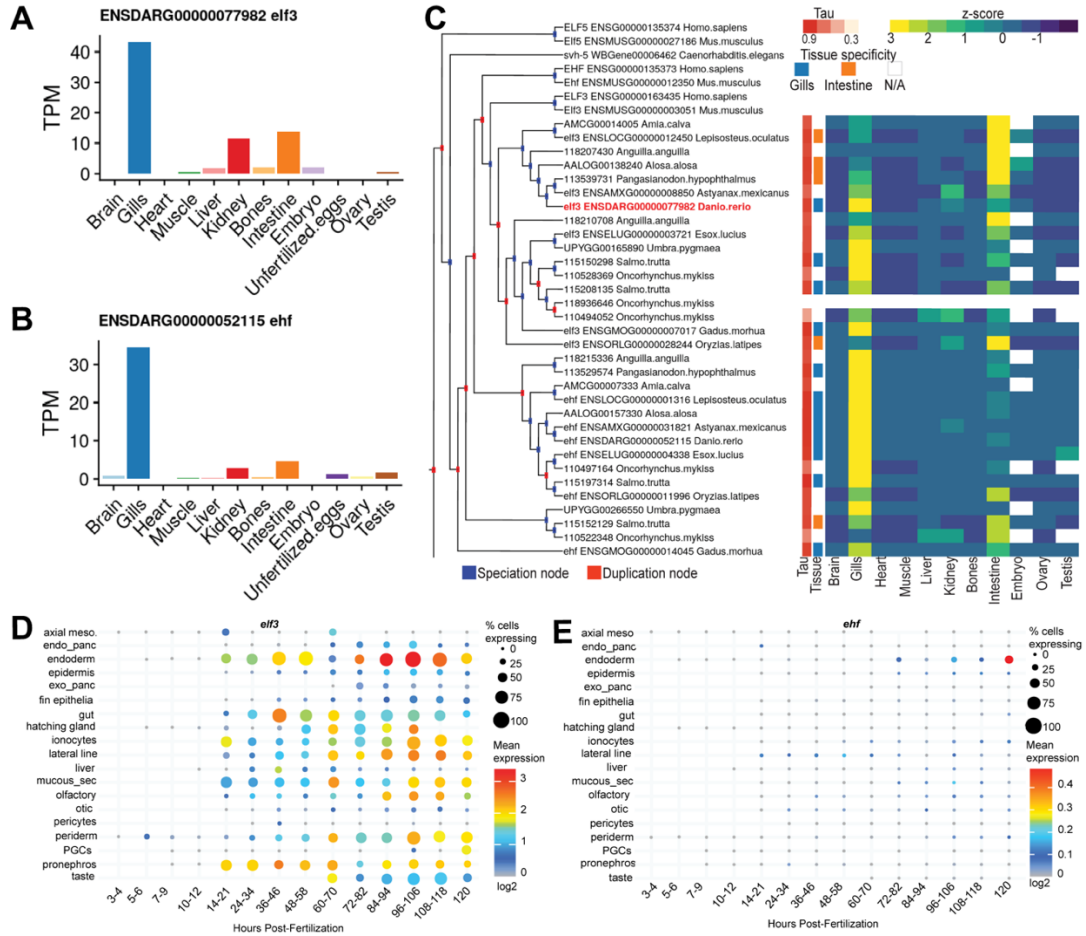


**Figure 2: *elf3* is expressed in diverse tissues in adult and larval zebrafish.**

Bar plots generated by the FEVER transcriptomics web server (Montfort et al., 2024) that show the expression in transcripts per million (TPM) for *elf3* (A) and *ehf* (B) in adult zebrafish tissues. (C) FEVER evolutionary gene tree with blue duplication and red speciation nodes for ESE ETS TFs across 13 fishes and corresponding heatmap of z-scored gene expression in 11 tissues. The FEVER-calculated tissue-specificity indexes (Tau) are calculated for genes with no missing expression values and indicate high specificity when  $>0.9$ . Genes with Tau specificity ( $>0.9$ ) for the gills and intestine are indicated by the blue and orange boxes respectively. (D-E) Dot plot visualization from the Daniocell (Sur et al., 2023) scRNA-seq atlas of larval zebrafish showing, tissue-specific expression of *elf3* and *ehf* at the indicated developmental timepoints. Abbreviations: axial meso = axial mesoderm, endo\_panc = endocrine pancreas; exo\_panc = exocrine pancreas, mucous\_sec = mucous secreting, PGCs: primordial germ cells.

**Table 3: List of mouse and zebrafish studies used to compare CV/GF expression**

Species	Source (PubMed ID)	Geo Accession
Mouse	28939687	GSE102867
Mouse	22617837	GSE32513
Mouse	17055441	GSE5198
Mouse	29138692	GSE99018
Mouse	24799697	GSE46952
Mouse	28385711	GSE90462
Mouse	22570612	GSE35597
Mouse	24963153	GSE57919
Mouse	25157157	GSE60039
Mouse	21531334	GSE27950
Mouse	25118238	GSE59644
Zebrafish	28385711	GSE90462
Zebrafish	15070763	N/A

### 2.2.2 Generation of *elf3* mutant alleles

To test the role of *elf3* in host-microbe interactions and other aspects of zebrafish biology, we used CRISPR-Cas9 to generate zebrafish *elf3* mutant alleles. We isolated two mutant alleles that encode lesions in exons shared by all protein-coding isoforms of *elf3* (Fig.1F). The *elf3*<sup>rd<sup>102</sup></sup> allele harbors a 19 bp deletion in an early exon that encodes a frameshift mutation and early stop codon. The *elf3*<sup>rd<sup>103</sup></sup> allele harbors a 12 bp deletion near the end of the conserved ETS DNA binding domain that leads to a 4 amino acid in-frame deletion, including a highly conserved phenylalanine residue that when mutated disrupts ETS domain binding (Mavrothalassitis et al., 1994; Pio et al.,

1996) (Fig. 3A). Incrosses between adults that were heterozygous for either *elf3<sup>rd102</sup>* or *elf3<sup>rd103</sup>* yielded larvae at expected Mendelian ratios with no gross abnormalities in morphology or body size, suggesting *elf3* is not required for embryogenesis (Fig.3B-I). Similar results were obtained using incrossed adults that were homozygous for either *elf3<sup>rd102</sup>* or *elf3<sup>rd103</sup>*, indicating that there is no requirement for maternal provision of *elf3* transcript for embryonic development (not shown). We elected to focus our subsequent phenotyping efforts on the in-frame deletion allele *elf3<sup>rd103</sup>* to avoid the risk of transcriptional adaptation with other related ETS TFs that could occur in the frameshift *elf3<sup>rd102</sup>* allele (El-Brolosy et al., 2019).

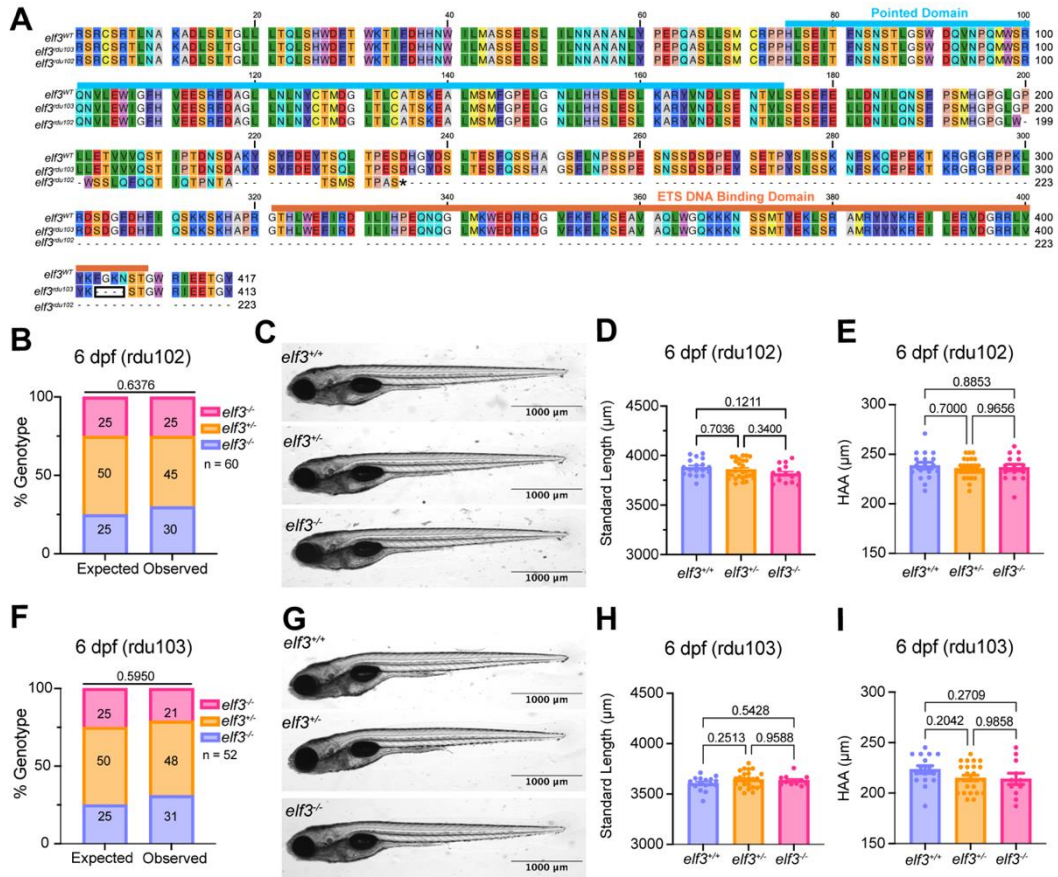


**Figure 3: Generation of *elf3* mutant alleles.**

(A) Alignment of the wild-type Elf3 protein sequence (ENSDARP00000124484.1) to the predicted mutated sequence for *elf3*<sup>rd102</sup> and *elf3*<sup>rd103</sup> alleles. The asterisk indicates the early stop codon of the *elf3*<sup>rd102</sup> frameshift mutation, and the black box highlights the 4 deleted amino acid residues of the *elf3*<sup>rd103</sup> 12 bp in-frame mutation. The predicted pointed and DNA-binding functional domains are indicated by the horizontal blue and orange lines respectively. (B) Comparison of the observed genotypic ratios from heterozygous in-cross of *elf3*<sup>rd102</sup> adults to expected Mendelian ratios. (C) Representative brightfield images of *elf3*<sup>rd102</sup> allele 6 dpf larvae. (D-E) Standard length (snout to caudal peduncle) and height at anterior of anal fin (HAA) of *elf3*<sup>rd102</sup> larvae with *n* per genotype (+/+ : 18, +/- : 27, -/- : 15). (F) Comparison of the observed genotypic ratios from heterozygous in-cross of *elf3*<sup>rd103</sup> adults to expected Mendelian ratios. (G) Representative brightfield images of *elf3*<sup>rd103</sup> 6 dpf larvae. (H-I) Morphometric analysis of the standard length (snout to caudal peduncle) and height at anterior of anal fin (HAA) of *elf3*<sup>rd103</sup> with *n* per genotype (+/+ : 16, +/- : 25, -/- : 11). Data are presented as mean ± SEM. *P*-values for (B & F) were calculated using a chi-square goodness-of-fit test and (D-E & H-I) using a one-way ANOVA with Tukey's multiple comparisons post-test.

### 2.2.3 Experimental design of larval bulk RNA-seq

To test the role of *elf3* in larval zebrafish and its impact on host-microbiota interactions, we performed bulk RNA sequencing on germ-free (GF) and conventionalized (CV) wild-type and mutant larvae at 6 days post-fertilization (dpf) (Fig.4A). Principal component analysis of the normalized RNA-seq counts revealed that biological replicates for the four conditions stratified based on microbial status and genotype (Fig.4B). This stratification was consistent with the identification of hundreds of significant differentially expressed genes in 4 comparisons (i.e., **microbial effect** in CVWT/GFWT and CVMut/GFMut, and **genotype effect** in GFMut/GFWT and CVMut/CVWT) (Fig.4C-D). We observed no clear differential expression of developmental markers between WT and mutant larvae (Fig.5A-F), which was consistent with our larval morphometric analyses (Fig.3), together indicating that the differential gene expression we observe here is not caused by differences in developmental progression (Yang et al., 2013). We continued our RNA-seq analyses to highlight 4 separate representations: **(1)** the effect of *elf3* genotype on transcriptional responses to microbiota (Fig. 4E), **(2)** the effect of *elf3* mutation on host gene expression independent of microbial status (Fig. 4F), **(3)** the interaction between genotype and microbial status (Fig.6), and **(4)** the underlying tissue specificity of the differentially expressed genes (Fig.7).

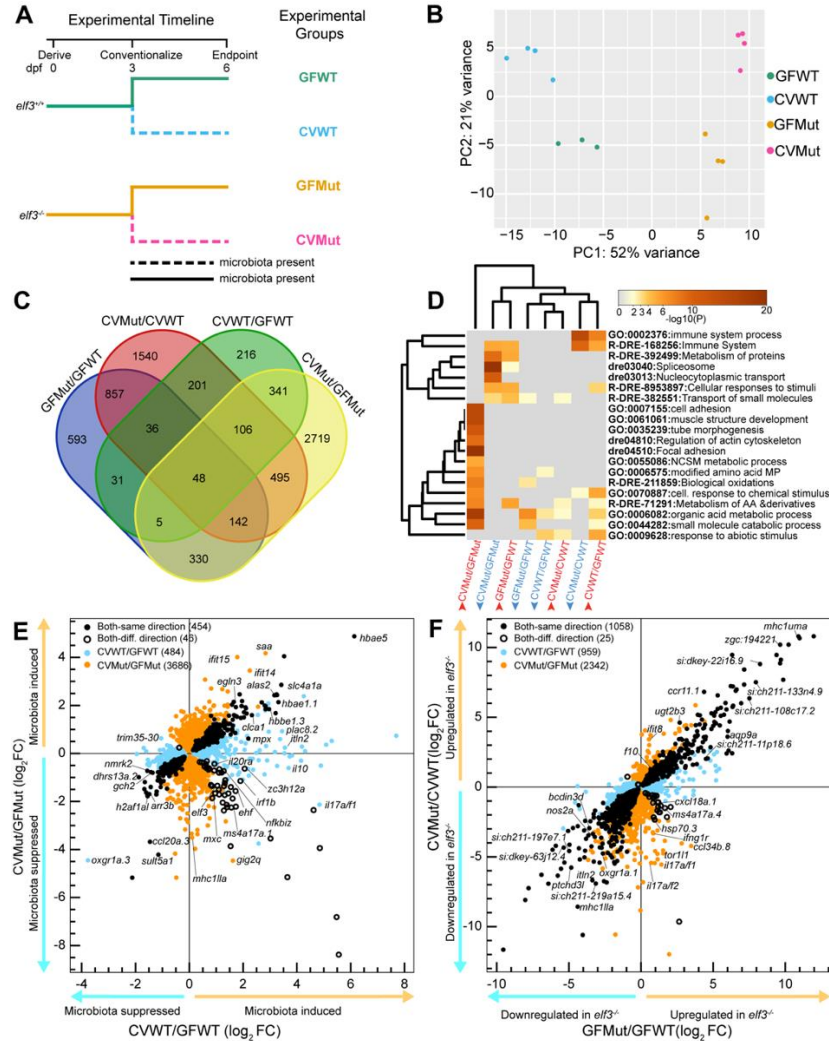


**Figure 4: *elf3* genotype and microbial status have effect the larval zebrafish transcriptome.**

(A) Schematic depicting the experimental conditions of the bulk RNA-seq experiment where clutches of *elf3*<sup>+/+</sup> and *elf3*<sup>-/-</sup> larvae produced from homozygous in-crosses were derived germ-free (GF). At 3 dpf, half of the larvae from each genotype were colonized with a conventional zebrafish microbiota (CV) (indicated with solid or dashed lines) and all groups were maintained until a 6 dpf endpoint, at which point pooled larval samples were prepared for sequencing (n = 6-16 larvae per pool). (B) PCA plot of the normalized counts for each experimental replicate (GFWT:3, GFMut:4, CVWT:4, CVMut:5). (C) Venn diagram overlap of the genes significantly differentially expressed (P adjusted < .05) in the 4 comparisons. (D) Metascape (Zhou et al., 2019) analysis of the enriched GO terms, biological processes, and signaling pathways that are upregulated (red lettering) and down-regulated (blue lettering) in each of the 4 RNA-seq comparisons. Abbreviations: NSCM metabolic process = nucleobase-containing small molecule metabolic process; modified amino acid MP = modified amino acid metabolic process; metabolism of AAs & derivatives = metabolism of amino acids and derivatives. (E) Scatterplot of the gene log<sub>2</sub> fold change for all significant differentially expressed genes in the CVWT/GFWT and CVMut/GFMut RNA-seq comparisons (P adjusted < .05), which assess the effect of microbial status on gene expression. (F) Scatterplot of the gene log<sub>2</sub> fold change for all significant differentially expressed genes in the GFMut/GFWT and CVMut/CVWT RNA-seq comparisons (P adjusted < .05), which assess the effect of *elf3* genotype on gene expression.

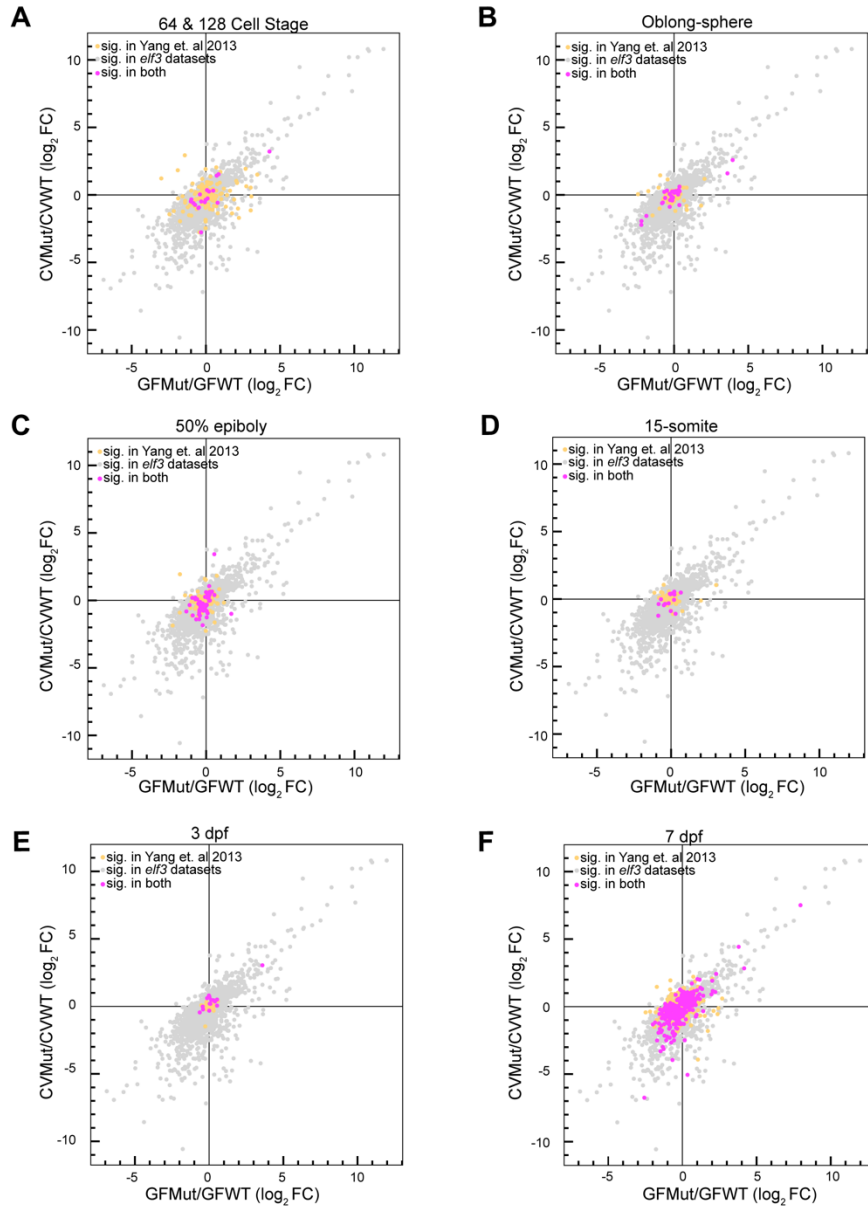


**Figure 5: *elf3* mutant larvae are not developmentally delayed.**

(A-F) Scatter plots of developmentally regulated genes overlaid on the larval *elf3* RNA-seq datasets (CVMut/CVWT and GFMut/GFWT comparison). Stages include (A) 64 & 128 cell stage, (B) oblong-sphere, (C) 50% epiboly, (D) 15-somite, (E) 3 dpf, and (F) 7 dpf (Yang et al., 2013) genes are colored yellow: developmental marker genes, gray: *elf3* datasets, and pink: significant in both.

### 2.2.4 *elf3* mediates host responses to the microbiota in larval zebrafish

To understand if *elf3* mutation affects transcriptional responses to microbiota, we first defined the normal host response as those genes differentially expressed in the CVWT/GFWT comparison (Fig.4E). Functional enrichment analysis (Zhou et al., 2019) indicated that microbial colonization induced expression of immune and defense response genes like *itln2*, *npsn*, and *mpx* similar to previous larval bulk transcriptomic studies (Kanther et al., 2011) (Fig.4D, Table 4). In agreement with our analyses in Fig. 1, we also observed upregulation of *elf3* upon colonization (Fig.2E). Consistent with previous studies (Davison et al., 2017), the microbiota suppressed genes involved in abiotic responses like circadian rhythm (*cry2*, *per1a*, and *bhlhe41*) as well as organic acid metabolic processes such as fatty acid metabolism (*cpt1b*, *hadhaa*, and *angptl4*) (Fig.4E, Table 4). Together, these data identify genes differentially expressed in response to microbiota in WT larvae.

Next, we assessed how the response to microbiota is affected by *elf3* mutation. We found 46% of the differentially expressed genes in the CVWT/GFWT comparison were similarly differential in the CVMut/GFMut comparison, indicating that there are substantial aspects of the host response to microbiota that are shared between genotypes (closed black circles in Fig. 4E). Enrichment analysis of this shared transcriptional program suggested that *elf3* is not required for microbial regulation of many processes, such as gas transport and hypoxia response, or suppression of iron homeostasis and phototransduction (Table 6, Table 7).

Beyond these similarities, we observed extensive differences in the transcriptional response to microbiota in WT and *elf3* mutant larvae (Fig.4D, Fig.4E). Because *elf3* is frequently upregulated in response to microbiota (Fig.1), we were particularly interested in differences between the genes upregulated in the CVWT/GFWT comparison and downregulated in the CVMut/CVWT comparison (Fig.4E). We were intrigued to find that genes involved in immune response were among those that differed in those two comparisons. For example, immune system

process was the top enriched biological process for genes induced by microbiota in WT animals, but it was not among the top 20 enriched terms in the *elf3* mutant response to microbiota (Fig.4D, Table 4, Table 8). In fact, the same immune system process category was the top enriched process downregulated in the CVMut/CVWT comparison, suggesting that *elf3* mutants fail to mount a normal immune response to microbiota (Fig.4D, Table 9). These *elf3*-dependent immune response genes included those involved in cytokine receptor signaling (*il10*, *il22*, and *tnfsf10*) (Bottiglione et al., 2020; Costa et al., 2013) and immune cell differentiation (*ikzf1* and *cebp1*) (Li et al., 2024; Willett et al., 2001) (Fig.4E). Furthermore, we were interested to find that a small subset of genes that were induced by microbiota in WT but suppressed by microbiota in *elf3* mutants were enriched for immune system functions and C-type lectin receptor signaling (open black circles in Fig.4E). This set included IRF TFs (*irf1a*, *irf1b*, *irf9*, and *irf10*). Together, these data suggest that microbial induction of immune genes observed in WT zebrafish is attenuated in *elf3* mutants.

We next evaluated how *elf3* mutation impacts the pattern of genes downregulated by microbiota. Genes downregulated response to microbiota in WT were enriched for organic acid metabolism and abiotic responses, which included circadian rhythm regulators (*cry2*, *per1a*, and *cipca*) (Table 5). However, those same pathways were not similarly suppressed in mutants (Fig. 4D, Table 9). These data highlight a putative role for *elf3* in mediating microbial suppression of circadian regulation.

**Table 4: Metascape (Zhou et al., 2019) enrichment for all significant genes upregulated in CVWT/GFWT**

CVWT/GFWT UP (description)	Term	Log P	Log q-value
Summary_immune system process	GO:0002376	-7.534674	-3.684104983
Member_immune system process	GO:0002376	-7.534674	-3.684104983
Member_myeloid cell differentiation	GO:0030099	-6.835031	-3.520995082
Member_erythrocyte differentiation	GO:0030218	-5.954666	-2.789729402
Member_erythrocyte homeostasis	GO:0034101	-5.839741	-2.789558581
Member_myeloid cell homeostasis	GO:0002262	-5.480313	-2.525118646
Member_homeostasis of number of cells	GO:0048872	-4.631207	-2.055235445
Member_hemopoiesis	GO:0030097	-4.045498	-1.576560173
Member_homeostatic process	GO:0042592	-3.222343	-1.008677909
Member_multicellular organismal-level homeostasis	GO:0048871	-3.126466	-0.954876869
Member_neutrophil differentiation	GO:0030223	-3.019082	-0.876887539
Member_regulation of erythrocyte differentiation	GO:0045646	-2.795823	-0.734397577
Member_erythrocyte development	GO:0048821	-2.74379	-0.694571618
Member_myeloid cell development	GO:0061515	-2.732653	-0.692775072
Member_granulocyte differentiation	GO:0030851	-2.673123	-0.651343467
Member_embryonic hemopoiesis	GO:0035162	-2.243519	-0.357617997
Member_leukocyte differentiation	GO:0002521	-2.177928	-0.329275154
Summary_reactive oxygen species metabolic process	GO:0072593	-7.396081	-3.684104983
Member_reactive oxygen species metabolic process	GO:0072593	-7.396081	-3.684104983
Member_gas transport	GO:0015669	-6.94571	-3.520995082
Member_oxygen transport	GO:0015671	-6.103641	-2.868786014
Member_hydrogen peroxide catabolic process	GO:0042744	-5.115286	-2.381033691
Member_hydrogen peroxide metabolic process	GO:0042743	-4.734846	-2.055235445
Member_Erythrocytes take up oxygen and release carbon dioxide	R-DRE-1247673	-2.795823	-0.734397577
Member_Erythrocytes take up carbon dioxide and release oxygen	R-DRE-1237044	-2.541029	-0.567578934
Member_O <sub>2</sub> /CO <sub>2</sub> exchange in erythrocytes	R-DRE-1480926	-2.541029	-0.567578934
Summary_response to external stimulus	GO:0009605	-6.869858	-3.520995082
Member_response to external stimulus	GO:0009605	-6.869858	-3.520995082

Member_defense response	GO:0006952	-5.802564	-2.789558581
Member_biological process involved in interspecies interaction between organisms	GO:0044419	-5.067253	-2.35527734
Member_response to external biotic stimulus	GO:0043207	-4.655577	-2.055235445
Member_response to other organism	GO:0051707	-4.655577	-2.055235445
Member_response to bacterium	GO:0009617	-4.646868	-2.055235445
Member_response to biotic stimulus	GO:0009607	-4.578765	-2.028157384
Member_defense response to other organism	GO:0098542	-3.213806	-1.007889092
Member_defense response to bacterium	GO:0042742	-2.894563	-0.805836699
Summary_Innate Immune System	R-DRE-168249	-5.899645	-2.789729402
Member_Innate Immune System	R-DRE-168249	-5.899645	-2.789729402
Member_Immune System	R-DRE-168256	-5.356563	-2.489685308
Member_Neutrophil degranulation	R-DRE-6798695	-4.645647	-2.055235445
Summary_response to hypoxia	GO:0001666	-5.458943	-2.525118646
Member_response to hypoxia	GO:0001666	-5.458943	-2.525118646
Member_response to decreased oxygen levels	GO:0036293	-5.407498	-2.508435382
Member_response to abiotic stimulus	GO:0009628	-5.235293	-2.452736478
Member_response to oxygen levels	GO:0070482	-5.209958	-2.452224688
Member_cellular response to hypoxia	GO:0071456	-4.122484	-1.602884846
Member_cellular response to decreased oxygen levels	GO:0036294	-3.993704	-1.56048195
Member_cellular response to oxygen levels	GO:0071453	-3.874681	-1.452739638
Summary_cellular response to chemical stimulus	GO:0070887	-5.326493	-2.48957867
Member_cellular response to chemical stimulus	GO:0070887	-5.326493	-2.48957867
Summary_Biosynthesis of protectins	R-DRE-9018681	-5.295646	-2.486760013
Member_Biosynthesis of protectins	R-DRE-9018681	-5.295646	-2.486760013
Member_Arachidonate metabolism	R-DRE-2142753	-2.947341	-0.831962697
Member_Eicosanoid synthesis	WP1318	-2.895011	-0.805836699
Member_cellular response to xenobiotic stimulus	GO:0071466	-2.793161	-0.734397577

Member_Biosynthesis of DHA-derived SPMs	R-DRE-9018677	-2.527506	-0.567578934
Member_Biosynthesis of specialized proresolving mediators (SPMs)	R-DRE-9018678	-2.527506	-0.567578934
Member_response to xenobiotic stimulus	GO:0009410	-2.509394	-0.55708569
Member_Synthesis of epoxy (EET) and dihydroxyeicosatrienoic acids (DHET)	R-DRE-2142670	-2.105921	-0.281344375
Member_Cytochrome P450 - arranged by substrate type	R-DRE-211897	-2.033145	-0.237623256
Summary_photoperiodism	GO:0009648	-4.622893	-2.055235445
Member_photoperiodism	GO:0009648	-4.622893	-2.055235445
Member_response to light stimulus	GO:0009416	-3.051622	-0.895949077
Member_phototransduction	GO:0007602	-2.904575	-0.805836699
Member_cellular response to light stimulus	GO:0071482	-2.63285	-0.628444262
Member_response to radiation	GO:0009314	-2.519625	-0.563524336
Member_detection of light stimulus	GO:0009583	-2.496043	-0.547494718
Member_cellular response to radiation	GO:0071478	-2.400796	-0.47161895
Member_cellular response to abiotic stimulus	GO:0071214	-2.095693	-0.281344375
Member_cellular response to environmental stimulus	GO:0104004	-2.095693	-0.281344375
Summary_Cellular response to chemical stress	R-DRE-9711123	-4.621083	-2.055235445
Member_Cellular response to chemical stress	R-DRE-9711123	-4.621083	-2.055235445
Member_Cytoprotection by HMOX1	R-DRE-9707564	-4.110741	-1.602884846
Member_Cellular responses to stimuli	R-DRE-8953897	-3.487206	-1.136958102
Member_Cellular responses to stress	R-DRE-2262752	-3.346223	-1.064488773
Summary_superoxide metabolic process	GO:0006801	-4.41675	-1.880865102
Member_superoxide metabolic process	GO:0006801	-4.41675	-1.880865102
Member_superoxide anion generation	GO:0042554	-3.003403	-0.876887539
Member_RHO GTPases Activate NADPH Oxidases	R-DRE-5668599	-2.795823	-0.734397577
Member_VEGFA-VEGFR2 Pathway	R-DRE-4420097	-2.276056	-0.379337036
Member_Detoxification of Reactive Oxygen Species	R-DRE-3299685	-2.271769	-0.379337036
Member_Signaling by VEGF	R-DRE-194138	-2.201835	-0.344802477

Summary_C-type lectin receptor signaling pathway	dre04625	-4.066559	-1.576560173
Member_C-type lectin receptor signaling pathway	dre04625	-4.066559	-1.576560173
Member_Toll like receptor signaling pathway	WP1384	-2.226589	-0.349821753
Summary_ADP metabolic process	GO:0046031	-4.05175	-1.576560173
Member_ADP metabolic process	GO:0046031	-4.05175	-1.576560173
Member_purine nucleoside diphosphate metabolic process	GO:0009135	-3.994354	-1.56048195
Member_purine ribonucleoside diphosphate metabolic process	GO:0009179	-3.994354	-1.56048195
Member_ribonucleoside diphosphate metabolic process	GO:0009185	-3.831005	-1.420059066
Member_organic acid metabolic process	GO:0006082	-3.635049	-1.245292629
Member_nucleoside diphosphate metabolic process	GO:0009132	-3.584477	-1.205828947
Member_purine-containing compound catabolic process	GO:0072523	-3.549555	-1.189761518
Member_pyruvate metabolic process	GO:0006090	-3.364721	-1.067718814
Member_Glycolysis / Gluconeogenesis	dre00010	-3.307973	-1.035330075
Member_glycolytic process	GO:0006096	-3.281417	-1.02428622
Member_ADP catabolic process	GO:0046032	-3.281417	-1.02428622
Member_purine nucleoside diphosphate catabolic process	GO:0009137	-3.229525	-1.00891085
Member_purine ribonucleoside diphosphate catabolic process	GO:0009181	-3.229525	-1.00891085
Member_ribonucleoside diphosphate catabolic process	GO:0009191	-3.229525	-1.00891085
Member_carboxylic acid metabolic process	GO:0019752	-3.207982	-1.007889092
Member_oxoacid metabolic process	GO:0043436	-3.164322	-0.970860248
Member_pyridine nucleotide catabolic process	GO:0019364	-3.130188	-0.954876869
Member_pyridine-containing compound catabolic process	GO:0072526	-3.130188	-0.954876869
Member_nucleoside diphosphate catabolic process	GO:0009134	-3.082595	-0.920847675
Member_Glycolysis	R-DRE-70171	-3.019082	-0.876887539
Member_Biosynthesis of amino acids	dre01230	-3.004449	-0.876887539
Member_Glycolysis and gluconeogenesis	WP1356	-2.904575	-0.805836699
Member_ATP metabolic process	GO:0046034	-2.732653	-0.692775072

Member_purine ribonucleotide catabolic process	GO:0009154	-2.63285	-0.628444262
Member_ribonucleotide catabolic process	GO:0009261	-2.63285	-0.628444262
Member_Glucose metabolism	R-DRE-70326	-2.574362	-0.582545285
Member_purine nucleotide catabolic process	GO:0006195	-2.400796	-0.47161895
Member_purine ribonucleoside triphosphate metabolic process	GO:0009205	-2.33534	-0.416120468
Member_generation of precursor metabolites and energy	GO:0006091	-2.332216	-0.416120468
Member_purine nucleoside triphosphate metabolic process	GO:0009144	-2.243519	-0.357617997
Member_Gluconeogenesis	R-DRE-70263	-2.213608	-0.349821753
Member_nucleotide catabolic process	GO:0009166	-2.199446	-0.344802477
Member_ribonucleoside triphosphate metabolic process	GO:0009199	-2.156653	-0.313908547
Member_carbohydrate derivative catabolic process	GO:1901136	-2.099476	-0.281344375
Member_carbohydrate catabolic process	GO:0016052	-2.095693	-0.281344375
Summary_Metabolism of porphyrins	R-DRE-189445	-3.660852	-1.260629775
Member_Metabolism of porphyrins	R-DRE-189445	-3.660852	-1.260629775
Member_Heme biosynthesis	R-DRE-189451	-3.575382	-1.205828947
Member_protoporphyrinogen IX biosynthetic process	GO:0006782	-3.404862	-1.09942605
Member_protoporphyrinogen IX metabolic process	GO:0046501	-3.404862	-1.09942605
Member_Glycine, serine and threonine metabolism	dre00260	-2.862881	-0.784373656
Member_hemoglobin biosynthetic process	GO:0042541	-2.619817	-0.619647997
Member_hemoglobin metabolic process	GO:0020027	-2.541029	-0.567578934
Member_heme biosynthetic process	GO:0006783	-2.271769	-0.379337036
Member_porphyrin-containing compound biosynthetic process	GO:0006779	-2.213608	-0.349821753
Member_tetrapyrrole biosynthetic process	GO:0033014	-2.213608	-0.349821753
Summary_regulation of immune system process	GO:0002682	-3.468319	-1.127411159
Member_regulation of immune system process	GO:0002682	-3.468319	-1.127411159

Member_regulation of leukocyte migration	GO:0002685	-2.63285	-0.628444262
Member_regulation of cell adhesion	GO:0030155	-2.015124	-0.227427433
Summary_Phenylalanine and tyrosine metabolism	R-DRE-8963691	-3.404862	-1.09942605
Member_Phenylalanine and tyrosine metabolism	R-DRE-8963691	-3.404862	-1.09942605
Member_L-phenylalanine metabolic process	GO:0006558	-3.255526	-1.013372089
Member_L-phenylalanine catabolic process	GO:0006559	-3.255526	-1.013372089
Member_erythrose 4-phosphate/phosphoenolpyruvate family amino acid catabolic process	GO:1902222	-3.122785	-0.954876869
Member_tyrosine metabolic process	GO:0006570	-3.003403	-0.876887539
Member_proteinogenic amino acid catabolic process	GO:0170040	-2.400796	-0.47161895
Member_Metabolism of amino acids and derivatives	R-DRE-71291	-2.310433	-0.401230507
Member_L-amino acid catabolic process	GO:0170035	-2.282427	-0.379337036
Member_erythrose 4-phosphate/phosphoenolpyruvate family amino acid metabolic process	GO:1902221	-2.271769	-0.379337036
Member_aromatic amino acid family catabolic process	GO:0009074	-2.213608	-0.349821753
Member_small molecule catabolic process	GO:0044282	-2.208481	-0.347763202
Member_proteinogenic amino acid metabolic process	GO:0170039	-2.065212	-0.258949443
Summary_regulation of neutrophil differentiation	GO:0045658	-3.404862	-1.09942605
Member_regulation of neutrophil differentiation	GO:0045658	-3.404862	-1.09942605
Member_regulation of myeloid cell differentiation	GO:0045637	-2.862881	-0.784373656
Member_regulation of granulocyte differentiation	GO:0030852	-2.704456	-0.672413339
Member_regulation of hemopoiesis	GO:1903706	-2.703148	-0.672413339
Member_IL 4 signaling pathway	WP1376	-2.131648	-0.294733217
Member_regulation of leukocyte differentiation	GO:1902105	-2.065129	-0.258949443
Summary_Cytokine-cytokine receptor interaction	dre04060	-3.345101	-1.064488773
Member_Cytokine-cytokine receptor interaction	dre04060	-3.345101	-1.064488773
Summary_response to oxygen-containing compound	GO:1901700	-2.990798	-0.86988683

Member_response to oxygen-containing compound	GO:1901700	-2.990798	-0.86988683
Member_regulation of defense response	GO:0031347	-2.750659	-0.696694051
Member_regulation of response to external stimulus	GO:0032101	-2.698382	-0.672147613
Member_regulation of inflammatory response	GO:0050727	-2.562958	-0.575258185
Member_response to lipopolysaccharide	GO:0032496	-2.529142	-0.567578934
Member_cellular response to lipopolysaccharide	GO:0071222	-2.527506	-0.567578934
Member_cellular response to molecule of bacterial origin	GO:0071219	-2.482201	-0.537381173
Member_response to molecule of bacterial origin	GO:0002237	-2.463634	-0.522510464
Member_cellular response to biotic stimulus	GO:0071216	-2.314809	-0.40217337
Member_response to lipid	GO:0033993	-2.194862	-0.343224024
Member_cellular response to oxygen-containing compound	GO:1901701	-2.01739	-0.227427433
Summary_Apoptosis	WP1351	-2.920582	-0.810665664
Member_Apoptosis	WP1351	-2.920582	-0.810665664
Summary_vasculogenesis	GO:0001570	-2.597518	-0.601545463
Member_vasculogenesis	GO:0001570	-2.597518	-0.601545463

**Table 5: Metascape (Zhou et al., 2019) enrichment for all significant genes downregulated in CVWT/GFWT**

CVWT/GFWT DOWN (description)	Term	Log P	Log q-value
Summary_circadian regulation of gene expression	GO:0032922	-6.13752222	-2.124516368
Member_circadian regulation of gene expression	GO:0032922	-6.13752222	-2.124516368
Member_regulation of circadian rhythm	GO:0042752	-5.42126007	-1.709284216
Member_circadian rhythm	GO:0007623	-5.10913548	-1.681480859
Member_rhythmic process	GO:0048511	-5.09242672	-1.681480859
Member_entrainment of circadian clock by photoperiod	GO:0043153	-4.27867142	-1.094518848
Member_entrainment of circadian clock	GO:0009649	-4.13840888	-1.074615166
Member_response to abiotic stimulus	GO:0009628	-3.72005604	-0.834843613

Member_response to temperature stimulus	GO:0009266	-3.70172143	-0.834843613
Member_photoperiodism	GO:0009648	-3.40274684	-0.690770985
Member_response to radiation	GO:0009314	-2.54683257	-0.253530928
Member_response to light stimulus	GO:0009416	-2.47673622	-0.204093061
Member_negative regulation of RNA metabolic process	GO:0051253	-2.44169903	-0.190662973
Member_negative regulation of nucleobase-containing compound metabolic process	GO:0045934	-2.05865622	-0.009438196
Member_negative regulation of DNA-templated transcription	GO:0045892	-2.00782803	0
Member_negative regulation of RNA biosynthetic process	GO:1902679	-2.00782803	0
Summary_fatty acid metabolic process	GO:0006631	-4.89235788	-1.578322032
Member_fatty acid metabolic process	GO:0006631	-4.89235788	-1.578322032
Member_monocarboxylic acid metabolic process	GO:0032787	-3.52868595	-0.744261285
Member_carboxylic acid metabolic process	GO:0019752	-3.25772696	-0.606448946
Member_oxoacid metabolic process	GO:0043436	-3.21380716	-0.581012547
Member_organic acid metabolic process	GO:0006082	-2.87324789	-0.404310086
Member_organic acid catabolic process	GO:0016054	-2.44024083	-0.190662973
Member_carboxylic acid catabolic process	GO:0046395	-2.44024083	-0.190662973
Member_fatty acid beta-oxidation	GO:0006635	-2.41048276	-0.182568384
Member_fatty acid oxidation	GO:0019395	-2.252788	-0.091040497
Member_lipid oxidation	GO:0034440	-2.04719125	-0.002668353
Member_cellular catabolic process	GO:0044248	-2.03584116	0
Summary_Fatty acid metabolism	dre01212	-4.26242666	-1.094518848
Member_Fatty acid metabolism	dre01212	-4.26242666	-1.094518848
Member_Fatty acid elongation	dre00062	-4.13337851	-1.074615166
Member_lipid biosynthetic process	GO:0008610	-3.52681821	-0.744261285
Member_fatty acid biosynthetic process	GO:0006633	-3.04348497	-0.468486561
Member_very long-chain fatty acid metabolic process	GO:0000038	-3.03433438	-0.468486561
Member_fatty acid elongation, saturated fatty acid	GO:0019367	-2.90683072	-0.425303784

Member_fatty acid elongation, unsaturated fatty acid	GO:0019368	-2.90683072	-0.425303784
Member_fatty acid elongation, monounsaturated fatty acid	GO:0034625	-2.90683072	-0.425303784
Member_fatty acid elongation, polyunsaturated fatty acid	GO:0034626	-2.90683072	-0.425303784
Member_monocarboxylic acid biosynthetic process	GO:0072330	-2.75333908	-0.356376735
Member_small molecule biosynthetic process	GO:0044283	-2.60273787	-0.273475822
Member_fatty acid elongation	GO:0030497	-2.5526385	-0.253530928
Member_Biosynthesis of unsaturated fatty acids	dre01040	-2.54226091	-0.253530928
Member_very long-chain fatty acid biosynthetic process	GO:0042761	-2.4097707	-0.182568384
Summary_organic acid transmembrane transport	GO:1903825	-3.88839162	-0.875385766
Member_organic acid transmembrane transport	GO:1903825	-3.88839162	-0.875385766
Member_organic anion transport	GO:0015711	-3.82584372	-0.854230551
Member_Amino acid transport across the plasma membrane	R-DRE-352230	-3.4886744	-0.730941056
Member_Transport of inorganic cations/anions and amino acids/oligopeptides	R-DRE-425393	-3.30483876	-0.629660791
Member_organic acid transport	GO:0015849	-3.30024396	-0.629660791
Member_carboxylic acid transmembrane transport	GO:1905039	-3.1748522	-0.576819696
Member_Glutamate Neurotransmitter Release Cycle	R-DRE-210500	-3.01527471	-0.464666855
Member_organic cation transport	GO:0015695	-2.84029275	-0.395488622
Member_carboxylic acid transport	GO:0046942	-2.74131919	-0.356376735
Member_SLC-mediated transmembrane transport	R-DRE-425407	-2.73195866	-0.356376735
Member_amino acid transport	GO:0006865	-2.57494638	-0.260910534
Member_amino acid import across plasma membrane	GO:0089718	-2.34465603	-0.137830155
Member_neutral amino acid transport	GO:0015804	-2.32928925	-0.135827338
Member_Neurotransmitter release cycle	R-DRE-112310	-2.28317089	-0.109014126
Member_L-alpha-amino acid transmembrane transport	GO:1902475	-2.18052397	-0.070520902
Member_amino acid transmembrane transport	GO:0003333	-2.11247056	-0.04885472
Summary_monoatomic anion transport	GO:0006820	-3.77310883	-0.839284227

Member_monoatomic anion transport	GO:0006820	-3.77310883	-0.839284227
Member_inorganic anion transport	GO:0015698	-2.48725908	-0.206646987
Member_chloride transport	GO:0006821	-2.40318254	-0.182568384
Member_inorganic anion transmembrane transport	GO:0098661	-2.38766002	-0.173994716
Member_chloride transmembrane transport	GO:1902476	-2.14585626	-0.057129697
Member_monoatomic ion transport	GO:0006811	-2.08346499	-0.029500536
Summary_intracellular iron ion homeostasis	GO:0006879	-3.64864296	-0.811728369
Member_intracellular iron ion homeostasis	GO:0006879	-3.64864296	-0.811728369
Member_Ferroptosis	dre04216	-3.18845628	-0.576819696
Member_chemical homeostasis	GO:0048878	-2.66573547	-0.324827474
Member_monoatomic ion homeostasis	GO:0050801	-2.3057635	-0.125266564
Member_homeostatic process	GO:0042592	-2.23077905	-0.087014083
Member_inorganic ion homeostasis	GO:0098771	-2.19166022	-0.070520902
Member_intracellular monoatomic ion homeostasis	GO:0006873	-2.00713918	0
Member_intracellular monoatomic cation homeostasis	GO:0030003	-2.00713918	0
Member_monoatomic cation homeostasis	GO:0055080	-2.00394158	0
Summary_Complex IV assembly	R-DRE-9864848	-3.41689218	-0.690770985
Member_Complex IV assembly	R-DRE-9864848	-3.41689218	-0.690770985
Summary_modified amino acid biosynthetic process	GO:0042398	-2.9093942	-0.425303784
Member_modified amino acid biosynthetic process	GO:0042398	-2.9093942	-0.425303784
Member_modified amino acid metabolic process	GO:0006575	-2.33165339	-0.135827338
Summary_Phototransduction	dre04744	-2.84029275	-0.395488622
Member_Phototransduction	dre04744	-2.84029275	-0.395488622
Summary_neurotransmitter transport	GO:0006836	-2.81396382	-0.38074157
Member_neurotransmitter transport	GO:0006836	-2.81396382	-0.38074157
Member_regulation of neurotransmitter secretion	GO:0046928	-2.4097707	-0.182568384
Member_regulation of neurotransmitter transport	GO:0051588	-2.22495867	-0.087014083

Summary_visual perception	GO:0007601	-2.74131919	-0.356376735
Member_visual perception	GO:0007601	-2.74131919	-0.356376735
Member_sensory perception of light stimulus	GO:0050953	-2.68649434	-0.336246327
Summary_Keratinization	R-DRE-6805567	-2.71617007	-0.356376735
Member_Keratinization	R-DRE-6805567	-2.71617007	-0.356376735
Member_Formation of the cornified envelope	R-DRE-6809371	-2.71617007	-0.356376735
Summary_Hypertrophy model	WP1327	-2.71617007	-0.356376735
Member_Hypertrophy model	WP1327	-2.71617007	-0.356376735
Summary_sulfur compound metabolic process	GO:0006790	-2.59628559	-0.273475822
Member_sulfur compound metabolic process	GO:0006790	-2.59628559	-0.273475822
Member_sulfur compound biosynthetic process	GO:0044272	-2.13418848	-0.050601551
Summary_blood circulation	GO:0008015	-2.3057635	-0.125266564
Member_blood circulation	GO:0008015	-2.3057635	-0.125266564
Member_heart contraction	GO:0060047	-2.22849694	-0.087014083
Member_circulatory system process	GO:0003013	-2.20013727	-0.070520902
Member_heart process	GO:0003015	-2.15602161	-0.062093848
Summary_hormone-mediated signaling pathway	GO:0009755	-2.27135773	-0.10344992
Member_hormone-mediated signaling pathway	GO:0009755	-2.27135773	-0.10344992
Member_response to hormone	GO:0009725	-2.0877453	-0.029500536
Summary_one-carbon metabolic process	GO:0006730	-2.22495867	-0.087014083
Member_one-carbon metabolic process	GO:0006730	-2.22495867	-0.087014083
Summary_steroid biosynthetic process	GO:0006694	-2.18974455	-0.070520902
Member_steroid biosynthetic process	GO:0006694	-2.18974455	-0.070520902
Summary_skeletal myofibril assembly	GO:0014866	-2.1697129	-0.070520902
Member_skeletal myofibril assembly	GO:0014866	-2.1697129	-0.070520902
Summary_regulation of glucose metabolic process	GO:0010906	-2.1697129	-0.070520902
Member_regulation of glucose metabolic process	GO:0010906	-2.1697129	-0.070520902

**Table 6: Metascape (Zhou et al., 2019) shared upregulated microbial response**

<b>Shared Microbial Response_Up</b>	<b>Term</b>	<b>LogP</b>	<b>Log(q-value)</b>
Summary_gas transport	GO:0015669	-8.922885	-4.90987868
Member_gas transport	GO:0015669	-8.922885	-4.90987868
Member_oxygen transport	GO:0015671	-7.797163	-4.38621746
Member_reactive oxygen species metabolic process	GO:0072593	-7.015639	-3.78078489
Member_hydrogen peroxide catabolic process	GO:0042744	-6.523311	-3.48808436
Member_hydrogen peroxide metabolic process	GO:0042743	-6.133814	-3.16220059
Member_Erythrocytes take up oxygen and release carbon dioxide	R-DRE-1247673	-3.628691	-1.26889745
Member_Erythrocytes take up carbon dioxide and release oxygen	R-DRE-1237044	-3.365818	-1.08362234
Member_O2/CO2 exchange in erythrocytes	R-DRE-1480926	-3.365818	-1.08362234
Member_Transport of small molecules	R-DRE-382551	-2.465387	-0.40662354
Summary_response to hypoxia	GO:0001666	-7.880006	-4.38621746
Member_response to hypoxia	GO:0001666	-7.880006	-4.38621746
Member_response to decreased oxygen levels	GO:0036293	-7.825314	-4.38621746
Member_response to oxygen levels	GO:0070482	-7.614795	-4.30075923
Member_response to abiotic stimulus	GO:0009628	-5.292389	-2.48350278
Member_cellular response to hypoxia	GO:0071456	-5.246333	-2.4637757
Member_cellular response to decreased oxygen levels	GO:0036294	-5.114658	-2.38040564
Member_cellular response to oxygen levels	GO:0071453	-4.992742	-2.28076635
Summary_erythrocyte differentiation	GO:0030218	-6.921516	-3.75360783
Member_erythrocyte differentiation	GO:0030218	-6.921516	-3.75360783
Member_erythrocyte homeostasis	GO:0034101	-6.820019	-3.71010341
Member_myeloid cell homeostasis	GO:0002262	-6.50109	-3.48808436
Member_homeostasis of number of cells	GO:0048872	-5.737286	-2.86925601

Member_myeloid cell differentiation	GO:0030099	-5.532155	-2.69524052
Member_homeostatic process	GO:0042592	-4.318643	-1.73700135
Member_hemopoiesis	GO:0030097	-4.002697	-1.54833994
Member_multicellular organismal-level homeostasis	GO:0048871	-3.854008	-1.42078574
Member_embryonic hemopoiesis	GO:0035162	-3.710862	-1.33132446
Member_myeloid cell development	GO:0061515	-3.258626	-1.01647232
Member_erythrocyte development	GO:0048821	-2.96036	-0.78205679
Member_immune system process	GO:0002376	-2.956214	-0.78205679
Summary_cellular response to chemical stimulus	GO:0070887	-5.975689	-3.0418643
Member_cellular response to chemical stimulus	GO:0070887	-5.975689	-3.0418643
Member_cellular response to xenobiotic stimulus	GO:0071466	-4.323794	-1.73700135
Member_response to xenobiotic stimulus	GO:0009410	-4.009793	-1.54833994
Member_Arachidonate metabolism	R-DRE-2142753	-3.130461	-0.90984694
Member_Cytochrome P450 - arranged by substrate type	R-DRE-211897	-3.060039	-0.85994689
Member_Synthesis of epoxy (EET) and dihydroxyeicosatrienoic acids (DHET)	R-DRE-2142670	-2.911991	-0.74408355
Member_Biosynthesis of DHA-derived SPMs	R-DRE-9018677	-2.433406	-0.38582988
Member_Biosynthesis of specialized proresolving mediators (SPMs)	R-DRE-9018678	-2.433406	-0.38582988
Member_Phase I - Functionalization of compounds	R-DRE-211945	-2.430353	-0.38582988
Member_Biological oxidations	R-DRE-211859	-2.294388	-0.28002671
Member_xenobiotic metabolic process	GO:0006805	-2.125493	-0.1617049
Summary_Cytoprotection by HMOX1	R-DRE-9707564	-5.736134	-2.86925601
Member_Cytoprotection by HMOX1	R-DRE-9707564	-5.736134	-2.86925601
Member_Cellular response to chemical stress	R-DRE-9711123	-5.139349	-2.38161572

Member_Cellular responses to stress	R-DRE-2262752	-4.046842	-1.54833994
Member_Cellular responses to stimuli	R-DRE-8953897	-3.723964	-1.33420751
Member_TP53 Regulates Metabolic Genes	R-DRE-5628897	-2.992837	-0.7993747
Member_Aerobic respiration and respiratory electron transport	R-DRE-1428517	-2.586349	-0.49762284
Member_Respiratory electron transport	R-DRE-611105	-2.153085	-0.17750599
Summary_organic acid metabolic process	GO:0006082	-4.848242	-2.15745561
Member_organic acid metabolic process	GO:0006082	-4.848242	-2.15745561
Member_carboxylic acid metabolic process	GO:0019752	-4.031519	-1.54833994
Member_oxoacid metabolic process	GO:0043436	-3.993144	-1.54833994
Member_small molecule catabolic process	GO:0044282	-3.480514	-1.13026602
Member_proteinogenic amino acid catabolic process	GO:0170040	-2.670483	-0.56056711
Member_L-amino acid catabolic process	GO:0170035	-2.569358	-0.48949265
Member_cellular catabolic process	GO:0044248	-2.362647	-0.33191246
Member_alpha-amino acid catabolic process	GO:1901606	-2.284432	-0.28002671
Member_proteinogenic amino acid metabolic process	GO:0170039	-2.153969	-0.17750599
Member_amino acid catabolic process	GO:0009063	-2.135366	-0.16768336
Member_L-amino acid metabolic process	GO:0170033	-2.101388	-0.14907972
Member_organic acid catabolic process	GO:0016054	-2.001727	-0.08563083
Member_carboxylic acid catabolic process	GO:0046395	-2.001727	-0.08563083
Summary_Neutrophil degranulation	R-DRE-6798695	-4.731062	-2.06047871
Member_Neutrophil degranulation	R-DRE-6798695	-4.731062	-2.06047871
Member_Innate Immune System	R-DRE-168249	-3.386489	-1.08362234
Member_Immune System	R-DRE-168256	-2.4005	-0.36521814
Summary_ADP metabolic process	GO:0046031	-4.41269	-1.76141161

Member_ADP metabolic process	GO:0046031	-4.41269	-1.76141161
Member_purine nucleoside diphosphate metabolic process	GO:0009135	-4.36342	-1.74835433
Member_purine ribonucleoside diphosphate metabolic process	GO:0009179	-4.36342	-1.74835433
Member_purine-containing compound catabolic process	GO:0072523	-4.290255	-1.72440696
Member_ribonucleoside diphosphate metabolic process	GO:0009185	-4.222798	-1.68691303
Member_Glycolysis and gluconeogenesis	WP1356	-4.222798	-1.68691303
Member_Glycolysis / Gluconeogenesis	dre00010	-4.06902	-1.54833994
Member_nucleoside diphosphate metabolic process	GO:0009132	-4.009383	-1.54833994
Member_generation of precursor metabolites and energy	GO:0006091	-3.82197	-1.40688483
Member_pyruvate metabolic process	GO:0006090	-3.817831	-1.40688483
Member_Biosynthesis of amino acids	dre01230	-3.788233	-1.38801057
Member_glycolytic process	GO:0006096	-3.406988	-1.08362234
Member_ADP catabolic process	GO:0046032	-3.406988	-1.08362234
Member_purine nucleoside diphosphate catabolic process	GO:0009137	-3.364234	-1.08362234
Member_purine ribonucleoside diphosphate catabolic process	GO:0009181	-3.364234	-1.08362234
Member_ribonucleoside diphosphate catabolic process	GO:0009191	-3.364234	-1.08362234
Member_pyridine nucleotide catabolic process	GO:0019364	-3.282193	-1.02506159
Member_pyridine-containing compound catabolic process	GO:0072526	-3.282193	-1.02506159
Member_ATP metabolic process	GO:0046034	-3.258626	-1.01647232
Member_nucleoside diphosphate catabolic process	GO:0009134	-3.242791	-1.00793592
Member_purine ribonucleoside triphosphate metabolic process	GO:0009205	-2.899144	-0.73739681
Member_purine ribonucleotide catabolic process	GO:0009154	-2.867075	-0.71739173
Member_ribonucleotide catabolic process	GO:0009261	-2.867075	-0.71739173
Member_purine nucleoside triphosphate metabolic process	GO:0009144	-2.814957	-0.67118291
Member_Glycolysis	R-DRE-70171	-2.808896	-0.67095177

Member_ribonucleoside triphosphate metabolic process	GO:0009199	-2.734872	-0.60267944
Member_purine nucleotide catabolic process	GO:0006195	-2.670483	-0.56056711
Member_nucleoside triphosphate metabolic process	GO:0009141	-2.568	-0.48949265
Member_nucleotide catabolic process	GO:0009166	-2.498088	-0.42956496
Member_Glucose metabolism	R-DRE-70326	-2.469502	-0.40662354
Member_carbohydrate catabolic process	GO:0016052	-2.408507	-0.36862884
Member_nucleoside phosphate catabolic process	GO:1901292	-2.304323	-0.28254302
Member_pyridine nucleotide metabolic process	GO:0019362	-2.284432	-0.28002671
Member_nicotinamide nucleotide metabolic process	GO:0046496	-2.284432	-0.28002671
Member_pyridine-containing compound metabolic process	GO:0072524	-2.207758	-0.20758919
Member_carbohydrate metabolic process	GO:0005975	-2.197526	-0.20155331
Member_carbohydrate derivative catabolic process	GO:1901136	-2.180996	-0.18917994
Summary_regulation of erythrocyte differentiation	GO:0045646	-3.628691	-1.26889745
Member_regulation of erythrocyte differentiation	GO:0045646	-3.628691	-1.26889745
Member_regulation of hemopoiesis	GO:1903706	-3.232171	-1.00449534
Member_regulation of myeloid cell differentiation	GO:0045637	-3.060039	-0.85994689
Member_regulation of multicellular organismal development	GO:2000026	-2.34867	-0.32243544
Member_regulation of immune system process	GO:0002682	-2.147258	-0.17564439
Member_regulation of leukocyte differentiation	GO:1902105	-2.073175	-0.13571646
Member_regulation of multicellular organismal process	GO:0051239	-2.024025	-0.09737921
Summary_Metabolism of porphyrins	R-DRE-189445	-3.28948	-1.02506159
Member_Metabolism of porphyrins	R-DRE-189445	-3.28948	-1.02506159
Summary_Glycine, serine and threonine metabolism	dre00260	-3.060039	-0.85994689
Member_Glycine, serine and threonine metabolism	dre00260	-3.060039	-0.85994689

Summary_superoxide metabolic process	GO:0006801	-2.967148	-0.78205679
Member_superoxide metabolic process	GO:0006801	-2.967148	-0.78205679
Member_response to oxygen-containing compound	GO:1901700	-2.724872	-0.59835703
Summary_endothelial cell migration	GO:0043542	-2.714189	-0.59327765
Member_endothelial cell migration	GO:0043542	-2.714189	-0.59327765
Summary_transforming growth factor beta receptor signaling pathway	GO:0007179	-2.626665	-0.53273732
Member_transforming growth factor beta receptor signaling pathway	GO:0007179	-2.626665	-0.53273732
Member_response to transforming growth factor beta	GO:0071559	-2.626665	-0.53273732
Member_cellular response to transforming growth factor beta stimulus	GO:0071560	-2.626665	-0.53273732
Member_cell surface receptor protein serine/threonine kinase signaling pathway	GO:0007178	-2.171053	-0.18521764
Member_response to endogenous stimulus	GO:0009719	-2.16884	-0.18521764
Member_cellular response to growth factor stimulus	GO:0071363	-2.114353	-0.15442607
Member_response to growth factor	GO:0070848	-2.101388	-0.14907972
Member_cellular response to endogenous stimulus	GO:0071495	-2.085848	-0.13729986
Member_enzyme-linked receptor protein signaling pathway	GO:0007167	-2.010213	-0.08711181
Summary_organic hydroxy compound metabolic process	GO:1901615	-2.518539	-0.44505262
Member_organic hydroxy compound metabolic process	GO:1901615	-2.518539	-0.44505262
Summary_supramolecular fiber organization	GO:0097435	-2.077075	-0.13571646
Member_supramolecular fiber organization	GO:0097435	-2.077075	-0.13571646
Summary_phototransduction	GO:0007602	-2.073175	-0.13571646
Member_phototransduction	GO:0007602	-2.073175	-0.13571646
Summary_positive regulation of macromolecule metabolic process	GO:0010604	-2.042542	-0.10871769

Member_positive regulation of macromolecule metabolic process	GO:0010604	-2.042542	-0.10871769
Summary_defense response	GO:0006952	-2.036221	-0.10600092
Member_defense response	GO:0006952	-2.036221	-0.10600092

**Table 7: Metascape (Zhou et al., 2019) shared downregulated microbial response**

<b>Shared Microbial Response Down</b>	<b>Term</b>	<b>LogP</b>	<b>Log(q-value)</b>
Summary_intracellular iron ion homeostasis	GO:0006879	-5.162922	-1.149916365
Member_intracellular iron ion homeostasis	GO:0006879	-5.162922	-1.149916365
Member_intracellular monoatomic ion homeostasis	GO:0006873	-3.243483	-0.075574855
Member_intracellular monoatomic cation homeostasis	GO:0030003	-3.243483	-0.075574855
Member_cellular homeostasis	GO:0019725	-2.974457	0
Member_intracellular chemical homeostasis	GO:0055082	-2.951219	0
Member_Ferroptosis	dre04216	-2.774416	0
Member_monoatomic cation homeostasis	GO:0055080	-2.765476	0
Member_monoatomic ion homeostasis	GO:0050801	-2.617604	0
Member_iron ion transport	GO:0006826	-2.431303	0
Member_Necroptosis	dre04217	-2.336136	0
Member_inorganic ion homeostasis	GO:0098771	-2.259782	0
Summary_Phototransduction	dre04744	-4.303841	-0.591865137
Member_Phototransduction	dre04744	-4.303841	-0.591865137
Summary_modified amino acid biosynthetic process	GO:0042398	-4.115881	-0.579996234
Member_modified amino acid biosynthetic process	GO:0042398	-4.115881	-0.579996234
Member_modified amino acid metabolic process	GO:0006575	-3.036541	0
Summary_visual perception	GO:0007601	-3.43065	-0.075574855
Member_visual perception	GO:0007601	-3.43065	-0.075574855
Member_sensory perception of light stimulus	GO:0050953	-3.382315	-0.075574855

Member_regulation of G protein-coupled receptor signaling pathway	GO:0008277	-2.223597	0
Summary_sulfur compound metabolic process	GO:0006790	-2.850005	0
Member_sulfur compound metabolic process	GO:0006790	-2.850005	0
Summary_mitochondrial transport	GO:0006839	-2.833677	0
Member_mitochondrial transport	GO:0006839	-2.833677	0
Member_protein transmembrane import into intracellular organelle	GO:0044743	-2.607578	0
Member_protein targeting to mitochondrion	GO:0006626	-2.337463	0
Member_protein transmembrane transport	GO:0071806	-2.307869	0
Member_mitochondrial transmembrane transport	GO:1990542	-2.295771	0
Member_protein localization to mitochondrion	GO:0070585	-2.250972	0
Member_establishment of protein localization to mitochondrion	GO:0072655	-2.250972	0
Summary_small molecule biosynthetic process	GO:0044283	-2.741628	0
Member_small molecule biosynthetic process	GO:0044283	-2.741628	0
Member_fatty acid metabolic process	GO:0006631	-2.439774	0
Member_Fatty acid metabolism	dre01212	-2.410559	0
Member_Fatty acid elongation	dre00062	-2.307869	0
Summary_cellular respiration	GO:0045333	-2.569802	0
Member_cellular respiration	GO:0045333	-2.569802	0
Member_Respiratory electron transport	R-DRE-611105	-2.277569	0
Member_Aerobic respiration and respiratory electron transport	R-DRE-1428517	-2.052244	0
Summary_protein dephosphorylation	GO:0006470	-2.343753	0
Member_protein dephosphorylation	GO:0006470	-2.343753	0
Summary_carboxylic acid transmembrane transport	GO:1905039	-2.259616	0

Member_carboxylic acid transmembrane transport	GO:1905039	-2.259616	0
Member_L-alpha-amino acid transmembrane transport	GO:1902475	-2.250972	0
Member_organic acid transmembrane transport	GO:1903825	-2.224432	0
Member_L-amino acid transport	GO:0015807	-2.096249	0
Summary_chloride transport	GO:0006821	-2.224432	0
Member_chloride transport	GO:0006821	-2.224432	0
Member_chloride transmembrane transport	GO:1902476	-2.223597	0

**Table 8: Metascape (Zhou et al., 2019) enrichment for all significant genes upregulated in CVMut/GFMut**

<b>CVMut/GFMut_UP (description)</b>	<b>Term</b>	<b>Log P</b>	<b>Log(q-value)</b>
Summary_Focal adhesion	dre04510	-20.31317	-16.300165
Member_Focal adhesion	dre04510	-20.31317	-16.300165
Member_Cytoskeleton in muscle cells	dre04820	-19.77598	-16.064003
Member_ECM-receptor interaction	dre04512	-17.58459	-14.048707
Summary_organic acid metabolic process	GO:0006082	-17.45004	-14.039092
Member_organic acid metabolic process	GO:0006082	-17.45004	-14.039092
Member_carboxylic acid metabolic process	GO:0019752	-15.36579	-12.051754
Member_oxoacid metabolic process	GO:0043436	-15.13085	-11.896
Member_monocarboxylic acid metabolic process	GO:0032787	-10.18781	-7.3508917
Member_fatty acid metabolic process	GO:0006631	-2.525482	-1.0968069
Summary_cell adhesion	GO:0007155	-14.77553	-11.607622
Member_cell adhesion	GO:0007155	-14.77553	-11.607622
Member_cell-cell adhesion	GO:0098609	-2.6394	-1.1934204
Summary_muscle structure development	GO:0061061	-14.63036	-11.520444
Member_muscle structure development	GO:0061061	-14.63036	-11.520444
Member_muscle organ development	GO:0007517	-14.0598	-11.001038
Member_muscle cell differentiation	GO:0042692	-8.884606	-6.1499305
Member_skeletal muscle organ development	GO:0060538	-8.734112	-6.0221358
Member_muscle cell development	GO:0055001	-8.286662	-5.6715963

Member_striated muscle tissue development	GO:0014706	-7.847791	-5.2971834
Member_muscle tissue development	GO:0060537	-7.490255	-5.0213172
Member_skeletal muscle tissue development	GO:0007519	-6.935244	-4.5582123
Member_striated muscle cell development	GO:0055002	-4.872485	-2.9422647
Member_striated muscle cell differentiation	GO:0051146	-4.750283	-2.8478667
Member_skeletal muscle fiber development	GO:0048741	-4.22969	-2.4361307
Member_myotube cell development	GO:0014904	-4.149051	-2.3664945
Member_myotube differentiation	GO:0014902	-3.547183	-1.8805298
Summary_cell-substrate adhesion	GO:0031589	-12.44628	-9.433275
Member_cell-substrate adhesion	GO:0031589	-12.44628	-9.433275
Member_cell-matrix adhesion	GO:0007160	-8.312104	-5.6793096
Member_integrin-mediated signaling pathway	GO:0007229	-5.949566	-3.8225229
Member_cell adhesion mediated by integrin	GO:0033627	-4.351687	-2.5147727
Summary_tube morphogenesis	GO:0035239	-11.66685	-8.6952374
Member_tube morphogenesis	GO:0035239	-11.66685	-8.6952374
Member_blood vessel morphogenesis	GO:0048514	-11.27118	-8.3373585
Member_blood vessel development	GO:0001568	-10.90167	-8.0026033
Member_vasculature development	GO:0001944	-10.419	-7.5521214
Member_angiogenesis	GO:0001525	-7.568646	-5.0607897
Member_sprouting angiogenesis	GO:0002040	-6.828149	-4.4872405
Summary_small molecule catabolic process	GO:0044282	-9.762035	-6.9531493
Member_small molecule catabolic process	GO:0044282	-9.762035	-6.9531493
Member_alpha-amino acid catabolic process	GO:1901606	-8.606175	-5.915388
Member_alpha-amino acid metabolic process	GO:1901605	-8.327211	-5.6793096
Member_amino acid catabolic process	GO:0009063	-7.673506	-5.1518617
Member_cellular catabolic process	GO:0044248	-7.536545	-5.0550177
Member_Metabolism of amino acids and derivatives	R-DRE-71291	-7.301819	-4.8451158
Member_organic acid catabolic process	GO:0016054	-7.203241	-4.7812995
Member_carboxylic acid catabolic process	GO:0046395	-7.203241	-4.7812995

Member_dicarboxylic acid metabolic process	GO:0043648	-6.927765	-4.5582123
Member_L-amino acid metabolic process	GO:0170033	-6.712236	-4.4316241
Member_amino acid metabolic process	GO:0006520	-6.693868	-4.4212253
Member_proteinogenic amino acid metabolic process	GO:0170039	-5.941291	-3.8203799
Member_L-amino acid catabolic process	GO:0170035	-5.86179	-3.7572695
Member_proteinogenic amino acid catabolic process	GO:0170040	-4.947416	-3.0025958
Member_glutamate metabolic process	GO:0006536	-2.897777	-1.3808938
Summary_Regulation of actin cytoskeleton	dre04810	-9.093799	-6.3112418
Member_Regulation of actin cytoskeleton	dre04810	-9.093799	-6.3112418
Summary_enzyme-linked receptor protein signaling pathway	GO:0007167	-8.884183	-6.1499305
Member_enzyme-linked receptor protein signaling pathway	GO:0007167	-8.884183	-6.1499305
Member_cell surface receptor protein tyrosine kinase signaling pathway	GO:0007169	-8.014645	-5.4487973
Member_Calcium signaling pathway	dre04020	-4.551091	-2.690373
Member_positive regulation of cell population proliferation	GO:0008284	-4.367908	-2.5251641
Member_regulation of cell population proliferation	GO:0042127	-3.793384	-2.0830731
Member_MAPK signaling pathway	dre04010	-2.85667	-1.3566065
Member_ERK1 ERK2 MAPK cascade	WP402	-2.832137	-1.3389595
Summary_wound healing	GO:0042060	-8.385165	-5.7145816
Member_wound healing	GO:0042060	-8.385165	-5.7145816
Member_response to wounding	GO:0009611	-6.497004	-4.2763903
Member_regulation of body fluid levels	GO:0050878	-5.40655	-3.366672
Member_blood coagulation	GO:0007596	-4.662051	-2.782584
Member_hemostasis	GO:0007599	-4.662051	-2.782584
Member_coagulation	GO:0050817	-4.662051	-2.782584
Member_protein activation cascade	GO:0072376	-2.98147	-1.4441358
Member_blood coagulation, fibrin clot formation	GO:0072378	-2.98147	-1.4441358
Member_homotypic cell-cell adhesion	GO:0034109	-2.856395	-1.3566065
Member_platelet activation	GO:0030168	-2.510618	-1.0886394
Summary_Carbon metabolism	dre01200	-8.154311	-5.561075

Member_Carbon metabolism	dre01200	-8.154311	-5.561075
Member_Glycolysis / Gluconeogenesis	dre00010	-6.858821	-4.5085733
Member_carbohydrate metabolic process	GO:0005975	-6.752826	-4.4387902
Member_ribonucleoside diphosphate metabolic process	GO:0009185	-6.626047	-4.3689157
Member_pyridine nucleotide metabolic process	GO:0019362	-6.506075	-4.2783991
Member_nicotinamide nucleotide metabolic process	GO:0046496	-6.506075	-4.2783991
Member_ADP metabolic process	GO:0046031	-6.407602	-4.2075092
Member_purine nucleoside diphosphate metabolic process	GO:0009135	-6.258742	-4.0882412
Member_purine ribonucleoside diphosphate metabolic process	GO:0009179	-6.258742	-4.0882412
Member_purine-containing compound catabolic process	GO:0072523	-6.256149	-4.0882412
Member_pyridine-containing compound metabolic process	GO:0072524	-6.111431	-3.9557579
Member_pyruvate metabolic process	GO:0006090	-6.067849	-3.9181661
Member_nucleoside diphosphate metabolic process	GO:0009132	-5.949038	-3.8225229
Member_Glycolysis and gluconeogenesis	WP1356	-5.840822	-3.7416302
Member_glycolytic process	GO:0006096	-5.377743	-3.3515089
Member_ADP catabolic process	GO:0046032	-5.377743	-3.3515089
Member_Glucose metabolism	R-DRE-70326	-5.302882	-3.2811023
Member_purine nucleoside diphosphate catabolic process	GO:0009137	-5.238897	-3.2470803
Member_purine ribonucleoside diphosphate catabolic process	GO:0009181	-5.238897	-3.2470803
Member_ribonucleoside diphosphate catabolic process	GO:0009191	-5.238897	-3.2470803
Member_nucleobase-containing small molecule metabolic process	GO:0055086	-5.197687	-3.2099868
Member_purine-containing compound metabolic process	GO:0072521	-5.183866	-3.2002441
Member_carbohydrate catabolic process	GO:0016052	-5.168555	-3.188973
Member_purine ribonucleotide catabolic process	GO:0009154	-5.004375	-3.0405871
Member_ribonucleotide catabolic process	GO:0009261	-5.004375	-3.0405871
Member_pyridine nucleotide catabolic process	GO:0019364	-4.976074	-3.0275264

Member_pyridine-containing compound catabolic process	GO:0072526	-4.976074	-3.0275264
Member_generation of precursor metabolites and energy	GO:0006091	-4.900486	-2.9630269
Member_nucleoside diphosphate catabolic process	GO:0009134	-4.851531	-2.9319471
Member_Biosynthesis of amino acids	dre01230	-4.764053	-2.8582574
Member_nucleoside phosphate catabolic process	GO:1901292	-4.734046	-2.8349839
Member_Gluconeogenesis	R-DRE-70263	-4.709575	-2.8171427
Member_organophosphate catabolic process	GO:0046434	-4.623833	-2.7507059
Member_purine nucleotide catabolic process	GO:0006195	-4.31735	-2.4918645
Member_nucleotide catabolic process	GO:0009166	-4.312185	-2.4895104
Member_Glycolysis	R-DRE-70171	-4.035067	-2.2626108
Member_organophosphate metabolic process	GO:0019637	-3.909759	-2.1602926
Member_ATP metabolic process	GO:0046034	-3.254178	-1.6594735
Member_nucleoside phosphate metabolic process	GO:0006753	-3.249689	-1.6566386
Member_purine nucleotide metabolic process	GO:0006163	-3.156229	-1.5777918
Member_carbohydrate derivative catabolic process	GO:1901136	-2.902818	-1.3808938
Member_purine ribonucleoside triphosphate metabolic process	GO:0009205	-2.85027	-1.3518123
Member_Metabolism of carbohydrates	R-DRE-71387	-2.654819	-1.2005222
Member_purine nucleoside triphosphate metabolic process	GO:0009144	-2.647298	-1.1977728
Member_nucleotide metabolic process	GO:0009117	-2.640134	-1.1934204
Member_ribonucleoside triphosphate metabolic process	GO:0009199	-2.459073	-1.0502935
Member_ribonucleotide metabolic process	GO:0009259	-2.335423	-0.955886
Member_purine ribonucleotide metabolic process	GO:0009150	-2.325663	-0.9491446
Member_ribose phosphate metabolic process	GO:0019693	-2.158149	-0.8342275
Member_nucleoside triphosphate metabolic process	GO:0009141	-2.082925	-0.7817262
Summary_Glycine, serine and threonine metabolism	dre00260	-8.142717	-5.561075
Member_Glycine, serine and threonine metabolism	dre00260	-8.142717	-5.561075

Summary_Biological oxidations	R-DRE-211859	-7.826292	-5.2904076
Member_Biological oxidations	R-DRE-211859	-7.826292	-5.2904076
Member_Phase I - Functionalization of compounds	R-DRE-211945	-6.575553	-4.3259753
Member_Biosynthesis of DHA-derived SPMs	R-DRE-9018677	-5.990695	-3.8527506
Member_Biosynthesis of specialized proresolving mediators (SPMs)	R-DRE-9018678	-5.990695	-3.8527506
Member_cellular response to xenobiotic stimulus	GO:0071466	-5.704356	-3.6258486
Member_response to xenobiotic stimulus	GO:0009410	-5.40655	-3.366672
Member_Cytochrome P450 - arranged by substrate type	R-DRE-211897	-4.97843	-3.0275264
Member_xenobiotic metabolic process	GO:0006805	-4.614939	-2.7449482
Member_Biosynthesis of maresins	R-DRE-9018682	-4.409053	-2.5604003
Member_Aspirin ADME	R-DRE-9749641	-4.264117	-2.4579371
Member_Biosynthesis of maresin-like SPMs	R-DRE-9027307	-4.035067	-2.2626108
Member_Xenobiotics	R-DRE-211981	-3.868784	-2.1480343
Member_Synthesis of epoxy (EET) and dihydroxyeicosatrienoic acids (DHET)	R-DRE-2142670	-3.513276	-1.8562962
Member_Miscellaneous substrates	R-DRE-211958	-3.379185	-1.7397348
Member_Metabolism of lipids	R-DRE-556833	-2.715042	-1.2485788
Member_Arachidonate metabolism	R-DRE-2142753	-2.6267	-1.1830681
Member_CYP2E1 reactions	R-DRE-211999	-2.263271	-0.9120777
Member_Fatty acids	R-DRE-211935	-2.160979	-0.8355021
Summary_heart development	GO:0007507	-7.538567	-5.0550177
Member_heart development	GO:0007507	-7.538567	-5.0550177
Member_tissue morphogenesis	GO:0048729	-4.834553	-2.9184576
Member_morphogenesis of an epithelium	GO:0002009	-3.718352	-2.0234099
Member_epithelial tube morphogenesis	GO:0060562	-3.566633	-1.8980197
Member_heart morphogenesis	GO:0003007	-3.046601	-1.4929874

Member_embryonic heart tube development	GO:0035050	-2.282856	-0.9240267
Summary_One carbon pool by folate	dre00670	-7.250182	-4.8053774
Member_One carbon pool by folate	dre00670	-7.250182	-4.8053774
Member_one-carbon metabolic process	GO:0006730	-5.681345	-3.6128215
Member_One carbon metabolism	WP1355	-3.814146	-2.0999936
Member_tetrahydrofolate interconversion	GO:0035999	-2.70796	-1.2464045
Member_glycine biosynthetic process	GO:0006545	-2.383322	-0.9956282
Member_tetrahydrofolate metabolic process	GO:0046653	-2.362912	-0.9803339
Member_Glyoxylate and dicarboxylate metabolism	dre00630	-2.185307	-0.8562484
Member_Folate transport and metabolism	dre04981	-2.076241	-0.7784028
Summary_actin cytoskeleton organization	GO:0030036	-7.181643	-4.7706971
Member_actin cytoskeleton organization	GO:0030036	-7.181643	-4.7706971
Member_actin filament-based process	GO:0030029	-7.010625	-4.620868
Member_supramolecular fiber organization	GO:0097435	-5.58907	-3.530307
Member_cytoskeleton organization	GO:0007010	-4.822937	-2.910302
Member_actomyosin structure organization	GO:0031032	-4.597093	-2.7333067
Member_myofibril assembly	GO:0030239	-2.921519	-1.3942344
Member_cellular component assembly involved in morphogenesis	GO:0010927	-2.895589	-1.3808938
Member_cellular anatomical entity morphogenesis	GO:0032989	-2.895589	-1.3808938
Member_sarcomere organization	GO:0045214	-2.44458	-1.0368796
Summary_Arginine and proline metabolism	dre00330	-7.03478	-4.6345578
Member_Arginine and proline metabolism	dre00330	-7.03478	-4.6345578
Member_modified amino acid metabolic process	GO:0006575	-6.520049	-4.2783991
Member_phosphagen metabolic process	GO:0006599	-3.892265	-2.1602926
Member_phosphocreatine metabolic process	GO:0006603	-3.892265	-2.1602926
Member_phosphagen biosynthetic process	GO:0042396	-3.892265	-2.1602926
Member_phosphocreatine biosynthetic process	GO:0046314	-3.892265	-2.1602926

Member_modified amino acid biosynthetic process	GO:0042398	-3.008655	-1.4610316
Member_Creatine metabolism	R-DRE-71288	-2.108058	-0.8043218
Summary_cellular response to endogenous stimulus	GO:0071495	-6.903387	-4.5435937
Member_cellular response to endogenous stimulus	GO:0071495	-6.903387	-4.5435937
Member_cellular response to chemical stimulus	GO:0070887	-6.784084	-4.4612741
Member_response to endogenous stimulus	GO:0009719	-6.413762	-4.2075092
Member_cellular response to hormone stimulus	GO:0032870	-3.707743	-2.0148837
Member_response to hormone	GO:0009725	-3.368922	-1.7343141
Summary_regulation of cell migration	GO:0030334	-6.811756	-4.4799912
Member_regulation of cell migration	GO:0030334	-6.811756	-4.4799912
Member_regulation of cell motility	GO:2000145	-5.760593	-3.6718663
Member_positive regulation of cell migration	GO:0030335	-5.49357	-3.4396051
Member_regulation of locomotion	GO:0040012	-4.981992	-3.0275264
Member_positive regulation of cell motility	GO:2000147	-4.89556	-2.9617352
Member_positive regulation of locomotion	GO:0040017	-4.623833	-2.7507059
Member_positive regulation of leukocyte migration	GO:0002687	-3.889797	-2.1600925
Member_regulation of leukocyte migration	GO:0002685	-3.136839	-1.5599962
Member_positive regulation of leukocyte chemotaxis	GO:0002690	-3.061903	-1.5008938
Member_regulation of leukocyte chemotaxis	GO:0002688	-2.869688	-1.3618323
Member_positive regulation of chemotaxis	GO:0050921	-2.105491	-0.8034485
Member_regulation of neutrophil migration	GO:1902622	-2.064973	-0.7704686
Summary_aromatic amino acid family catabolic process	GO:0009074	-6.728169	-4.4326448
Member_aromatic amino acid family catabolic process	GO:0009074	-6.728169	-4.4326448
Member_aromatic amino acid metabolic process	GO:0009072	-5.624816	-3.5612002
Member_erythrose 4-phosphate/phosphoenolpyruvate family amino acid metabolic process	GO:1902221	-3.979963	-2.2246355
Member_Phenylalanine metabolism	dre00360	-3.057534	-1.5008938

Member_tyrosine metabolic process	GO:0006570	-2.856395	-1.3566065
Member_L-phenylalanine metabolic process	GO:0006558	-2.285635	-0.9248758
Member_L-phenylalanine catabolic process	GO:0006559	-2.285635	-0.9248758
Member_erythrose 4-phosphate/phosphoenolpyruvate family amino acid catabolic process	GO:1902222	-2.116615	-0.8043218
Member_Tyrosine metabolism	dre00350	-2.042705	-0.7531552

**Table 9: Metascape (Zhou et al., 2019) enrichment for significant genes downregulated in CVMut/GFMut**

<b>CVMut/GFMut_DOWN (description)</b>	<b>Term</b>	<b>Log P</b>	<b>Log(q-value)</b>
Summary_Spliceosome	dre03040	-22.913548	-18.90054227
Member_Spliceosome	dre03040	-22.913548	-18.90054227
Member_RNA splicing	GO:0008380	-18.718413	-15.00643701
Member_mRNA processing	GO:0006397	-18.49077	-14.95488554
Member_mRNA metabolic process	GO:0016071	-18.268753	-14.85780758
Member_mRNA processing	WP467	-17.490689	-14.17665342
Member_RNA splicing, via transesterification reactions	GO:0000375	-16.394064	-13.28414849
Member_RNA splicing, via transesterification reactions with bulged adenosine as nucleophile	GO:0000377	-16.394064	-13.28414849
Member_mRNA splicing, via spliceosome	GO:0000398	-16.394064	-13.28414849
Member_RNA biosynthetic process	GO:0032774	-13.935668	-10.8769044
Member_mRNA Splicing - Major Pathway	R-DRE-72163	-12.435304	-9.501479233
Member_mRNA Splicing	R-DRE-72172	-12.435304	-9.501479233
Member_Processing of Capped Intron-Containing Pre-mRNA	R-DRE-72203	-12.435304	-9.501479233
Member_RNA processing	GO:0006396	-12.376541	-9.477478528
Member_Metabolism of RNA	R-DRE-8953854	-7.7905407	-5.139262665
Summary_Nucleocytoplasmic transport	dre03013	-10.632004	-7.765126493
Member_Nucleocytoplasmic transport	dre03013	-10.632004	-7.765126493
Member_mRNA transport	GO:0051028	-8.8427784	-6.043465302
Member_nucleic acid transport	GO:0050657	-8.1960471	-5.484071242
Member_RNA transport	GO:0050658	-8.1960471	-5.484071242

Member_establishment of RNA localization	GO:0051236	-8.1960471	-5.484071242
Member_RNA localization	GO:0006403	-7.5737864	-4.940991781
Member_nuclear export	GO:0051168	-7.291735	-4.676669113
Member_RNA export from nucleus	GO:0006405	-6.2689904	-3.739848317
Member_mRNA export from nucleus	GO:0006406	-6.2614925	-3.739848317
Member_nucleocytoplasmic transport	GO:0006913	-6.2357144	-3.727858534
Member_nuclear transport	GO:0051169	-6.1509904	-3.656498483
Member_nucleobase-containing compound transport	GO:0015931	-5.0484396	-2.716675002
Member_poly(A)+ mRNA export from nucleus	GO:0016973	-2.9579669	-0.993826807
Summary_Metabolism of proteins	R-DRE-392499	-9.0276952	-6.190780627
Member_Metabolism of proteins	R-DRE-392499	-9.0276952	-6.190780627
Member_Post-translational protein modification	R-DRE-597592	-8.8260222	-6.043465302
Member_Class I MHC mediated antigen processing & presentation	R-DRE-983169	-5.371386	-2.971164055
Member_Adaptive Immune System	R-DRE-1280218	-4.3496126	-2.121936567
Member_Antigen processing: Ubiquitination & Proteasome degradation	R-DRE-983168	-3.8502525	-1.697550399
Member_Neddylaton	R-DRE-8951664	-3.100778	-1.108961474
Summary_mitochondrial respirasome assembly	GO:0097250	-7.9105623	-5.219775711
Member_mitochondrial respirasome assembly	GO:0097250	-7.9105623	-5.219775711
Member_mitochondrial respiratory chain complex assembly	GO:0033108	-7.0799871	-4.481954645
Member_cytochrome complex assembly	GO:0017004	-6.0154157	-3.533888755
Member_mitochondrion organization	GO:0007005	-5.7982176	-3.364995376
Member_mitochondrial cytochrome c oxidase assembly	GO:0033617	-3.1108073	-1.114834812
Member_respiratory chain complex IV assembly	GO:0008535	-2.9376456	-0.98909775
Summary_ribonucleoprotein complex biogenesis	GO:0022613	-7.8771886	-5.20660543
Member_ribonucleoprotein complex biogenesis	GO:0022613	-7.8771886	-5.20660543
Member_rRNA processing	GO:0006364	-3.4716107	-1.393222063
Member_ribosome biogenesis	GO:0042254	-3.3419856	-1.302107597

Member_rRNA metabolic process	GO:0016072	-3.1959149	-1.195746248
Member_Ribosome biogenesis in eukaryotes	dre03008	-2.0846823	-0.393895785
Summary_protein-containing complex assembly	GO:0065003	-6.6919226	-4.110280538
Member_protein-containing complex assembly	GO:0065003	-6.6919226	-4.110280538
Member_protein-containing complex organization	GO:0043933	-5.8079077	-3.364995376
Member_protein-RNA complex assembly	GO:0022618	-5.0218395	-2.699029711
Member_spliceosomal snRNP assembly	GO:0000387	-4.870392	-2.572732072
Member_protein-RNA complex organization	GO:0071826	-4.7599034	-2.471173448
Member_spliceosomal complex assembly	GO:0000245	-2.6495396	-0.763638593
Summary_Oxidative phosphorylation	dre00190	-6.6127225	-4.046874634
Member_Oxidative phosphorylation	dre00190	-6.6127225	-4.046874634
Member_Respiratory electron transport	R-DRE-611105	-3.8355005	-1.691726395
Member_respiratory electron transport chain	GO:0022904	-2.9576146	-0.993826807
Member_aerobic electron transport chain	GO:0019646	-2.6544105	-0.765256306
Member_mitochondrial ATP synthesis coupled electron transport	GO:0042775	-2.6544105	-0.765256306
Member_electron transport chain	GO:0022900	-2.613029	-0.751248888
Member_cellular respiration	GO:0045333	-2.5737095	-0.722897523
Member_ATP synthesis coupled electron transport	GO:0042773	-2.4622432	-0.645137041
Member_Aerobic respiration and respiratory electron transport	R-DRE-1428517	-2.458554	-0.644205276
Member_oxidative phosphorylation	GO:0006119	-2.121919	-0.421907066
Summary_Cellular responses to stress	R-DRE-2262752	-6.3130203	-3.762412454
Member_Cellular responses to stress	R-DRE-2262752	-6.3130203	-3.762412454
Member_Cellular responses to stimuli	R-DRE-8953897	-5.2093221	-2.868414112
Member_Gene expression (Transcription)	R-DRE-74160	-5.0117066	-2.697670721
Member_RNA Polymerase II Transcription	R-DRE-73857	-4.2802812	-2.066615874
Member_TP53 Regulates Metabolic Genes	R-DRE-5628897	-3.256348	-1.234568255

Member_Transcriptional Regulation by TP53	R-DRE-3700989	-2.8849414	-0.95111679
Member_Generic Transcription Pathway	R-DRE-212436	-2.5715505	-0.722897523
Summary_protein folding	GO:0006457	-5.9086606	-3.439722844
Member_protein folding	GO:0006457	-5.9086606	-3.439722844
Member_protein maturation	GO:0051604	-3.2290837	-1.224678063
Member_'de novo' protein folding	GO:0006458	-2.5517092	-0.708965076
Member_'de novo' post-translational protein folding	GO:0051084	-2.1210457	-0.421907066
Summary_Iron uptake and transport	R-DRE-917937	-5.8274906	-3.370787205
Member_Iron uptake and transport	R-DRE-917937	-5.8274906	-3.370787205
Member_Transferrin endocytosis and recycling	R-DRE-917977	-5.260296	-2.900502648
Member_Amino acids regulate mTORC1	R-DRE-9639288	-5.260296	-2.900502648
Member_Cellular response to starvation	R-DRE-9711097	-5.260296	-2.900502648
Member_Insulin receptor recycling	R-DRE-77387	-4.6141204	-2.358705616
Member_Signaling by Insulin receptor	R-DRE-74752	-4.1730477	-1.966221843
Member_ROS and RNS production in phagocytes	R-DRE-1222556	-3.6562079	-1.535296681
Member_Phagosome	dre04145	-2.500157	-0.674671901
Member_proton transmembrane transport	GO:1902600	-2.4500085	-0.638399764
Summary_Proteasome assembly	R-DRE-9907900	-5.6206256	-3.19868433
Member_Proteasome assembly	R-DRE-9907900	-5.6206256	-3.19868433
Member_Proteasome	dre03050	-3.8206111	-1.682666528
Member_Regulation of mRNA stability by proteins that bind AU-rich elements	R-DRE-450531	-2.9483676	-0.98909775
Member_Mitotic G2-G2/M phases	R-DRE-453274	-2.524526	-0.690497057
Member_G2/M Transition	R-DRE-69275	-2.524526	-0.690497057
Member_Nuclear events mediated by NFE2L2	R-DRE-9759194	-2.2037775	-0.478573418
Member_KEAP1-NFE2L2 pathway	R-DRE-9755511	-2.1890823	-0.468332522
Member_Cellular response to chemical stress	R-DRE-9711123	-2.0269799	-0.371908867
Summary_mRNA surveillance pathway	dre03015	-5.4391826	-3.028236783

Member_mRNA surveillance pathway	dre03015	-5.4391826	-3.028236783
Member_RNA catabolic process	GO:0006401	-3.4734026	-1.393222063
Member_nucleic acid catabolic process	GO:0141188	-3.044656	-1.061033912
Member_mRNA catabolic process	GO:0006402	-2.5039774	-0.67566297
Member_nuclear-transcribed mRNA catabolic process, nonsense-mediated decay	GO:0000184	-2.3036107	-0.548283463
Member_nuclear-transcribed mRNA catabolic process	GO:0000956	-2.2293757	-0.490527663
Summary_RNA polymerase II transcribes snRNA genes	R-DRE-6807505	-5.3034598	-2.9137032
Member_RNA polymerase II transcribes snRNA genes	R-DRE-6807505	-5.3034598	-2.9137032
Member_transcription by RNA polymerase II	GO:0006366	-4.4377184	-2.20232374
Member_transcription initiation at RNA polymerase II promoter	GO:0006367	-3.8054194	-1.673227112
Member_DNA-templated transcription initiation	GO:0006352	-3.4957465	-1.396554499
Member_Estrogen signaling	WP1330	-2.524526	-0.690497057
Member_DNA-templated transcription	GO:0006351	-2.4416408	-0.632754966
Member_Formation of TC-NER Pre-Incision Complex	R-DRE-6781823	-2.1210457	-0.421907066
Member_TP53 Regulates Transcription of DNA Repair Genes	R-DRE-6796648	-2.0367496	-0.379464692
Summary_Immune System	R-DRE-168256	-5.2433372	-2.893089231
Member_Immune System	R-DRE-168256	-5.2433372	-2.893089231
Member_Innate Immune System	R-DRE-168249	-2.718325	-0.809122882
Summary_establishment of protein localization	GO:0045184	-4.8697346	-2.572732072
Member_establishment of protein localization	GO:0045184	-4.8697346	-2.572732072
Member_intracellular transport	GO:0046907	-4.4371783	-2.20232374
Member_intracellular protein transport	GO:0006886	-2.8069883	-0.88034233
Summary_Mitochondrial translation elongation	R-DRE-5389840	-4.7116071	-2.438963962
Member_Mitochondrial translation elongation	R-DRE-5389840	-4.7116071	-2.438963962
Member_Mitochondrial translation termination	R-DRE-5419276	-4.7116071	-2.438963962

Member_Mitochondrial translation	R-DRE-5368287	-4.6207114	-2.358705616
Member_Translation	R-DRE-72766	-2.6367337	-0.757960296
Summary_Phototransduction	dre04744	-4.6082835	-2.358705616
Member_Phototransduction	dre04744	-4.6082835	-2.358705616
Member_Inactivation, recovery and regulation of the phototransduction cascade	R-DRE-2514859	-4.0653492	-1.871887292
Member_The phototransduction cascade	R-DRE-2514856	-3.8472334	-1.697550399
Member_Visual phototransduction	R-DRE-2187338	-3.2367427	-1.22547074
Member_Sensory Perception	R-DRE-9709957	-2.0090728	-0.357794799
Summary_Activation of BH3-only proteins	R-DRE-114452	-4.3323861	-2.111771956
Member_Activation of BH3-only proteins	R-DRE-114452	-4.3323861	-2.111771956
Member_Intrinsic Pathway for Apoptosis	R-DRE-109606	-3.4662971	-1.393222063
Member_Activation of BAD and translocation to mitochondria	R-DRE-111447	-3.4617452	-1.393222063
Member_Regulation of localization of FOXO transcription factors	R-DRE-9614399	-2.9579669	-0.993826807
Member_Apoptosis	R-DRE-109581	-2.6156451	-0.751248888
Member_FOXO-mediated transcription	R-DRE-9614085	-2.5732464	-0.722897523
Member_Programmed Cell Death	R-DRE-5357801	-2.369939	-0.589929262
Summary_protein localization to organelle	GO:0033365	-4.1413025	-1.941210047
Member_protein localization to organelle	GO:0033365	-4.1413025	-1.941210047
Member_mitochondrial transport	GO:0006839	-3.7699274	-1.643412228
Member_protein localization to mitochondrion	GO:0070585	-2.6119664	-0.751248888
Member_establishment of protein localization to mitochondrion	GO:0072655	-2.6119664	-0.751248888
Member_establishment of protein localization to organelle	GO:0072594	-2.5676353	-0.721946788
Member_mitochondrial transmembrane transport	GO:1990542	-2.5077332	-0.676570986
Summary_regulation of RNA splicing	GO:0043484	-4.023135	-1.836203964
Member_regulation of RNA splicing	GO:0043484	-4.023135	-1.836203964
Member_regulation of alternative mRNA splicing, via spliceosome	GO:0000381	-2.369939	-0.589929262

Member_regulation of mRNA splicing, via spliceosome	GO:0048024	-2.1756634	-0.459322734
---	------------	------------	--------------

### 2.2.5 *elf3* regulates gene expression in larval zebrafish independent of microbial status

Having evaluated the impact of *elf3* mutation on host response to microbiota, we next wanted to evaluate how *elf3* mutation affects gene expression beyond the microbial response. To do this, we identified *elf3*-dependent genes that are similarly differential in both the CVMut/GFMut and GFMut/GFWT comparisons. We found that 52% of *elf3*-dependent genes were up- or downregulated in both microbial conditions (Fig.4D, closed black circles in Fig.4F). This common genotypic effect included enrichment of genes involved in mRNA stability, proline metabolism, and response to cellular stress (Table 8). Conversely, pyruvate and glycerophospholipid metabolic pathways along with mucins and mucin-associated genes (*muc13a*, *muc5e*, and *mucms1*) were downregulated independent of microbial status in *elf3* mutants. We also identified defense response genes (*irg1l*, *nos2a*, *crp7*) among the shared downregulated genes, indicating potential immunologic roles for *elf3* independent of microbial stimulation. Together, these results uncover diverse *elf3*-dependent transcriptional programs in zebrafish larvae.

**Table 10: Metascape (Zhou et al., 2019) enrichment upregulated genotypic response**

<b>Shared genotype response Upregulated in CVMut/CVWT and GFMut/GFWT</b>	<b>Term</b>	<b>LogP</b>	<b>Log(q-value)</b>
Summary_Regulation of mRNA stability by proteins that bind AU-rich elements	R-DRE-450531	-4.48202323	-0.46901738
Member_Regulation of mRNA stability by proteins that bind AU-rich elements	R-DRE-450531	-4.48202323	-0.46901738
Member_KEAP1-NFE2L2 pathway	R-DRE-9755511	-4.00670694	-0.33467607
Member_Class I MHC mediated antigen processing & presentation	R-DRE-983169	-3.51518332	-0.33467607
Member_Neddylaton	R-DRE-8951664	-3.5114984	-0.33467607
Member_Assembly of the pre-replicative complex	R-DRE-68867	-3.47432511	-0.33467607
Member_DNA Replication Pre-Initiation	R-DRE-69002	-3.47432511	-0.33467607
Member_Regulation of PTEN stability and activity	R-DRE-8948751	-3.38260464	-0.33467607
Member_Antigen processing: Ubiquitination & Proteasome degradation	R-DRE-983168	-3.34547961	-0.33467607
Member_DNA Replication	R-DRE-69306	-3.25466982	-0.33467607
Member_Proteasome assembly	R-DRE-9907900	-3.25466982	-0.33467607
Member_Cellular responses to stress	R-DRE-2262752	-3.22612135	-0.33467607
Member_Cellular response to chemical stress	R-DRE-9711123	-3.20473837	-0.33467607
Member_Adaptive Immune System	R-DRE-1280218	-3.20155389	-0.33467607
Member_Deubiquitination	R-DRE-5688426	-3.16417095	-0.32725636
Member_Cyclin E associated events during G1/S transition	R-DRE-69202	-3.06312155	-0.25423568
Member_Cyclin A:Cdk2-associated events at S phase entry	R-DRE-69656	-3.0276197	-0.24506277
Member_Antigen processing-Cross presentation	R-DRE-1236975	-2.95909997	-0.23522609
Member_PTEN Regulation	R-DRE-6807070	-2.95909997	-0.23522609
Member_Cellular responses to stimuli	R-DRE-8953897	-2.9469402	-0.23522609
Member_G1/S Transition	R-DRE-69206	-2.92601264	-0.23522609
Member_S Phase	R-DRE-69242	-2.7710928	-0.12340987
Member_ubiquitin-dependent protein catabolic process	GO:0006511	-2.76701094	-0.12340987
Member_Ub-specific processing proteases	R-DRE-5689880	-2.75620448	-0.12340987
Member_Proteasome	dre03050	-2.71354701	-0.11103028

Member_modification-dependent protein catabolic process	GO:0019941	-2.68679106	-0.10514898
Member_modification-dependent macromolecule catabolic process	GO:0043632	-2.66934319	-0.10349537
Member_Activation of NF-kappaB in B cells	R-DRE-1169091	-2.53426018	-0.08585798
Member_Degradation of GLI1 by the proteasome	R-DRE-5610780	-2.53426018	-0.08585798
Member_Mitotic G1 phase and G1/S transition	R-DRE-453279	-2.52892788	-0.08585798
Member_Metabolism of amino acids and derivatives	R-DRE-71291	-2.52501461	-0.08585798
Member_Cross-presentation of soluble exogenous antigens (endosomes)	R-DRE-1236978	-2.49445524	-0.08585798
Member_Autodegradation of the E3 ubiquitin ligase COP1	R-DRE-349425	-2.49445524	-0.08585798
Member_Regulation of ornithine decarboxylase (ODC)	R-DRE-350562	-2.49445524	-0.08585798
Member_Stabilization of p53	R-DRE-69541	-2.49445524	-0.08585798
Member_Ubiquitin-dependent degradation of Cyclin D	R-DRE-75815	-2.49445524	-0.08585798
Member_RUNX1 regulates transcription of genes involved in differentiation of HSCs	R-DRE-8939236	-2.49445524	-0.08585798
Member_Degradation of AXIN	R-DRE-4641257	-2.45600828	-0.08585798
Member_The role of GTSE1 in G2/M progression after G2 checkpoint	R-DRE-8852276	-2.45600828	-0.08585798
Member_Downstream signaling events of B Cell Receptor (BCR)	R-DRE-1168372	-2.41883546	-0.08585798
Member_AUF1 (hnRNP D0) binds and destabilizes mRNA	R-DRE-450408	-2.41883546	-0.08585798
Member_Regulation of RUNX2 expression and activity	R-DRE-8939902	-2.41883546	-0.08585798
Member_GSK3B and BTRC:CUL1-mediated-degradation of NFE2L2	R-DRE-9762114	-2.41883546	-0.08585798
Member_Degradation of DVL	R-DRE-4641258	-2.38286048	-0.08585798
Member_UCH proteinases	R-DRE-5689603	-2.38286048	-0.08585798
Member_CDK-mediated phosphorylation and removal of Cdc6	R-DRE-69017	-2.38286048	-0.08585798
Member_Switching of origins to a post-replicative state	R-DRE-69052	-2.38286048	-0.08585798
Member_Synthesis of DNA	R-DRE-69239	-2.38286048	-0.08585798
Member_Regulation of RUNX3 expression and activity	R-DRE-8941858	-2.38286048	-0.08585798
Member_Nuclear events mediated by NFE2L2	R-DRE-9759194	-2.38286048	-0.08585798

Member_FBXL7 down-regulates AURKA during mitotic entry and in early mitosis	R-DRE-8854050	-2.34801369	-0.0674016
Member_p53-Dependent G1 DNA Damage Response	R-DRE-69563	-2.31423133	-0.06465347
Member_p53-Dependent G1/S DNA damage checkpoint	R-DRE-69580	-2.31423133	-0.06465347
Member_G1/S DNA Damage Checkpoints	R-DRE-69615	-2.31423133	-0.06465347
Member_Transcriptional regulation by RUNX3	R-DRE-8878159	-2.31423133	-0.06465347
Member_Metabolism of polyamines	R-DRE-351202	-2.2814549	-0.05377888
Member_GLI3 is processed to GLI3R by the proteasome	R-DRE-5610785	-2.2814549	-0.05377888
Member_Signaling by the B Cell Receptor (BCR)	R-DRE-983705	-2.2814549	-0.05377888
Member_Transcriptional regulation by RUNX2	R-DRE-8878166	-2.24963059	-0.03596528
Member_SCF(Skp2)-mediated degradation of p27/p21	R-DRE-187577	-2.18864365	0
Member_Hedgehog ligand biogenesis	R-DRE-5358346	-2.18864365	0
Member_Asymmetric localization of PCP proteins	R-DRE-4608870	-2.13091676	0
Member_proteolysis involved in protein catabolic process	GO:0051603	-2.10716772	0
Member_G2/M Checkpoints	R-DRE-69481	-2.10317906	0
Member_Hedgehog 'on' state	R-DRE-5632684	-2.07614561	0
Member_TCF dependent signaling in response to WNT	R-DRE-201681	-2.02177326	0
Member_protein catabolic process	GO:0030163	-2.01649833	0
Member_Transcriptional regulation by RUNX1	R-DRE-8878171	-2.00511646	0
Summary_proline metabolic process	GO:0006560	-3.67735539	-0.33467607
Member_proline metabolic process	GO:0006560	-3.67735539	-0.33467607
Member_Arginine and proline metabolism	dre00330	-2.45678835	-0.08585798
Summary_regulation of cilium assembly	GO:1902017	-2.70906278	-0.11103028
Member_regulation of cilium assembly	GO:1902017	-2.70906278	-0.11103028
Member_photoreceptor cell development	GO:0042461	-2.05577029	0
Summary_cellular response to stress	GO:0033554	-2.35591349	-0.0674016
Member_cellular response to stress	GO:0033554	-2.35591349	-0.0674016
Member_DNA damage response	GO:0006974	-2.27325443	-0.05264027
Member_DNA repair	GO:0006281	-2.05278262	0

Summary_protein-containing complex localization	GO:0031503	-2.18253225	0
Member_protein-containing complex localization	GO:0031503	-2.18253225	0
Summary_Arachidonate metabolism	R-DRE-2142753	-2.04978467	0
Member_Arachidonate metabolism	R-DRE-2142753	-2.04978467	0

**Table 11: Metascape (Zhou et al., 2019) enrichment for downregulated genotypic response**

<b>Downregulated in CVMut/CVWT and GFMut/GFWT</b>	<b>Term</b>	<b>LogP</b>	<b>Log(q-value)</b>
Summary_Pyruvate metabolism	dre00620	-2.681571	0
Member_Pyruvate metabolism	dre00620	-2.681571	0
Summary_glycerophospholipid biosynthetic process	GO:0046474	-2.608686	0
Member_glycerophospholipid biosynthetic process	GO:0046474	-2.608686	0
Member_glycerolipid biosynthetic process	GO:0045017	-2.438718	0
Member_phosphatidylinositol phosphate biosynthetic process	GO:0046854	-2.425476	0
Member_phospholipid biosynthetic process	GO:0008654	-2.176605	0
Member_lipid biosynthetic process	GO:0008610	-2.149296	0
Member_Phosphatidylinositol signaling system	dre04070	-2.11776	0
Summary_regulation of cell shape	GO:0008360	-2.516644	0
Member_regulation of cell shape	GO:0008360	-2.516644	0
Member_regulation of neurogenesis	GO:0050767	-2.285668	0
Member_positive regulation of cell development	GO:0010720	-2.279603	0
Member_regulation of cell morphogenesis	GO:0022604	-2.175305	0
Summary_defense response	GO:0006952	-2.228793	0
Member_defense response	GO:0006952	-2.228793	0

## 2.2.6 Interaction genes integrate microbial status and *elf3*-genotype

After examining the separate effects of microbial status and *elf3* genotype on the larval transcriptome, we investigated the effects of interactions between both variables on gene

expression. For example, transcription factor *stat4* is downregulated in mutants and fails to be microbially induced at a magnitude comparable to WT (Fig.6A), suggesting its expression results from the integration of both genotypic and microbial information. When we compared the overlap of up- and down-regulated genes for each of our 4 RNA-seq comparisons, we noted strong overlap (43%) between genes upregulated in the CVWT/GFWT comparison and those downregulated in the CVMut/GFMut comparison (Fig.6B). This overlap, which is representative of genes like *stat4*, was consistent with our functional enrichment analysis (Fig.2D). In contrast, there was less (28%) overlap between the genes downregulated in the CVWT/GFWT comparison and those upregulated in CVMut/CVWT (Fig.6B). These data support the predictions of our functional genomic meta-analyses (Fig.1) that *elf3* is preferentially required for microbially induced responses.

As a more stringent approach to interrogate interactions between *elf3* genotype and microbial status, we generated likelihood ratio test (LRT) data for our RNA-seq (Lickwar et al., 2022; Love et al., 2014). This LRT analysis identified several gene expression patterns that have either a negative or positive interaction  $\log_2$  fold change that describes how the genes behave across our four conditions (Fig. 6C, Fig.6D). Immune processes like cytokine signaling and MHC class I antigen presentation were enriched in the negative  $\log_2$  fold change interaction gene signature (Table 12). In fact, approximately 20% of this interaction signature can be classified as putative immune response genes (Fig.6C). Closer inspection of immune gene expression across all 4 conditions revealed 3 major patterns. The first pattern consisted of immune genes that are induced by microbiota in WT but not *elf3* mutants like *stat4* and other immune responsive transcription factors (*irf1b* and *irf1a*) as well as mediators of cytokine signaling (*il17rel*, *il20ra*, *soc3b*) (Fig.6E). Notably, we also identified ETS TF *ehf*, which has emerging roles in inflammation and immune response (Oyelakin et al., 2022; Wu et al., 2008), in this pattern (Fig.6F). The second pattern identified immune genes that failed to be microbially induced in *elf3*

mutants but exhibited high expression in GF mutants. The *elf3* gene fell into this category, suggesting that *elf3* might regulate its own expression in addition to expression of immune regulators like IRF TFs (*irf9* and *irf10*) and genes important for viral responses (*mxr*) (Fig.6F). Lastly, we also observed immune genes like *sting1*, *ifi35*, and *malt3* (Ge et al., 2015; Levraud et al., 2019) that were significantly downregulated in mutants in CV conditions despite not being significantly upregulated by microbiota in WT larvae. Together, these data indicate that *elf3* mutants have an attenuated immune response to microbial colonization. Interestingly, the positive log2 fold change interaction (96 out of total 393 genes) signature revealed upregulation of intermediate filament and extracellular matrix components specifically in mutants under CV conditions (Table 13) suggesting that these components might be compensatory for the blunted immune response.

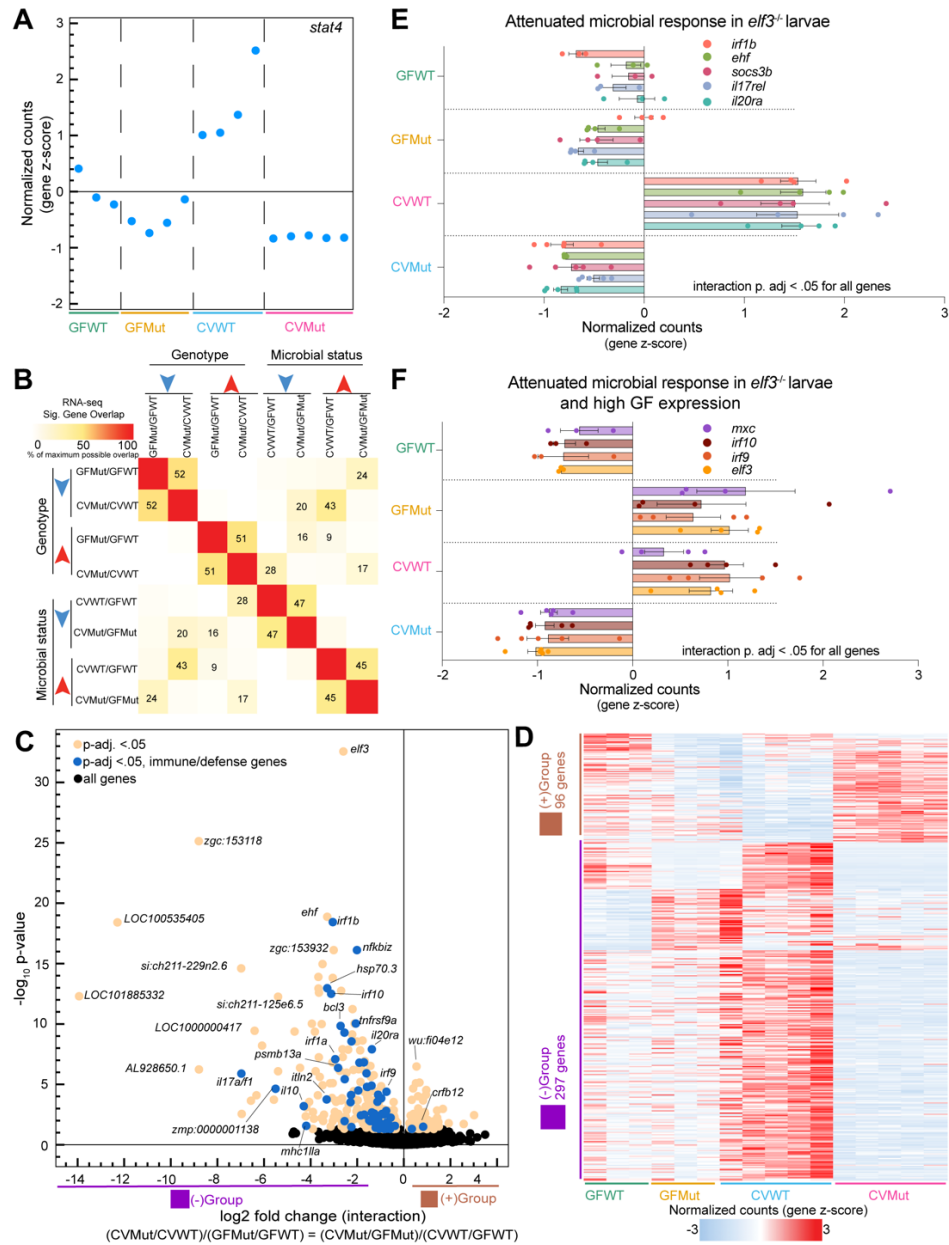


**Figure 6: Identification of interaction genes that integrate *elf3* genotype and microbial status.** (A) Plot of the z-scored normalized counts for significant interaction gene *stat4* where each dot represents 1 replicate for the indicated experimental condition (P adjusted <.05). (B) Pairwise comparisons of maximum possible overlap between the significant up-or-downregulated genes for each of the 4 RNA-seq comparisons. (C) Volcano plot depicting the  $\log_2$  fold change (x-axis) vs.  $-\log_{10}$  p-value (y-axis) for significant interaction genes identified via likelihood ratio test (LRT) analysis (P adjusted <.05). (D) Heatmap of the z-scored normalized counts for all significant interaction genes. Out of a total of 393 genes, 96 genes have a positive  $\log_2$ FC and 297 genes have a negative  $\log_2$ FC (P adjusted <.05). (E) Bar plot of the z-scored normalized counts for genes representative of the attenuated microbial response in *elf3* mutant larval. All depicted genes are significant interaction genes (P adjusted <.05). (F) Bar plot of the z-scored normalized counts for example immune response genes that fail to be microbially induced in *elf3* mutant larval at a magnitude comparable to wild-type and additionally exhibit high expression in GF conditions. All depicted genes are significant interaction genes (P adjusted <.05).

**Table 12: Metascape (Zhou et al., 2019) negative log<sub>2</sub>FC interaction**

<b>negative log<sub>2</sub>FC (description)</b>	<b>Term</b>	<b>LogP</b>	<b>Log(q-value)</b>
Summary_immune system process	GO:0002376	-11.32902	-7.316016343
Member_immune system process	GO:0002376	-11.32902	-7.316016343
Member_biological process involved in interspecies interaction between organisms	GO:0044419	-9.884043	-6.172067363
Member_response to external biotic stimulus	GO:0043207	-9.124343	-5.724295477
Member_response to other organism	GO:0051707	-9.124343	-5.724295477
Member_response to biotic stimulus	GO:0009607	-9.038331	-5.724295477
Member_response to bacterium	GO:0009617	-6.903142	-3.793226436
Member_response to external stimulus	GO:0009605	-6.511313	-3.49830671
Member_defense response	GO:0006952	-5.916525	-3.017462588
Member_immune response	GO:0006955	-5.249651	-2.467094412
Member_defense response to bacterium	GO:0042742	-5.217497	-2.459763317
Member_defense response to other organism	GO:0098542	-4.979939	-2.245687241
Member_regulation of inflammatory response	GO:0050727	-4.26647	-1.684827731
Member_regulation of defense response	GO:0031347	-3.779185	-1.243300479
Member_regulation of response to stress	GO:0080134	-2.931608	-0.608798541
Member_defense response to symbiont	GO:0140546	-2.911994	-0.606558329
Member_regulation of response to external stimulus	GO:0032101	-2.856356	-0.583713237
Member_innate immune response	GO:0045087	-2.077078	0
Summary_Antigen Presentation: Folding, assembly and peptide loading of class I MHC	R-DRE-983170	-7.790317	-4.555462625
Member_Antigen Presentation: Folding, assembly and peptide loading of class I MHC	R-DRE-983170	-7.790317	-4.555462625
Member_Class I MHC mediated antigen processing & presentation	R-DRE-983169	-6.048658	-3.114833262
Member_Immune System	R-DRE-168256	-5.481414	-2.614535802
Member_antigen processing and presentation of peptide antigen via MHC class I	GO:0002474	-5.426288	-2.589373475

Member_Adaptive Immune System	R-DRE-1280218	-4.76188	-2.078150972
Member_antigen processing and presentation of peptide antigen	GO:0048002	-4.748734	-2.078150972
Member_ER-Phagosome pathway	R-DRE-1236974	-4.358732	-1.760699721
Member_Endosomal/Vacuolar pathway	R-DRE-1236977	-4.358732	-1.760699721
Member_antigen processing and presentation	GO:0019882	-4.137209	-1.571361541
Member_Antigen processing-Cross presentation	R-DRE-1236975	-3.353011	-0.942065259
Member_Innate Immune System	R-DRE-168249	-2.973293	-0.63250161
Member_Neutrophil degranulation	R-DRE-6798695	-2.754517	-0.51966212
Member_positive regulation of cell adhesion	GO:0045785	-2.038833	0
Summary_Herpes simplex virus 1 infection	dre05168	-7.534102	-4.366193769
Member_Herpes simplex virus 1 infection	dre05168	-7.534102	-4.366193769
Member_Cytosolic DNA-sensing pathway	dre04623	-2.814586	-0.55745508
Member_NOD-like receptor signaling pathway	dre04621	-2.758256	-0.51966212
Summary_Proteasome	dre03050	-6.73885	-3.680086312
Member_Proteasome	dre03050	-6.73885	-3.680086312
Member_Proteasome assembly	R-DRE-9907900	-6.310617	-3.33900346
Member_Post-translational protein modification	R-DRE-597592	-2.688498	-0.460822294
Member_proteasomal protein catabolic process	GO:0010498	-2.434015	-0.24708436
Summary_C-type lectin receptor signaling pathway	dre04625	-5.302595	-2.493709334
Member_C-type lectin receptor signaling pathway	dre04625	-5.302595	-2.493709334
Summary_reactive oxygen species metabolic process	GO:0072593	-4.832123	-2.120147625
Member_reactive oxygen species metabolic process	GO:0072593	-4.832123	-2.120147625
Member_gas transport	GO:0015669	-4.591491	-1.940212678
Member_Erythrocytes take up oxygen and release carbon dioxide	R-DRE-1247673	-3.886099	-1.335491193
Member_hydrogen peroxide catabolic process	GO:0042744	-3.621649	-1.152711086
Member_Erythrocytes take up carbon dioxide and release oxygen	R-DRE-1237044	-3.621649	-1.152711086
Member_O <sub>2</sub> /CO <sub>2</sub> exchange in erythrocytes	R-DRE-1480926	-3.621649	-1.152711086

Member_oxygen transport	GO:0015671	-3.404204	-0.982262327
Member_hydrogen peroxide metabolic process	GO:0042743	-3.404204	-0.982262327
Summary_nucleotide-sugar metabolic process	GO:0009225	-4.518225	-1.885430649
Member_nucleotide-sugar metabolic process	GO:0009225	-4.518225	-1.885430649
Member_nucleotide-sugar biosynthetic process	GO:0009226	-3.621649	-1.152711086
Member_Biosynthesis of nucleotide sugars	dre01250	-3.459081	-1.014277292
Member_Amino sugar and nucleotide sugar metabolism	dre00520	-2.862782	-0.583713237
Summary_Cytokine-cytokine receptor interaction	dre04060	-3.672899	-1.152711086
Member_Cytokine-cytokine receptor interaction	dre04060	-3.672899	-1.152711086
Summary_response to virus	GO:0009615	-3.478296	-1.021592237
Member_response to virus	GO:0009615	-3.478296	-1.021592237
Member_Apoptosis	WP1351	-2.791083	-0.541505291
Summary_positive regulation of neuron apoptotic process	GO:0043525	-3.339572	-0.939350152
Member_positive regulation of neuron apoptotic process	GO:0043525	-3.339572	-0.939350152
Member_regulation of neuron apoptotic process	GO:0043523	-2.964294	-0.63250161
Summary_cytokine-mediated signaling pathway	GO:0019221	-3.163297	-0.77353999
Member_cytokine-mediated signaling pathway	GO:0019221	-3.163297	-0.77353999
Member_cellular response to cytokine stimulus	GO:0071345	-3.044007	-0.684213529
Member_response to cytokine	GO:0034097	-2.862142	-0.583713237
Member_response to peptide	GO:1901652	-2.862142	-0.583713237
Member_Signaling by Interleukins	R-DRE-449147	-2.442061	-0.248599057
Summary_response to lipopolysaccharide	GO:0032496	-3.102012	-0.722474714
Member_response to lipopolysaccharide	GO:0032496	-3.102012	-0.722474714
Member_response to molecule of bacterial origin	GO:0002237	-3.045365	-0.684213529
Member_cellular response to lipopolysaccharide	GO:0071222	-2.679849	-0.459235204
Member_cellular response to molecule of bacterial origin	GO:0071219	-2.644365	-0.430699409
Member_cellular response to biotic stimulus	GO:0071216	-2.512514	-0.312421365

Member_response to lipid	GO:0033993	-2.207137	-0.032980177
Summary_chaperone cofactor-dependent protein refolding	GO:0051085	-2.964266	-0.63250161
Member_chaperone cofactor-dependent protein refolding	GO:0051085	-2.964266	-0.63250161
Member_'de novo' post-translational protein folding	GO:0051084	-2.919151	-0.606558329
Member_'de novo' protein folding	GO:0006458	-2.833806	-0.568988161
Member_chaperone-mediated protein folding	GO:0061077	-2.609945	-0.40311916
Member_protein folding	GO:0006457	-2.312883	-0.132385684

**Table 13: Metascape (Zhou et al., 2019) positive log<sub>2</sub>FC Interaction Genes**

<b>positive log<sub>2</sub>FC (description)</b>	<b>Term</b>	<b>LogP</b>	<b>Log(q-value)</b>
Summary_intermediate filament-based process	GO:0045103	-3.566803	0
Member_intermediate filament-based process	GO:0045103	-3.566803	0
Member_intermediate filament cytoskeleton organization	GO:0045104	-3.566803	0
Member_wound healing	GO:0042060	-2.54381	0
Member_response to wounding	GO:0009611	-2.028539	0
Summary_striated muscle tissue development	GO:0014706	-3.242155	0
Member_striated muscle tissue development	GO:0014706	-3.242155	0
Member_muscle tissue development	GO:0060537	-3.189267	0
Member_muscle structure development	GO:0061061	-2.985631	0
Member_muscle cell differentiation	GO:0042692	-2.931658	0
Member_striated muscle cell development	GO:0055002	-2.677205	0
Member_positive regulation of transcription by RNA polymerase II	GO:0045944	-2.576577	0
Member_Adipogenesis	WP1331	-2.530511	0
Member_myofibril assembly	GO:0030239	-2.478823	0
Member_striated muscle cell differentiation	GO:0051146	-2.44626	0
Member_muscle cell development	GO:0055001	-2.379571	0
Member_cellular component assembly involved in morphogenesis	GO:0010927	-2.370528	0
Member_cellular anatomical entity morphogenesis	GO:0032989	-2.370528	0
Member_actomyosin structure organization	GO:0031032	-2.181278	0
Member_supramolecular fiber organization	GO:0097435	-2.16179	0
Member_skeletal muscle tissue development	GO:0007519	-2.07999	0
Member_positive regulation of macromolecule biosynthetic process	GO:0010557	-2.002798	0
Summary_Transport of inorganic cations/anions and amino acids/oligopeptides	R-DRE-425393	-3.099589	0
Member_Transport of inorganic cations/anions and amino acids/oligopeptides	R-DRE-425393	-3.099589	0

Member_SLC-mediated transmembrane transport	R-DRE-425407	-2.115726	0
Summary_negative regulation of RNA metabolic process	GO:0051253	-3.095561	0
Member_negative regulation of RNA metabolic process	GO:0051253	-3.095561	0
Member_negative regulation of nucleobase-containing compound metabolic process	GO:0045934	-2.864951	0
Member_negative regulation of DNA-templated transcription	GO:0045892	-2.505947	0
Member_negative regulation of RNA biosynthetic process	GO:1902679	-2.505947	0
Summary_extracellular matrix organization	GO:0030198	-2.900055	0
Member_extracellular matrix organization	GO:0030198	-2.900055	0
Member_extracellular structure organization	GO:0043062	-2.900055	0
Member_external encapsulating structure organization	GO:0045229	-2.889613	0
Summary_monoatomic anion transport	GO:0006820	-2.261394	0
Member_monoatomic anion transport	GO:0006820	-2.261394	0

**Table 14: Identification of Interaction Immune Genes**

	<b>Gene Symbol</b>
<b>negative log<sub>2</sub> fold change interaction term</b>	psmb9a
	il10
	irak3
	il13
	stat4
	socs3b
	il20ra
	il22ra2
	casp8l2
	mxr
	atf3
	tnfrsf1a
	irf1b
	tmem173
	il17a/f1
	il22
	il17ra1a
	tnfrsf9a
	cc119b
	casp8
	malt2
	irf9
	bc13
	malt3
	tapbp.1
	calr3a
	b2m
	casp3b
	mhc1zba
	tap1
	gbp1
	gbp2
	psmb8a
	psmb12
	caspb
	mpeg1.2

	irf10
	irf8
	irf1a
	zmp:0000001138
	itln2
	etv7
	tapbpl
	mhc1lla
	rbpms
	mpx
	npsn
	hspa5
	psmb13a
	uba7
	lonrf11
	hsp70.3
	hbbe2
	lyz
	agr2
	il17rel
	excl18a.1
	nfkbiz
	irf2
	psme1
	psme2
	psmb10
<b>positive log<sub>2</sub> fold change interaction term</b>	crfb12
	prlra

### 2.2.7 Mapping differentially expressed genes in larval zebrafish to cell-type specificity

Since the bulk RNA-seq data captured responses throughout the whole larvae, we sought to identify the cellular origins of the gene expression differences. To do this, we performed hierarchal clustering of all differentially expressed genes in the RNA-seq data and previously annotated cell-specific marker genes (Massaquoi et al., 2023) (Fig.7A). This analysis revealed that many of the genes differentially expressed as a function of microbial status and *elf3* genotype

are also strongly expressed by distinct cell types (Fig.7B-F, Fig.8A-B, Fig.9C-E). For example, *elf3* genotype had significant effects on the expression of pancreatic marker genes (Fig. 7D). We found pancreatic marker genes like *cel.1*, *cel.2*, and *cpa1* that were upregulated in mutants in both microbial conditions (Fig. 7D). This is interesting since previous work reveals that Elf3 expression levels in the pancreatic epithelium increase during development from embryonic days E12.5 to E18.5 in mice (Kobberup et al., 2007), and *elf3* regulates epithelial identity genes in a pancreatic adenocarcinoma cell line (CFPAC-1) (Diaferia et al., 2016). Microbial independent roles for Elf3 in epithelial tissue development is supported by the literature (Flentjar et al., 2007; Ng et al., 2002; Yoshida et al., 2000).

We also found microbially responsive transcriptional programs associated with specific cell types like the intestine and neurons that are unique to the *elf3* mutant genotype. We identified several genes that were specifically downregulated in mutants in GF conditions that were also marker genes for digestive tissues like the intestine (*apoea*, *cldn15a*, and *vill*) and liver (*f2* and *c8a*) (Fig.7B-C). Conversely, neuronal marker genes like *eno2*, *nrsn1*, and *sox4a* were downregulated in the CVMut condition (Fig. 9E).

Finally, we looked for cell-specific marker genes that followed the same gene expression pattern as the attenuated immune response we observed in colonized *elf3* mutants. Red blood cell (RBC) and immune cell marker genes followed this pattern (Fig.8E-F). We observed blunted induction of RBC (*hbbe1.1*, *hbbe1.3*, *hbbe2*) and leukocyte (*lcp1*, *coro1a*, *ikzf1*) marker genes (Table 4). We also found that several highly specific neutrophil marker genes (*lyz*, *npsn*, *mpx*, and *mmp13a*) were microbially induced in WT but not mutant larvae (Fig.8F). These data taken together suggest that *elf3* function regulates specific aspects of the hematopoietic response to colonization.

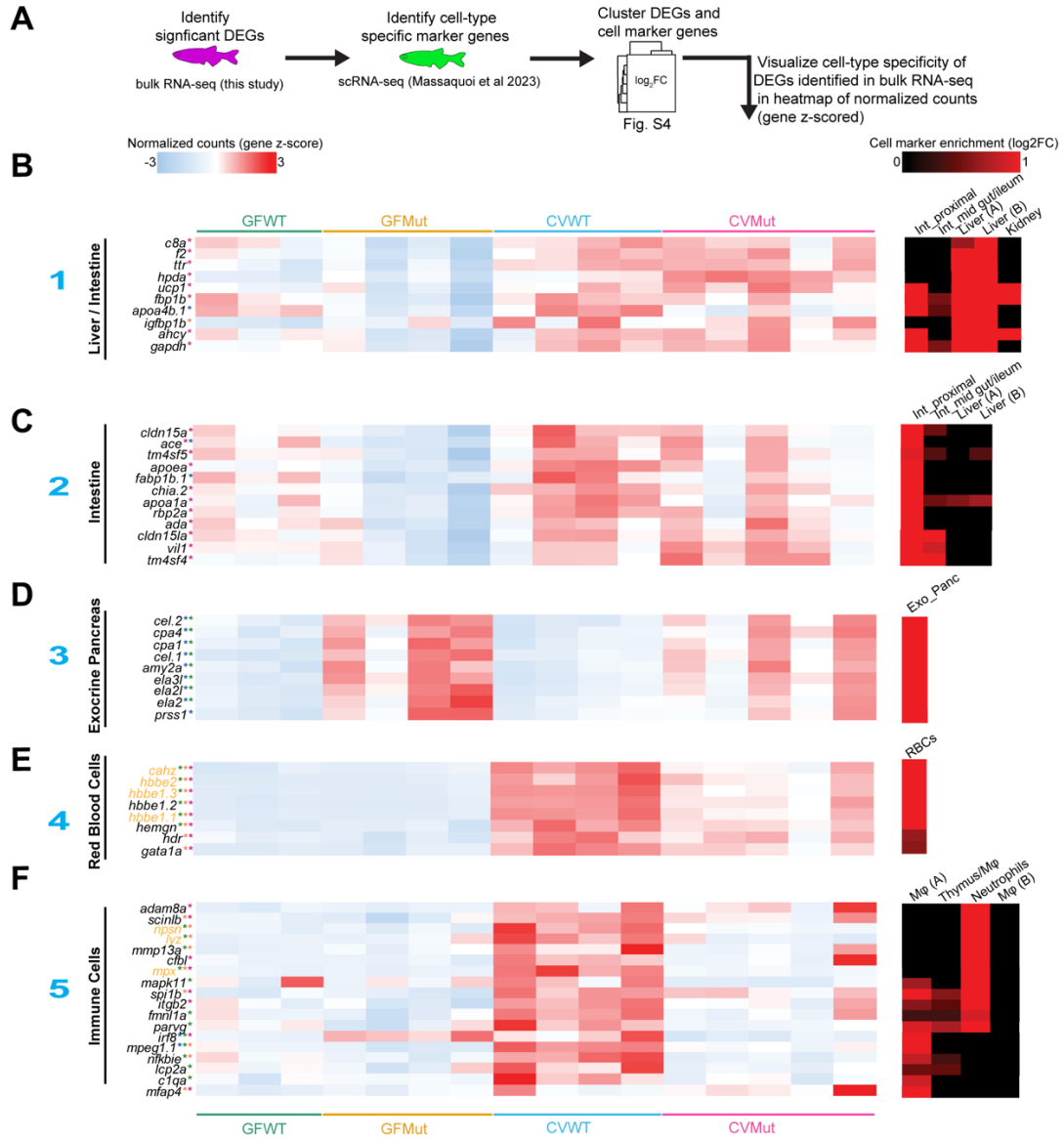


**Figure 7: Differentially expressed genes in larval RNA-seq exhibit cell-type specificity.**

(A) Schematic of application of cell-type specific calls to significant differentially expressed genes (DEGs) in the RNA-seq dataset. Significant DEGs were identified and clustered with cell marker genes identified in a scRNA-seq dataset generated from the dissociated cells of 6 dpf zebrafish (Massaquoi et al., 2023). The resulting clustered heatmap is featured in Fig.S4, and the heatmaps below are visualizations of example genes for each cell type. (B-G) Heatmaps of the gene z-scored normalized counts for diverse cell markers such as the liver/intestine (B), intestine (C), exocrine pancreas (D), red blood cells (RBCs) (E), and immune cells (F). All genes are significant in at least 1 of the 4 RNA-seq comparisons (P adjusted < .05). The color of the asterisk next to each gene indicates in which comparison(s) the gene is significantly differential (CVMut/GFMut: maroon, CVWT/GFWT: orange, GFMut/GFWT: blue, and CVMut/CVWT: green). Genes in yellow font are significant interaction genes. The blue numbers to the left of each heatmap indicate the cell type cluster the example marker genes represent (Fig. S2). The heatmaps on the far right show the log<sub>2</sub> fold change of the indicated gene as a function of cell marker enrichment (Massaquoi et al., 2023). Abbreviations: int\_proximal = intestine\_small/proximal; int\_mid gut/ileum = intestine mid gut/ileum; exo\_panc = exocrine pancreas; RBCs= red blood cells; Mφ = macrophages.



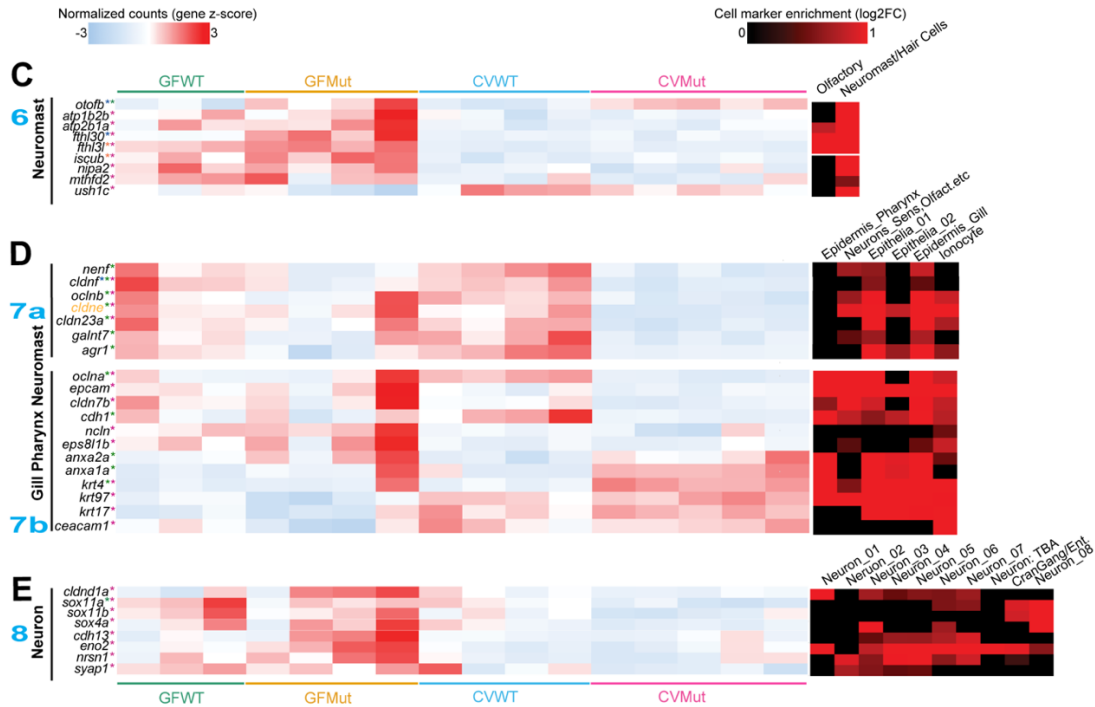


**Figure 9: Identification of putative cell-type specific responses among differentially expressed genes in larval RNA-seq (part 2).**

(C-E) Heatmaps of z-scored normalized counts for example (C) neuromasts, (D) gill/pharynx/neuromast tissue and (E) neuronal marker genes. All genes in the heatmap are significant in at least 1 RNA-seq comparison. The asterisk next to each gene is colored to indicate which comparison(s) the gene is significantly differential (CVMut/GFMut: maroon, CVWT/GFWT: orange, GFMut/GFWT: blue, and CVMut/CVWT: green). The blue numbers to the left of each blue, white, and red heatmap indicates the specific cell type cluster the example genes represent (Fig. S4A). The red and black heatmaps show the log<sub>2</sub> fold change enrichment of each gene for the indicated cell type (Massaquoi et al., 2023). Abbreviations: neuron\_01 = Cerebellum Purkinje cells; neuron\_02 = ZFIN-Habenula/Atlas-Sensory Neuron; neuron\_03 = forebrain; neuron\_04 = MHBNeurGlutAll; neuron\_05 = MHBNeurGlutAII/MHBNeurGABAII/Cranial ganglion; neuron\_06 = MHBNeurGlutAII/MHBNeurGABAII; neuron\_07 = RetDiff/CranGangAIIb, MHBNeurGABA/GlutAII/SCDiff; CranGang/Ent = Cranial Ganglion with Enteric Neurons, neuron\_8 = MHBNeurGABAII, MHBNeurGlutAII; neurons\_sens, olfact, etc = neurons/sensory/olfactory/hair cells; epithelia\_01 = epithelial: gill/basal/periderm/ionocyte; epithelia\_02: epithelial: gill/basal/periderm/ionocyte

### 2.2.8 *elf3* mutation reduces adult survival in zebrafish

Since *elf3* mutants fail to induce an appropriate immune response to the microbiota, we hypothesized that *elf3* mutant fish might develop immune-related pathologies. Adult *elf3* mutants of both sexes presented a range of clinical pathologies such as abnormal swimming behavior indicative of impaired swim bladder buoyancy, ulcer development on the body flank, or erythema (Fig.10A-B). Approximately 11% of evaluated mutants (30 out of 284) presented one or more of these observable pathologies compared to 1% of observed wild-type adults (5 out of 441) (Fig.10A-B&D). Overall, *elf3* mutant adults exhibit poor survival fitness, as we recovered  $\geq 40\%$  fewer mutants than expected when genotyping both alleles at adulthood (Fig.10E-F, Fig.11A-E).

To track the reduced survival, we longitudinally assayed animals in mixed *elf3* genotype heterozygous tanks as well as separate homozygous WT and mutant tanks starting from 2 months to approximately 12 months of age (Fig.8E-F, Fig.9C-E). Repeated genotyping of fish from heterozygous tanks revealed a (43%) reduction in mutant survival by 12 months of age (Fig.10E). To rule out that *elf3* mutant survival effect was driven by competition between genotypes, we assessed survival in homozygous tanks and observed similar reduced survival (51%) (Fig.10F).

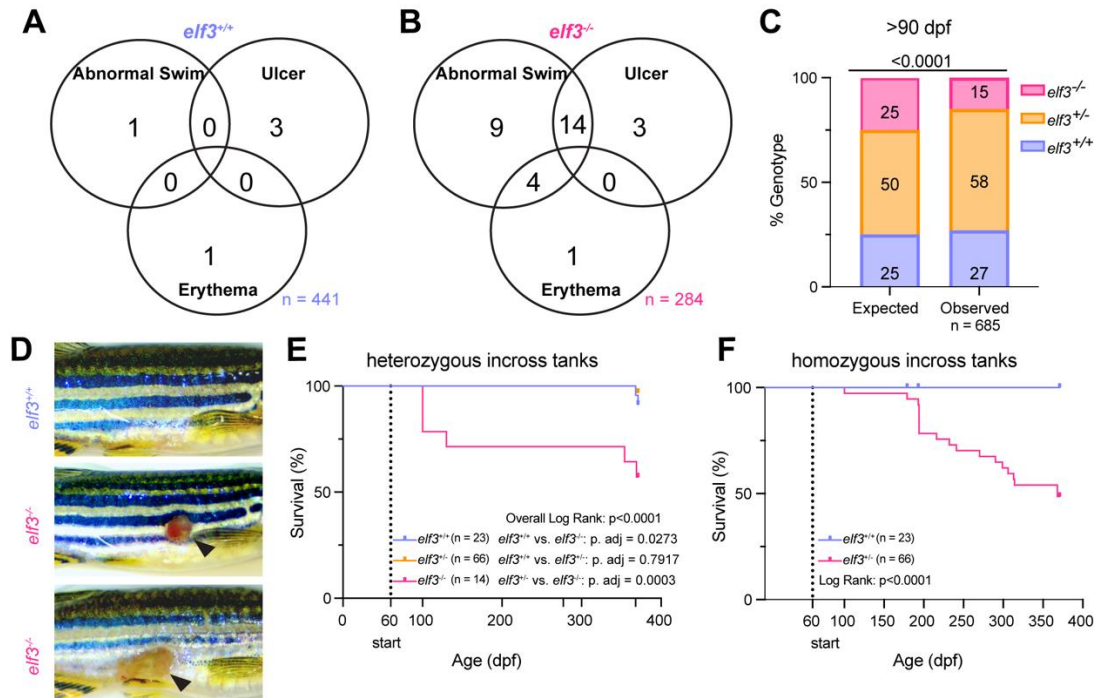


**Figure 10: *elf3*<sup>-/-</sup> adults present immune-related pathologies and exhibit poor survival.**

(A-B) Venn diagram of observed clinical signs of health deterioration, such as abnormal swimming, erythema, and ulcer development in *elf3*<sup>+/+</sup> (A) and *elf3*<sup>-/-</sup> (B) adults. (C) Comparison of the genotypic ratios observed in adult zebrafish > 90 dpf generated from heterozygous in-crosses of *elf3*<sup>+/-</sup> parents to expected Mendelian outcomes. (D) Representative images of severe (middle) and milder (bottom) ulcers in *elf3*<sup>-/-</sup> adults compared to healthy *elf3*<sup>+/+</sup> adults (top). (E) Kaplan Meier survival curve of co-housed *elf3* genotypes starting from the initial observation at 60 dpf (dotted line) and ending at 371 dpf. Repeated genotyping events occurred at 60 dpf, 100 dpf, 277 dpf, and 368 dpf. (F) Kaplan Meier survival curve of separately housed *elf3*<sup>+/+</sup> and *elf3*<sup>-/-</sup> adults starting from the initial observation at 60 dpf (dotted line) and ending at 371 dpf. P-values were calculated for (A) using a chi-square goodness-of-fit test and for (E-F) using an overall log-rank test followed by Bonferroni corrected log-rank tests for individual comparisons when required.

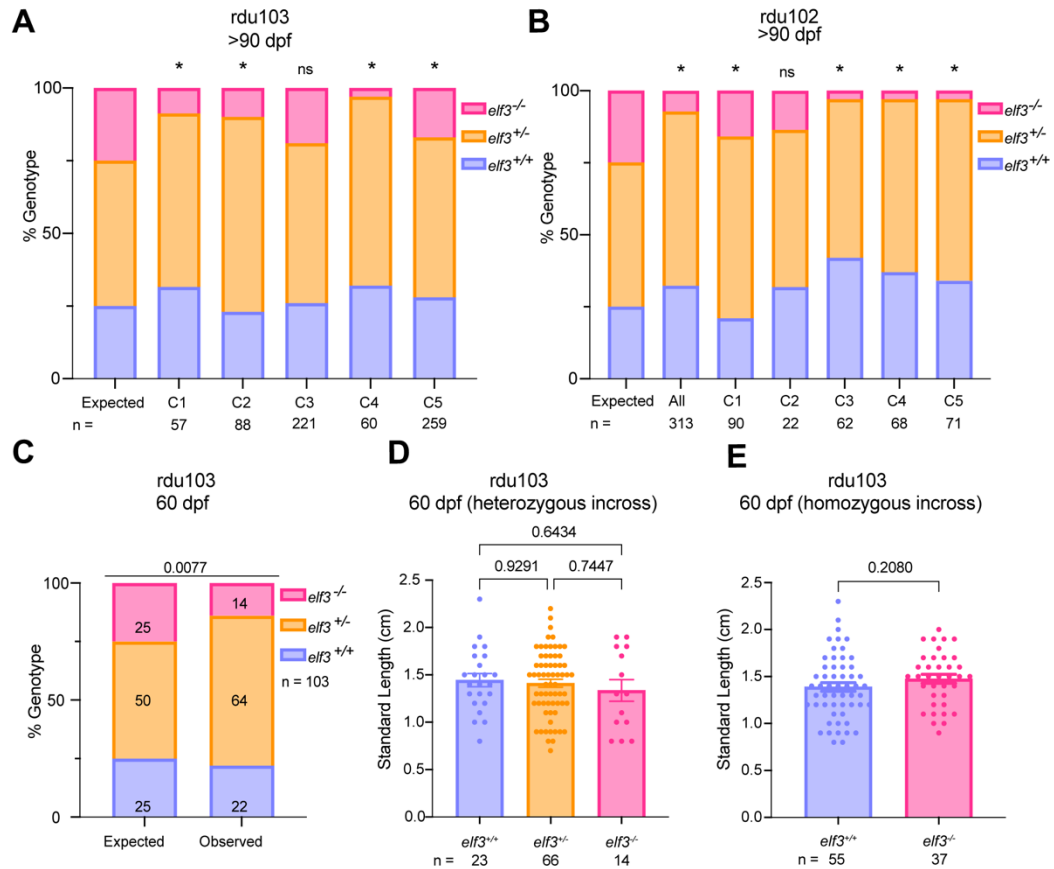


**Figure 11: *elf3*<sup>-/-</sup> adults of both alleles exhibit premature death.**

(A-B) Observed *elf3* allele genotyping cohorts [C] for rdu103 (A) and rdu102 (B) adults (> 90 dpf) compared to expected Mendelian outcomes. The data represented in (A) provide the cohort breakdown of the compiled genotyping presented in Fig.5A. (C) Comparison of observed genotypic ratios to expected Mendelian ratios of *elf3* genotypes (rdu103) at 60 dpf. These data represent the starting genotypic ratios for the longitudinal study in the heterozygous tanks referenced in Fig.5E (D-E) Standard length measurements of *elf3* genotypes in heterozygous (mixed genotype, D) or homozygous (*elf3*<sup>+/+</sup> or *elf3*<sup>-/-</sup> only, E) tanks at 60 dpf. These data represent the start of the longitudinal study referenced in Fig. 5F. *P*-values for (A-B) were calculated using a chi-square goodness-of-fit test and (D&E) using a one-way ANOVA with Tukey's multiple comparisons post-test.

### 2.2.9 *elf3* moribund mutants exhibit swim bladder inflammation

To understand the pathologies associated with reduced *elf3* mutant survival, we performed histological analysis on 14 moribund *elf3* mutants and healthy wild-type controls. Adults were defined as moribund based on presentation of the aforementioned clinical signs (abnormal swimming, ulcer, and/or erythema). Four moribund mutants had granulomas in locations including the liver, ovary, and coelomic cavity, while no granulomas were detected in WT animals (Fig.12A). Mycobacterial infections are a common cause of granulomas in zebrafish (Kent et al., 2004; Watral & Kent, 2007; Whipps et al., 2012), so we used detection methods such as acid-fast stain (Astrofsky et al., 2000) as well as an infection assay (Takaki et al., 2013) to assess susceptibility. All the granulomas were acid fast negative, suggesting non-mycobacterial contributions to granuloma formation (Fig.12A). When we injected standard doses of *Mycobacterium marinum* into 2 dpf wild-type and *elf3* mutant larvae, we observed no significant difference in bacterial burden between genotypes at 5 days post infection (dpi, or 7dpf) (Fig.12A). Therefore, while *elf3* appears to be required for aspects of the immune response to microbiota in larvae (Fig.4), it does not alter susceptibility to *M. marinum* infection during larval stages.

Our histological analysis also revealed extensive inflammation of the swim bladder and surrounding tissue (i.e. aerocystitis/peri-aerocystitis) in 13 out of 14 *elf3*<sup>-/-</sup> adults, whereas only 1 out of 14 *elf3*<sup>+/+</sup> controls had minimal inflammation between swim bladder compartments (Fig.12B-C). To test if the aerocystitis is associated with bacterial infection, the swim bladders of moribund *elf3* mutant zebrafish displaying aberrant swimming behavior and WT controls were removed, homogenized, and plated on rich media to evaluate the bacterial load. Whereas none of the tested WT animals (n = 4) showed significant bacterial burden associated with the homogenized swim bladders, the swim bladders in 4 out of 6 the *elf3* mutant animals displayed abundant bacterial growth with a single colony morphology emerging from each animal. 16S rRNA gene sequencing of the isolated bacteria revealed that two mutants were infected with hemolytic *Vibrio cholerae* and

two mutants were infected with nonhemolytic *Pseudomonas oleovorans*. Together, these results indicate that moribund status in adult *elf3* mutants is associated with aerocystitis/peri-aerocystitis and accompanying swim bladder infection, and/or non-mycobacterial granuloma formation.

We were curious if these histopathological phenotypes arose prior to reaching moribund status. Histopathological examination of *elf3* mutant and wild-type fish approximately 5 months in age (14 per genotype) that were free of the clinical signs of health deterioration did not show substantial inflammation phenotypes, suggesting that *elf3* mutants likely do not present long-term internal pathologies that precede external moribund presentations (Fig.13B-D). These histopathological data combined with our survival and clinical observations support a working model wherein *elf3* mutant adults are more susceptible to sporadic infection-associated aerocystitis, peri-aerocystitis, and granuloma formation, leading to abnormal swimming behavior and ultimately death.

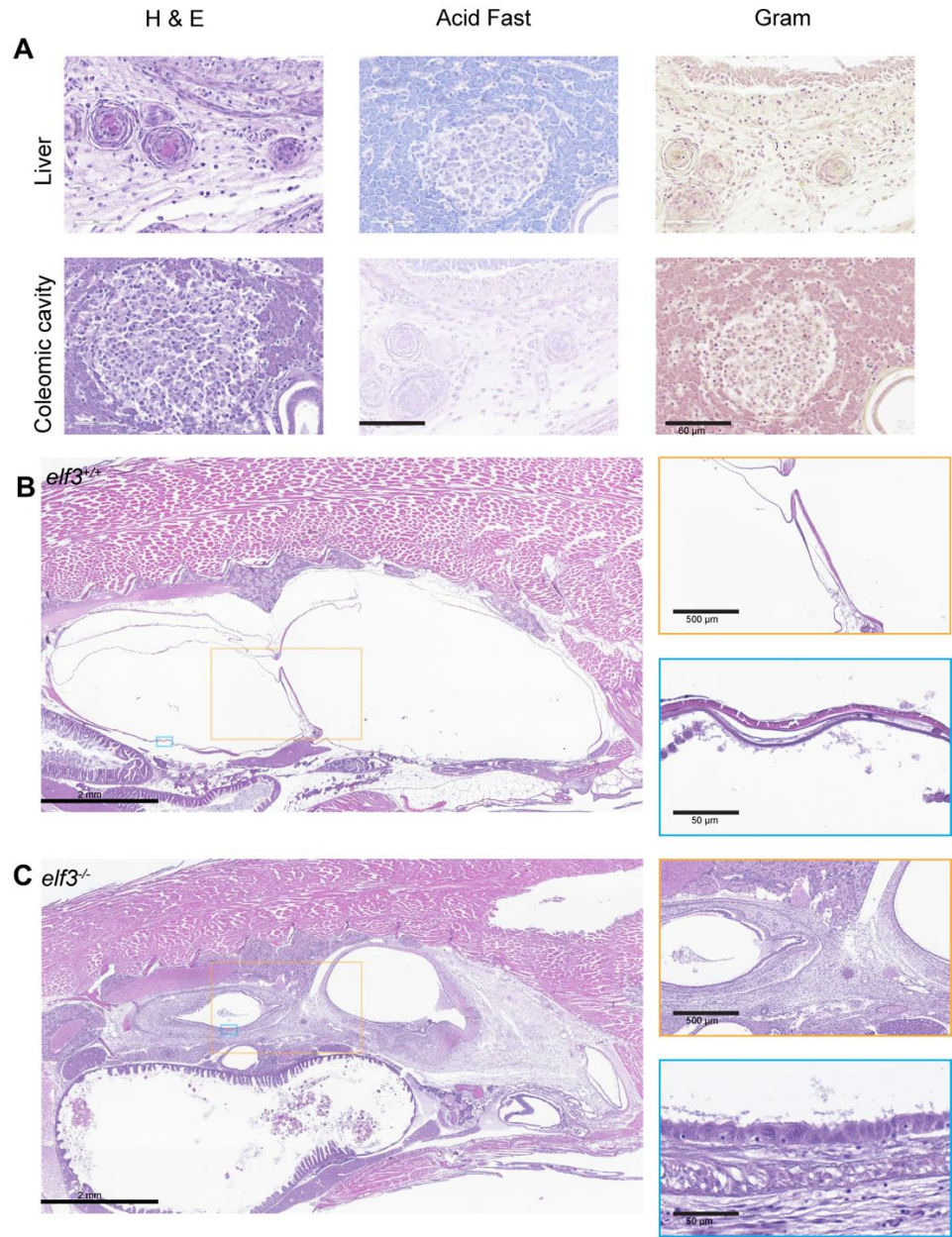


**Figure 12: moribund *elf3*<sup>-/-</sup> adults develop aerocystitis.**

(A) Representative images of granulomas that can develop in moribund *elf3*<sup>-/-</sup> adults in the liver and coelomic cavity. For each example granuloma, there is a hematoxylin and eosin (H&E) stained image, an acid-fast stained image, and a Gram-stained image to assess the overall morphology of the granuloma as well as test for the presence of Mycobacterium. (B-C) Representative images of the coelomic cavity of healthy appearing, wild-type controls (B) and moribund mutant (C) adults (histopathological evaluation of 14 moribund mutants and 14 wild-type controls). The two inset images featured below are magnified images of the swim bladder that highlight the inflammation observed in the anterior and posterior chambers of the moribund *elf3* mutant. Scanned images were rotated or vertically reflected for consistent body orientation across all images.

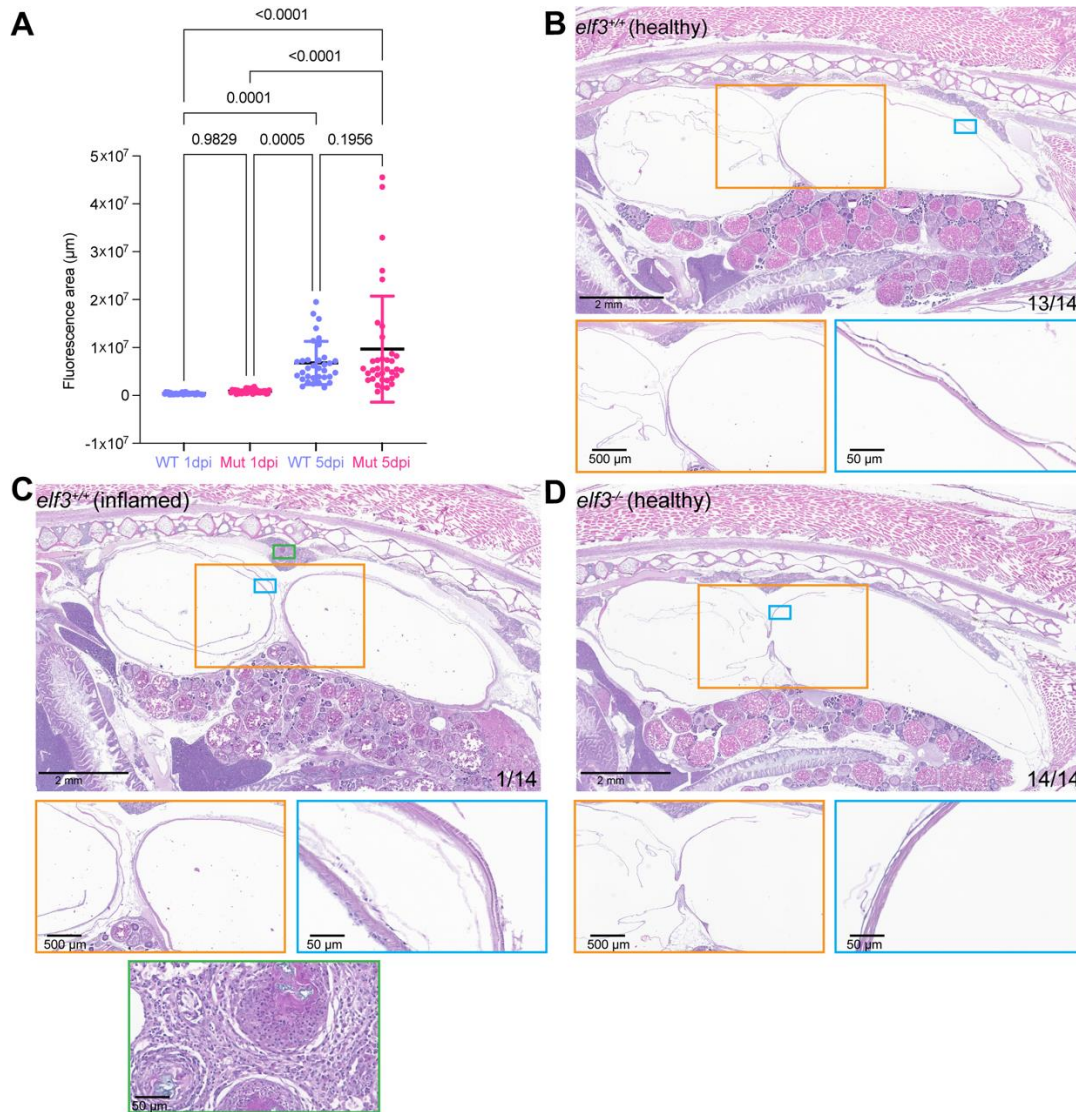


**Figure 13: Healthy appearing *elf3*<sup>-/-</sup> adults present normal histopathology.**

(A) Comparison of the bacterial burden of fluorescent *Mycobacterium marinum* (*Mm:tdTomato*) in *elf3* wild-type and mutant larvae 5-days post infection (dpi). Hematoxylin and eosin (H&E) stained images of wildtype (B,C) and mutant (D) adult zebrafish from our cross-sectional analysis of adults that appeared to be healthy based on external appearance and behavior. Panel C shows the one animal, a wild-type individual that displayed inflammation based on histologic analysis. This animal also had granulomatous inflammation in the kidney (green insert). The magnified insert images show the swim bladder (yellow) and layers of the swim bladder wall (blue). Scanned images were rotated or vertically reflected for consistent body orientation across all images (n = 13/14 normal wildtype, 1/14 inflamed wildtype, 14/14 normal mutant). *P*-values for (A) were calculated using a one-way ANOVA with Tukey's multiple comparisons post-test.

### 2.2.10 Discussion

Our findings here establish Elf3 as a microbially-regulated TF that is also required for mediating diverse host responses to microbiota. Our finding that *Elf3* genes are commonly induced by commensal microbiota in digestive tissues in zebrafish and mice is in accord with previous studies showing *Elf3* homologs are induced by bacterial pathogens (Haber et al., 2017; van der Vaart et al., 2013; van Soest et al., 2011) and symbionts (Chun et al., 2008) in diverse animal species. Previous literature indicated many roles for *elf3* including regulation of epithelial identity and differentiation (Ng et al., 2002; Suzuki et al., 2021), inflammation (Grall et al., 2005; Rudders et al., 2001; Wu et al., 2008), extracellular matrix (ECM) organization (Sarmah et al., 2022) and epithelial-mesenchymal transition (Lin et al., 2024; Yeung et al., 2017; Zheng et al., 2018). However, it remained unclear if *elf3* could integrate information derived from microbes to affect downstream host transcriptional processes and whether this would uncover additional physiologic roles. By comparing the transcriptome of mutant and wild-type zebrafish larvae reared in GF and CV conditions, our data suggest that *elf3* is indeed important for microbially responsive transcriptional programs. We observed attenuation of host immune genes in colonized *elf3* mutants that supports previous findings that Elf3 regulates cytokine expression in response to pro-inflammatory stimuli in human bronchial epithelial cells (Wu et al., 2008), synovial fibroblasts (Kouri et al., 2023), and chondrocytes (Otero et al., 2012). The attenuated host immune response also included several hematopoietic marker genes, which is consistent with a finding that *elf3* mediates T-cell priming in a murine model of pulmonary inflammation (Kushwah et al., 2011). Curiously, *elf3* is required for microbial upregulation of several hematopoietic cell markers despite not being strongly expressed in red blood or innate immune cells under conventionally-reared conditions (Fig.S1). However, it is important to note that as with all other transcriptional differences that we've discussed, we do not have evidence that *elf3* is directly involved in this effect. Previous literature indicates that epithelial cells can signal

through MMPs to enhance macrophage recruitment in response to *Mycobacterium marinum* (Volkman et al., 2010), and our dataset indicates that there is an attenuation of microbial induction of *mmp13a* in *elf3* mutants. It is possible that *elf3* mutation has direct or indirect effects on epithelial to immune cell crosstalk. We also found that *elf3* is required for full expression of other microbially induced TFs (i.e. IRFs) and cytokines that putatively facilitate the crosstalk between epithelial and other host tissues and the immune system. This aligns with emerging evidence that *elf3* directly binds to the IRF6 promoter in a human gastric cancer cell line (Li et al., 2019) and to the interferon epsilon (IFN $\epsilon$ ) in HEK293 cells (Fung et al., 2024).

Our findings also suggest there might be *elf3*-dependent transcriptional programs like ECM organization and assembly that are specific to the state of microbial colonization. For example, ECM organizational genes were previously demonstrated to be upregulated in conventionally-reared *elf3* knockdown larvae compared to controls (Sarmah et al., 2022). In accord, we found in our study that ECM organization genes were upregulated in *elf3* mutant larvae compared to wildtype only in CV conditions. We also note that not all the demonstrated functions of *elf3*, such as regulation of epithelial-mesenchymal transition seen in numerous human cell culture studies (Lin et al., 2024; Yeung et al., 2017; Zheng et al., 2018), exhibited a strong transcriptional signature in our work. This suggests that there might be a degree of genetic redundancy or species differences in *elf3* functions across species or certain tissues.

We found that *elf3* mutants exhibit reduced survival fitness as adults despite normal development and expected Mendelian ratios in larvae. One possibility for the lack of a survival phenotype in larvae includes differences in immune biology at developmental stages. The adaptive immune response in developing zebrafish is not mature and functional until approximately 4-6 weeks post-fertilization (Lam et al., 2004). Our 6 dpf RNA-seq results do not permit evaluation of how *elf3* mutation affects mature adaptive immune responses, which may have important implications for the spontaneous illness and death we observed *elf3*<sup>-/-</sup> adults. It is

also possible the reported adult phenotype in *elf3* mutants is due to differences in the microbial composition of relevant host tissues (e.g., swim bladder and intestine) and that these differences are less prevalent at larval stages. The microbiota associated with *elf3*<sup>-/-</sup> adult tissues for instance might be more differential and linked to increased infection susceptibility compared to wildtype animals. Future 16S rRNA sequencing studies are needed to assess the effects of *elf3* mutation on the microbiota at larval and adult stages as well as pre-clinical vs. clinical states.

Interestingly, we found that Elf3 is protective against spontaneous inflammation of the swim bladder (aerocystitis) even though *elf3* does not appear to be expressed in the adult swim bladder (Zheng et al., 2011). In larval zebrafish, *elf3* is expressed along the gastrointestinal tract including the esophagus, pharynx, and pneumatic duct (Fig.S1A). A putative cause for the aerocystitis is infectious agents, such as ascending bacteria, that could migrate from the digestive tract through the pneumatic duct to infect the swim bladder. Alternatively, or in concert, reduced function of the pneumatic duct in *elf3* mutants could cause or impair swim bladder buoyancy regulation and subsequently render the duct and swim bladder susceptible to inflammation and infection.

Taken together, our transcriptomic and whole animal histopathologic analyses indicate that *elf3* transcriptionally mediates host-microbiota interactions as well as microbe-independent programs important for animal physiology. Our model presents putative direct or indirect roles of *elf3* in the upregulation of immune/defense responses and hematopoiesis while facilitating the downregulation of abiotic responses and organic acid metabolism in response to microbes (Fig. 7). *elf3* also putatively mediates metabolic programs like proline and pyruvate metabolism and cellular stress responses in a microbe-independent manner (Fig. 7). Additional studies are needed to understand if the role of *elf3* in protection against aerocystitis is related to its role in host-microbiota interactions or not.

This study indicates that *elf3* transcriptionally mediates host immune responses to the microbiota and is important for adult survival under standard housing conditions. While our results establish putative direct and indirect target genes of *elf3* upon microbial stimulation, additional studies are needed to understand the larger upstream pathways involved in regulating *elf3* expression and microbial responsiveness as well as direct Elf3 target genes. Our identification of conserved NF- $\kappa$ B binding sites in the *elf3* promoter (Fig.1) is consistent with previous findings that these NF- $\kappa$ B mediates *elf3* expression in diverse cell types (Grall et al., 2003; Rudders et al., 2001; Wu et al., 2008). Future genetic or pharmacological studies that directly test the ability of these TFs to regulate *elf3* will provide additional context to its role mediating host-microbiota interactions.

## Putative indirect or direct function of *elf3* in zebrafish

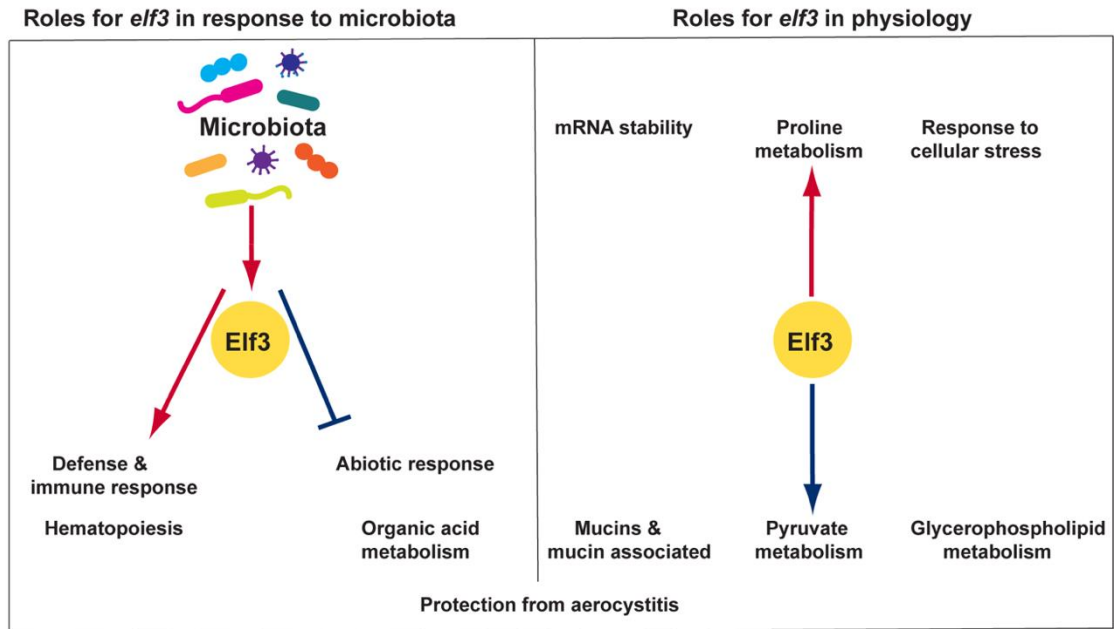


**Figure 14: Summary model indicating putative roles for *elf3* in zebrafish**

*elf3* has roles in mediating host transcriptional responses to the microbiota as well as transcriptional programs important for microbe-independent physiologic functions. In response to microbes, *elf3* mediates the upregulation of genes involved in immune and defense response well as hematopoietic marker genes while mediating the downregulation of genes with roles abiotic responses (e.g., circadian rhythm) and organic acid metabolism. Additionally, *elf3* mutation results in the upregulation of transcriptional programs like proline metabolism and response to stress and the downregulation of pyruvate and glycerophospholipid metabolism genes in a microbe-independent manner. *elf3* mutation has significant consequences for the survival of adult zebrafish; however, it remains unclear if this effect is related to the role of *elf3* in host-microbiota interactions. All the putative roles for *elf3* indicated in this model could be direct or indirect.

## **2.3 Methods**

### **2.3.1 Ethics Statement**

All zebrafish experiments were performed in accordance with the protocol approved by the Duke University Institutional Animal Care and Use Committee (IACUC protocol number A061-22-03).

### **2.3.2 Zebrafish husbandry**

Husbandry of conventionally reared zebrafish was performed as previously described (Murdoch et al., 2019; Wen et al., 2021). Zebrafish stocks maintained on a Ekkwill (EK) or a mixed EK/Tübingen long fin (TL) background were housed on a Pentair recirculating aquaculture system timed to a 14/10- hour light/dark cycle at 28°C (Wen et al., 2021). Early larval fish were given a Zeigler AP100 powered diet twice per day until 14 dpf, at which point the fish were fed *Artemia* (brine shrimp) in the morning followed by an afternoon feeding with powdered Gemma Micro diet. Fish are maintained on this two-part diet through adult stages.

Generation and maintenance of gnotobiotic larvae was performed as previously described (Pham et al., 2008) with the addendum that the “antibiotic-containing gnotobiotic zebrafish medium” (AB-GZM) was supplemented with 50 ug/ml gentamycin (Sigma-Aldrich, G1264) (Murdoch et al., 2019). Genotyping of larval and adult zebrafish was performed using standard whole larvae preparations or fin tissue resection methods with the extracted genomic DNA using the primers listed in Table 12. For imaging experiments, fish were anesthetized in buffered Tricaine prior to mounting.

### 2.3.3 Key resources

**Table 15: Biological reagents**

Type of reagent	Name of reagent	Source
<i>Danio rerio</i> mutant allele	<i>elf3</i> <sup>rd<sup>u</sup>102</sup> ( $\Delta$ 19 bp)	This study
<i>Danio rerio</i> mutant allele	<i>elf3</i> <sup>rd<sup>u</sup>103</sup> ( $\Delta$ 12 bp)	This study

**Table 16: Primers**

Name	Sequence	Source
elf3_rdu102_F	CCGAGTTTGAGCTACTAGACAACA	This study
elf3_rdu102_R	GAATTGTAGACTGGACCACCA	This study
elf3_rdu103_F	ACTCTTGCTCTTTCTGACAGGTA	This study
elf3_rdu103_R	AACCGGTCTCCTCTATCCTCC	This study
8F	AGAGTTTGATCCTGGCTCAG	(Weisburg et al., 1991)
1492R	GGTTACCTTGTTACGACTT	(Weisburg et al., 1991)

### 2.3.4 Generation of mutant zebrafish lines

The *elf3* locus was mutated via CRISPR/Cas9-based genome editing as previously described (Davison et al., 2017; Heppert et al., 2022; Wen et al., 2021). The “CRISPRscan” tool (<https://www.crisprscan.org/>) was used to identify the target sequence of both guide RNAs (gRNA). For *elf3*<sup>rd<sup>u</sup>102</sup>, the gRNA was generated via *in vitro* transcription. This gRNA (120 ng/uL) was injected into one-to-two cell stage, wild-type embryos in an injection mixture that included “Cas9 mRNA (150 ng/ul), 0.05% phenol red, 120 mM NaCl, and 20 mM Hepes Buffer (pH 7.0)” (Heppert et al., 2022; Murdoch et al., 2019; Wen et al., 2021). For *elf3*<sup>rd<sup>u</sup>103</sup>, a synthesized gRNA targeting the DNA binding domain was purchased from IDTDNA. One-to-two

cell stage, wild-type embryos were injected with a mixture of this gRNA (80 ng/uL), Cas9 protein (300 ng/ul), and 0.06% phenol red. For both alleles, mutagenesis events in injected embryos were detected via Heteroduplex Mobility Assay. Founders for both alleles were identified via Sanger sequencing of PCR products that spanned the CRISPR target site. *elf3<sup>rd102</sup>* was identified as a 19 bp deletion, which is predicted to result in a premature stop codon after amino acid 235 (Fig.S2). *elf3<sup>rd103</sup>* was identified as a 12 bp in frame deletion (Fig.S2). Founders were outcrossed to wild-type fish to propagate both alleles and generate stable lines.

### 2.3.5 Cell isolation and RNA extraction for total RNA sequencing

*elf3<sup>+/+</sup>* and *elf3<sup>rd103</sup>* larvae were pooled separately from at least two clutches of homozygous incrosses from parental cousins. Larvae were euthanized in buffered Tricaine (n= 6-16 pooled larvae per experimental replicate) and stored at 4°C in RNAlater (Thermo Fisher, AM7020) for 16 hours prior to long-term storage at -80°C. RNA extraction was performed as previously described (Heppert et al., 2022). To start the RNA extraction process, the larvae were washed in 1 mL of cold GZM. Next, 1 mL of TRIzol (Thermo Fisher, 15596026) was added to each replicate tube, and the larvae were homogenized with a 27-gauge needle and syringe (25 total passes). Following homogenization, the RNA extraction process was completed with the PureLink RNA Mini Kit (Invitrogen, 12183018A). To ensure high quality RNA for sequencing, the eluted RNA was prepared for additional clean up with the Zymo RNA Clean and Concentrator Kit (Zymo Research, R1017) Total RNA was stored indefinitely at -80°C until submission to the Duke Sequencing and Genomic Technologies Shared Resource (SGT). The SGT Core generated stranded mRNA libraries (KAPA HyperPrep) and performed 150 bp paired-end sequencing in one 10B lane of the NovaSeq X Plus.

### 2.3.6 Bulk RNA-seq analysis

Initiation of the bulk RNA-sequencing analysis was performed as previously described (Heppert et al., 2022). Raw sequencing files were uploaded to the Galaxy server, where the paired

reads were subsequently trimmed using Trim Galore! to remove adapter sequences and low-quality scoring reads. These reads were mapped to the *Danio rerio* reference genome (GRCz11) with default STAR RNA-seq (Dobin et al., 2013) parameters using the Lawson lab transcriptome annotations as a gene model (v4.3.2 GTF) (Lawson et al., 2020). Mapped reads per gene were quantified via FeatureCounts with default parameters (Liao et al., 2014) and the resulting counts for each replicate were used to compute differential expression analysis and likelihood ratio test (LRT) via DESeq2 (Lickwar et al., 2022; Love et al., 2014). DESeq2 and its plotPCA function were used to generate the PCA plot of normalized counts for each replicate. The Venn diagram of significant differentially expressed genes was generated online via (<http://bioinformatics.psb.ugent.be/webtools/Venn/>). To identify GO biological processes and other pathways enriched in our lists of differentially expressed genes, we used the default settings of Metascape (Zhou et al., 2019).

### **2.3.7 Brightfield and color camera images of zebrafish**

To generate brightfield images of larval zebrafish, anesthetized fish were mounted in 3% methylcellulose and imaged with a Leica DFC 365FX camera attached to a Leica M205 FA stereomicroscope similarly to the protocol described in (Murdoch et al., 2019). Colored images of anesthetized adult zebrafish were taken with a Leica DFC425 camera attached to a Nikon SMT-2T dissecting scope.

### **2.3.8 Longitudinal assessment of *elf3*<sup>rd<sup>u</sup>103</sup> survival**

We in-crossed *elf3*<sup>rd<sup>u</sup>103</sup> heterozygous adults and separately in-crossed *elf3*<sup>+/+</sup> and *elf3*<sup>-/-</sup> siblings to generate the heterozygous (n = 4 tanks) and homozygous (n = 2 tanks per genotype) that we observed over time. For the heterozygous tanks, we genotyped the fish with standard fin resection methods at 60 dpf to obtain the starting genotypic ratios and performed genotyping rounds at 100 dpf, 277 dpf, and 368 dpf to monitor ratios. For the homozygous tanks, we performed tank counts at the same timepoints that the genotyping was conducted with 4

additional timepoints (130 dpf, 194 dpf, 232 dpf, 313 dpf). All survival data is presented in the form of Kaplan Meier survival curves. A death event was defined as any fish that was found dead, euthanized for a humane endpoint, or fish presumed dead resulting from decreased “n” at time of tank count. Moribund fish presenting clinical signs of health deterioration such as abnormal swimming, ulcers, and erythema were euthanized for a humane endpoint. Several of these euthanized moribund fish were prepared for adult histopathological assessment. Wild-type controls that were euthanized specifically to serve as controls for the histopathological assessment were considered censored and are indicated as such in the Kaplan Meier survival curve as ticks.

### **2.3.9 Longitudinal assessment of *elf3*<sup>rd<sup>u</sup>103</sup> survival**

Moribund *elf3* mutant adults ranging from 202 to 501 dpf were euthanized along with sex-matched, similarly aged wild-type controls ( $\leq 20$  dpf difference) in preparation for paired analysis. For the cross-sectional cohort, mutant and wild-type adults (7 males and 7 females per genotype) were euthanized at 154 dpf. Euthanized fish were prepared for whole animal histology according to the ZIRC Public Wiki fixation protocol ([www.zebrafish.org](http://www.zebrafish.org)) with the addendum that the de-calcified fish were rinsed for 3 hours in running DI water before immersion in a graded ethanol series ranging from 25% to 70%. The fish were stored in 70% ethanol prior to shipping to the Oregon Veterinary Diagnostic Laboratory at Oregon State University, where the fish were embedded in paraffin blocks, sectioned (along the paramedial plane), and stained to produce hematoxylin and eosin (H&E), acid fast, and Gram-stained slides. The Duke BioRepository and Precision Pathology Center (BRPC) generated 40X whole slide scans using a Leica Aperio GT450 scanner. Histopathologic evaluation of the scanned slides was performed in a blinded analysis by a board-certified veterinary pathologist that was either paired (moribund) or unpaired (cross-sectional cohort). For consistency, all histology images depicted in the publication were either rotated or vertically reflected for head left orientation.

### **2.3.10 Larval zebrafish infections with *Mycobacterium marinum***

2 dpf larval zebrafish from homozygous incrosses of *elf3* wild-type and homozygous mutant parents were anesthetized with tricaine and approximately 200 fluorescent bacteria (FB) of wild-type, red fluorescent *M. marinum* were injected into the caudal vein of each larval zebrafish with a borosilicate needle. The infected zebrafish were subsequently recovered in E3 medium containing 1-phenyl 2-thiourea (PTU). Any embryos damaged in the process of injection or infected with incorrect dosage were removed from the experiment at 1 dpi. Final images were taken at 5 dpi. Fluorescent bacteria were quantified as previously described (Takaki et al., 2013).

### **2.3.11 Isolation and identification of swim bladder bacteria**

To evaluate swim bladder infection in *elf3* mutant zebrafish, we selected moribund mutant fish that were displaying aberrant swimming behavior and wild-type control siblings (n = 6 mutants and n = 4 wildtype). Immediately following euthanasia in buffered Tricaine, the fish were soaked in 10% PVP-iodine (Ricca 3955-16) for 2 minutes, gently scrubbed with PVP-iodine soaked kimwipes, and re-submerged in the iodine solution for an additional 2 minutes. Swim bladders were dissected with sterile instruments, homogenized with a pestle, and plated on blood agar plates (tryptic soy agar base with 5% sheep blood, VWR 10324-332) under aerobic and anaerobic conditions. Cultured bacteria were isolated and their 16S rRNA genes were PCR amplified (Table S1), Sanger sequenced and classified using SILVA (Glockner et al., 2017; Quast et al., 2013; Yilmaz et al., 2014).

### **3. Conclusions**

Animals are in constant interaction with the surrounding microbial environment. For over a century, scientists have questioned the effects of these microorganisms on basic aspects of animal physiology. Questions about the role of microbes in biological processes such as nutrient metabolism and immune function continue to fuel many areas of biomedical research. If microbes can influence so many diverse aspects of host physiology, then there must be sensing and response mechanisms in place that help to facilitate these interactions. The work presented in this manuscript provides additional insight for one highly conserved transcription factor (*elf3*) that has a role in mediating host responses in larval zebrafish. However, many questions remain about how this transcription factor acts within broader transcriptional networks for mediating this response and how conserved this finding might be to other vertebrates. In this conclusion, I have addressed the limitations of the current work as well as provided recommendations for future research that builds on these findings.

#### ***3.1 Limitations and future work***

##### **3.1.1 Characterizing Elf3 protein function and protein-protein interactions**

In this study, we used bulk RNA-sequencing to compare the transcriptional profile of *elf3* wildtype and mutant larvae reared with or without the presence of microbes. Our transcriptomic analyses allowed us to conclude that *elf3* has a role in mediating how larval zebrafish respond to microbial stimuli. We know that in our dataset as well as other datasets generated from the digestive tissue of zebrafish, that *elf3* mRNA transcript levels are increased in conventionalized (CV) larvae compared to germ-free (GF). However, it is important to note that mRNA levels are just one aspect of gene expression that we probed with our transcriptomic approach. We did not address Elf3 protein levels in this study. mRNAs serve as the template for protein translation, and it is assumed in many cases of differential expression that increases or decreases in mRNA transcript levels are correlated with respective changes in protein abundance (Buccitelli &

Selbach, 2020; Koussounadis et al., 2015). Curiously, it is estimated from genome wide mRNA-protein correlation studies in mammalian cells that roughly 40% of variation in protein abundance can be explained by changes in mRNA transcript levels (Buccitelli & Selbach, 2020). This correlation may be higher or lower for specific genes and can be cell-type dependent (Buccitelli & Selbach, 2020). We cannot conclude from this work whether the microbiota can induce Elf3 protein abundance or alter its sub-cellular localization (e.g., nuclear vs cytoplasmic). Future exploration of Elf3 protein might explicitly address these points even with the use of other systems such as cultured cells, organoids, and animal models. Previous studies indicate that Elf3 has distinct nuclear versus cytoplasmic roles in transforming mammary epithelial cells (Prescott et al., 2004) and that its expression is stronger and more nuclear in the inflamed colonic tissue of mice treated with dextran sulfate-sodium compared to controls (Li et al., 2015). These data suggest that subcellular localization can influence the biological roles of Elf3 and that inflammatory signaling might enhance nuclear translocation. It would be interesting to learn if the microbiota informs subcellular localization of Elf3 in epithelial cells and ask questions about what other proteins Elf3 interacts with to elicit a host response. What proteins does Elf3 interact with in the nucleus and/or cytoplasm that enhance or inhibit its activity? Are there Elf3 interactor proteins that are specific to the microbial status of the host? How does *elf3* mutation affect the protein-protein interactions between other immune responsive host factors? Previous *in vitro* studies indicate IL-1 $\beta$  induces the expression of the transcriptional co-activator complex p300-CBP, which in turn interacts with ELF3 to enhance transcription of target genes like nitric oxide synthase 2 (*NOS2*) (Wang et al., 2004). Conversely, Ku70 and Ku86 proteins inhibit the transcriptional activity of ELF3 (Wang et al., 2004). I am particularly interested to see if ELF3 interacts with transcriptional co-activators like NFKBIZ and other proteins that mediate NF- $\kappa$ B signaling (Kohda et al., 2016; Yamamoto et al., 2004). While some of this future protein-protein interaction work would be performed in cultured cells or organoids, there are also methods for

generating protein-protein interactions networks in zebrafish using proximity-based biotinylation assays (Pronobis et al., 2021; Xiong et al., 2021).

Another limitation of our work is our inability to determine where Elf3 protein binds in the genome. We are unable to distinguish between the direct and indirect target genes identified in our larval bulk RNA-seq dataset. While it was encouraging to see differentially expressed genes in our dataset that have been demonstrated as direct ELF3 targets in cell culture (e.g., zebrafish *mmp13a* and human *MMP13*), we do not have data that reveal what genes Elf3 directly regulates in response to microbes. This is particularly noteworthy because there are several immune responsive transcription factors like *irf1b* and *stat4* that fail to be induced by microbes in the *elf3* mutants. It is likely that these TFs also have a role in the attenuation of the immune response observed in colonized *elf3* mutants. ChIP-seq is approach that would help identify direct Elf3 targets; however, it is a strategy that hinges on availability of high-quality ChIP-grade antibodies that are not currently available in zebrafish or in mice. The “Biotin ChIP-seq” method is a newer protocol that leverages the affinity of biotin to streptavidin beads to circumvent the need for TF specific antibodies in zebrafish (Lukoseviciute et al., 2018; Lukoseviciute et al., 2020). In this approach, researchers generate a stable transgenic reporter line in which the transcription factor of interest is tagged by an AVI tag that is targeted by BirA biotin ligase (Lukoseviciute et al., 2020). This transgenic reporter is then crossed to another transgenic reporter in which biotin ligase is ubiquitously expressed in the nucleus of all cells (Lukoseviciute et al., 2020). In the resulting double transgenic progeny, the transcription factor of interest is biotinylated and thus after subsequent crosslinking of the protein to DNA, can be pulled down with streptavidin beads similarly to how antibody coated beads pulldown TF-DNA complexes in traditional ChIP-seq protocols (Lukoseviciute et al., 2020). This approach was previously used to elucidate the transcriptional program regulated by *foxd3* during neural crest development in zebrafish (Lukoseviciute et al., 2018). It is likely that this approach would need to be optimized to

work for *elf3*; however, I anticipate that approaches like this will continue to improve our ability to understand TF binding without the need for specific, high-quality antibodies. Overall, I think that there are exciting protein-based studies that can help further define the role of Elf3 in mediating host responses to microbes.

### 3.1.2 Generation of *elf3* transgenic reporters

While this work establishes that *elf3* is a microbially responsive transcription factor in larval zebrafish, we do not know what upstream host transcription factors and other mediators regulate its expression and microbial responsiveness. We were able to identify that the *elf3* promoter has conserved NF- $\kappa$ B and Egr1 binding motifs; however, attempts to perform structure-function analyses with the *elf3* promoter to identify cis-regulatory regions and test whether these TFs might regulate *elf3* expression were inconclusive. The biggest challenge in the success of these experiments is the presence of repetitive simple sequence in the upstream promoter of zebrafish *elf3*, which is not highly amenable to cloning. We were unable to clone or synthesize the approximately 1900 bp upstream promoter region containing both TF binding motifs; however, we were able to generate a transgenic reporter line with the roughly 300 bp more proximal promoter that contains the NF- $\kappa$ B motif (data not shown). This reporter recapitulates expression of *elf3* in epithelial tissues like the intestine, neuromasts, and pronephric duct observed in published *in situ* data (Sarmah et al., 2022) (data not shown). Preliminary qRT-PCR analysis of *GFP* transcript levels in GF and CV transgenic larvae suggest that reporter expression is not microbially responsive and thus does not recapitulate microbial induction of endogenous *elf3* (data not shown). Future studies are needed to more explicitly test the genetic requirements for NF- $\kappa$ B, Egr1, and other host factors for the microbial induction of *elf3* in larval zebrafish. Even though my thesis lab was previously successful in using the structure-function approach to identify a microbially responsive cis-regulatory region for *angptl4* (Camp et al., 2012), I would recommend future studies of *elf3* transcriptional control use other transgenesis and mutagenesis

approaches. Pharmacological inhibition is another way to test the requirement of these host factors for the microbial induction of *elf3*; however, identification of efficacious inhibitors for use in larval zebrafish is challenging.

My recommendation for addressing putative upstream regulators of *elf3* is to start with the generation a transgenic zebrafish reporter line using CRISPR-mediated knock-in strategies (Cronan & Tobin, 2019; Levic et al., 2021; Wilson et al., 2021). This approach can include designing and injecting a single guide RNA (sgRNA) that targets the last intron of *elf3* (Levic et al., 2021). The double stranded DNA break that is induced is then repaired with the assistance of a dsDNA PCR donor that contains the endogenous sequence for the gene fused to fluorescent protein and polyadenylation sequences (Levic et al., 2021). Success with this knock-in approach would result in a fluorescently tagged Elf3 protein amenable to visualization with confocal microscopy. Important considerations include the fact that this tagging might negatively impact the expression, localization, and activity of Elf3 in vivo, so validation experiments confirming that these processes are not impaired are recommended. This knock-in approach can also be used to generate a N-terminus tag, but due to the highly repetitive nature of the sequence upstream of *elf3* coding sequence, it might be challenging to identify effective sgRNAs that cut within the target region. This consideration should also be applied to CRISPR-mediated promoter knock-in strategies in which a fluorescent reporter driven by a minimal promoter [e.g., *heat shock protein 70* (*hsp70*) or *cellular oncogene fos* (*c-fos*)] is inserted approximately 200-600 base pairs upstream of the transcriptional start site (Auer et al., 2014; Kimura et al., 2014). Because the reporter is inserted so close to the TSS, its predicted that the regulatory landscape acting on the endogenous gene expression will similarly act upon the minimal promoter driving reporter gene expression (Auer et al., 2014; Kimura et al., 2014). Thus, it is anticipated that the reporter expression will closely recapitulate endogenous expression of the gene of interest (Auer et al., 2014; Kimura et al., 2014). These transgenesis strategies are quite promising, but what if they are

not successful for *elf3* specifically? Another method for visualizing *elf3* expression in larval zebrafish is to generate and hybridize hybridization chain reaction (HCR) probes to *elf3* mRNA transcripts using RNA-FISH protocols (Childers et al., 2024; Choi et al., 2018; Munjal et al., 2021). This variation on traditional, semi-quantitative *in situ* hybridization methods enables more precise quantification of mRNA molecules *in vivo* (Choi et al., 2018). Researchers can compare the fluorescence intensity of the probes between experimental conditions to generate hypotheses about the effects of the treatment on gene expression. This strategy for visualizing *elf3* expression is particularly advantageous when there are experimental time constraints. The probes can be used immediately in wildtype animals compared to the months long waiting process involved in the generation of stable transgenic reporters. Previously published *elf3 in situ* hybridization data in developing larvae indicate that *elf3* is expressed in diverse tissues like the gut, pronephric duct, neuromasts, notochord, among others (Sarmah et al., 2022). These data can be used to validate *elf3* expression patterns identified with the discussed tools.

Once the concern of generating *elf3* transgenic reporter or HCR probes has been addressed, there are so many exciting ways in which these tools could be applied to answer questions about the expression and microbial responsiveness of *elf3*. For instance, is there tissue specificity associated with upregulation of *elf3* in response to microbiota? One of the limitations of the current work is that the bulk RNA-seq experiments were performed using RNA extracted from whole larvae at a singular timepoint. As a result, we do not have the resolution to address the spatiotemporal dynamics of microbial induction of *elf3*. It would be informative to compare germ-free and conventionalized transgenic larvae at various timepoints following microbial exposure to identify if there are (1) specific tissue types in which reporter expression is induced and (2) the earliest and latest timepoints in which reporter expression is CV larvae is higher than GF. These imaging experiments could be coupled with qRT-PCR assessment of *elf3* mRNA levels in specific tissues to validate if the reporter recapitulates dynamic changes in endogenous

*elf3* transcripts. We could use the validated reporter to begin addressing if transcription factors like NF- $\kappa$ B, Egr1, or other immune signaling host factors (pattern recognition receptors, adapter proteins, etc.) mediate its expression and microbial responsiveness. Future work might start with injecting pools of sgRNAs targeting these host factors in transgenic embryos and comparing *elf3* reporter expression or HCR probe fluorescence to control fish injected with sgRNAs targeting pigmentation genes that produce obvious phenotypes when mutated (Sarmah et al., 2022). While it is possible that the host factors mediating the tissue-specific expression of *elf3* are differential to those that regulate its microbial responsiveness, completing these CRISPR pool experiments under conventional conditions is preferable for generation of a candidate gene list. A good candidate mediator is a gene for which CRISPR pool-mediated knockdown results in significant reductions in *elf3* reporter expression or HCR probe fluorescence. These experiments might ultimately lead to injecting CRISPR pools in gnotobiotic experiments for comparisons between GF and colonized animals; however, there may be pitfalls associated with keeping the injected fish GF. It might be more advantageous to perform these experiments once stable mutant lines of the candidates have been generated.

Additional uses of the proposed *elf3* transgenic and HCR probe approaches include performing monoassociation experiments with isolated bacterial strains to determine if there is specificity for microbial induction of *elf3*. Transcriptomic data from published larval monoassociations suggest that *elf3* expression is not induced following colonization by *Exiguobacterium* sp. ZWU0009, but it is induced in response to *Chryseobacterium* sp. ZOR0023 monoassociation (Koch et al., 2018). These data suggest that there are microbe-specific factors that contribute to the microbial responsiveness of *elf3*. Future gnotobiotic experiments featuring a panel of bacterial strains in wildtype larvae could address whether some microbes are more potent in their induction of *elf3* than others and putatively identify microbes that even suppress *elf3* expression. Interesting bacterial candidates identified in these experiments might lead to future

work testing whether it is a bacterial component or secreted effector that can induce *elf3* expression and eventually attempt to identify specific bacterial metabolites that mediate *elf3*. It is also possible to perform gnotobiotic experiments in which germ-free larvae are exposed to “microbe associated molecular patterns” (MAMPs) including flagellin, lipopolysaccharide, and peptidoglycan to determine whether these components can induce *elf3* expression in larvae (Newman et al., 2013). These data could also inform the CRISPR-pool mediated approaches for understanding upstream host factors that mediate *elf3* expression because many of these MAMPs are recognized by specific pattern recognition receptors (Akira et al., 2001; Li & Wu, 2021). For instance, a specific response to flagellin suggests that toll-like receptor 5 (*tlr5a/b*) is a putative mediator of *elf3* expression, and this could be further tested in gnotobiotic experiments with *tlr5* mutant larvae (Akira et al., 2001; Li & Wu, 2021). It would be preferable to perform imaging assays to visualize these effects; however, qRT-PCR analysis of *elf3* transcript levels in whole larvae or specific tissue types would suffice.

### **3.1.3 *elf3* infections models**

In this work, we observed that *elf3* mutant adults had poor survival that was associated with swim bladder inflammation. This observation has sparked several questions about the factors initiating health deterioration. What triggers the swim bladder inflammation? Are microbes causative? One of my greatest hopes for the future of the *elf3* project is investigation of putative causal microbes for swim bladder inflammation. I would like to see a much larger screen of bacteria cultured from the swim bladders of moribund *elf3*<sup>-/-</sup> mutants and wildtype controls. A larger “n” for these experiments compared to what we have reported here would help draw more definitive conclusions about whether there is a consistent pattern of culturable microbes within or surrounding the swim bladder of fish presenting abnormal swimming behaviors. Future work could then attempt to perform injection or immersion exposure models with candidate microbes and report whether *elf3* mutants are more susceptible than wildtype animals. Identification of a

causal microbe could also be used to address questions about the disparity in survival between *elf3* larvae and adults. Are there unique aspects of the role of *elf3* in larval zebrafish that render them more resistant to infection? These experiments could be performed if there is a way to experimentally induce swim bladder inflammation at both developmental stages.

While the idea of isolating a putative causal microbe is proactive, there are several pitfalls that would make this work particularly challenging. It is possible that the swim bladder inflammation we observe in mutants precedes colonization of the swim bladder by opportunistic microbes, and thus, isolated microbes are not causal but are simply able to take advantage of the pre-existing inflamed environment. Another important consideration is that there is potential for the causal microbe or microbes to be viral or fungal and not bacterial. Previous research indicates that an isolated Rhabdovirus can cause swim bladder infection in carp (Bachmann & Ahne, 1974). Techniques for culturing virus from the swim bladders of *elf3* mutant swim bladders would require additional expertise. Finally, it is also possible that there is a causal microbe or consortium of microbes that cannot be cultured using standard laboratory techniques, and thus, a limitation in current available tools might prevent the establishment of an *elf3* infection model.

The other perspective of an *elf3* infection model is to apply the *elf3* allele to current infection models in zebrafish and evaluate whether mutants have an increased susceptibility to infection. The data from the larval bulk RNA-seq experiments suggest that *elf3* mutants exhibit an attenuated immune response in response to microbes. It is possible that this attenuated immune response might leave *elf3* mutant larvae and adults more susceptible to opportunistic microbes and other pathogens. My hope is that the *elf3* mutants can serve as a resource for the zebrafish community similarly to how other immune signaling mutants (e.g., *myd88*, *tlr2*, etc.) are used to investigate host factors mediating responses to infection (van der Sar et al., 2006; van der Vaart et al., 2013; van Soest et al., 2011).

### ***3.2 Concluding remarks***

In this work, we identified epithelial transcription factor *elf3* as a mediator of host-microbiota interactions in larval zebrafish. I remain extremely optimistic that many of the remaining questions introduced in this chapter will be addressed by the field within the next few years. Humans and other animals are constantly navigating the push and pull between beneficial and harmful interactions with microbes, and thus a greater understanding of what facilitates these interactions has important implications for improving human health and combatting disease. I believe that investigation of host-microbiota interactions will remain an important scientific field for innovation and therapeutic intervention as we continue to navigate dynamic changes (e.g., climate change, urbanization, etc.) on our planet.

## References

- Abt, M. C., Osborne, L. C., Monticelli, L. A., Doering, T. A., Alenghat, T., Sonnenberg, G. F., Paley, M. A., Antenus, M., Williams, K. L., Erikson, J., Wherry, E. J., & Artis, D. (2012). Commensal bacteria calibrate the activation threshold of innate antiviral immunity. *Immunity*, *37*(1), 158-170. <https://doi.org/10.1016/j.immuni.2012.04.011>
- Akira, S., Takeda, K., & Kaisho, T. (2001). Toll-like receptors: critical proteins linking innate and acquired immunity. *Nat Immunol*, *2*(8), 675-680. <https://doi.org/10.1038/90609>
- Al-Asmakh, M., & Zadjali, F. (2015). Use of Germ-Free Animal Models in Microbiota-Related Research. *J Microbiol Biotechnol*, *25*(10), 1583-1588. <https://doi.org/10.4014/jmb.1501.01039>
- Albino, D., Longoni, N., Curti, L., Mello-Grand, M., Pinton, S., Civenni, G., Thalmann, G., D'Ambrosio, G., Sarti, M., Sessa, F., Chiorino, G., Catapano, C. V., & Carbone, G. M. (2012). ESE3/EHF controls epithelial cell differentiation and its loss leads to prostate tumors with mesenchymal and stem-like features. *Cancer Res*, *72*(11), 2889-2900. <https://doi.org/10.1158/0008-5472.CAN-12-0212>
- Astrofsky, K. M., Schrenzel, M. D., Bullis, R. A., Smolowitz, R. M., & Fox, J. G. (2000). Diagnosis and management of atypical Mycobacterium spp. infections in established laboratory zebrafish (*Brachydanio rerio*) facilities. *Comp Med*, *50*(6), 666-672. <https://www.ncbi.nlm.nih.gov/pubmed/11200575>
- Auer, T. O., Duroure, K., De Cian, A., Concordet, J. P., & Del Bene, F. (2014). Highly efficient CRISPR/Cas9-mediated knock-in in zebrafish by homology-independent DNA repair. *Genome Res*, *24*(1), 142-153. <https://doi.org/10.1101/gr.161638.113>
- Bachmann, P. A., & Ahne, W. (1974). Biological properties and identification of the agent causing swim bladder inflammation in carp. *Arch Gesamte Virusforsch*, *44*(3), 261-269. <https://doi.org/10.1007/BF01240614>
- Backhed, F., Ding, H., Wang, T., Hooper, L. V., Koh, G. Y., Nagy, A., Semenkovich, C. F., & Gordon, J. I. (2004). The gut microbiota as an environmental factor that regulates fat storage. *Proc Natl Acad Sci U S A*, *101*(44), 15718-15723. <https://doi.org/10.1073/pnas.0407076101>
- Basic, M., & Bleich, A. (2019). Gnotobiotics: Past, present and future. *Lab Anim*, *53*(3), 232-243. <https://doi.org/10.1177/0023677219836715>

- Bates, J. M., Akerlund, J., Mittge, E., & Guillemin, K. (2007). Intestinal alkaline phosphatase detoxifies lipopolysaccharide and prevents inflammation in zebrafish in response to the gut microbiota. *Cell Host Microbe*, 2(6), 371-382. <https://doi.org/10.1016/j.chom.2007.10.010>
- Bates, J. M., Mittge, E., Kuhlman, J., Baden, K. N., Cheesman, S. E., & Guillemin, K. (2006). Distinct signals from the microbiota promote different aspects of zebrafish gut differentiation. *Dev Biol*, 297(2), 374-386. <https://doi.org/10.1016/j.ydbio.2006.05.006>
- Bek, J. W., Shochat, C., De Clercq, A., De Saffel, H., Boel, A., Metz, J., Rodenburg, F., Karasik, D., Willaert, A., & Coucke, P. J. (2021). Lrp5 Mutant and Crispant Zebrafish Faithfully Model Human Osteoporosis, Establishing the Zebrafish as a Platform for CRISPR-Based Functional Screening of Osteoporosis Candidate Genes. *J Bone Miner Res*, 36(9), 1749-1764. <https://doi.org/10.1002/jbmr.4327>
- Belele, C. L., English, M. A., Chahal, J., Burnetti, A., Finckbeiner, S. M., Gibney, G., Kirby, M., Sood, R., & Liu, P. P. (2009). Differential requirement for Gata1 DNA binding and transactivation between primitive and definitive stages of hematopoiesis in zebrafish. *Blood*, 114(25), 5162-5172. <https://doi.org/10.1182/blood-2009-05-224709>
- Bennett, C. M., Kanki, J. P., Rhodes, J., Liu, T. X., Paw, B. H., Kieran, M. W., Langenau, D. M., Delahaye-Brown, A., Zon, L. I., Fleming, M. D., & Look, A. T. (2001). Myelopoiesis in the zebrafish, *Danio rerio*. *Blood*, 98(3), 643-651. <https://doi.org/10.1182/blood.v98.3.643>
- Bertrand, J. Y., Chi, N. C., Santoso, B., Teng, S., Stainier, D. Y., & Traver, D. (2010). Haematopoietic stem cells derive directly from aortic endothelium during development. *Nature*, 464(7285), 108-111. <https://doi.org/10.1038/nature08738>
- Bhaya, D., Davison, M., & Barrangou, R. (2011). CRISPR-Cas systems in bacteria and archaea: versatile small RNAs for adaptive defense and regulation. *Annu Rev Genet*, 45, 273-297. <https://doi.org/10.1146/annurev-genet-110410-132430>
- Bi, X., Wang, K., Yang, L., Pan, H., Jiang, H., Wei, Q., Fang, M., Yu, H., Zhu, C., Cai, Y., He, Y., Gan, X., Zeng, H., Yu, D., Zhu, Y., Jiang, H., Qiu, Q., Yang, H., Zhang, Y. E.,...Zhang, G. (2021). Tracing the genetic footprints of vertebrate landing in non-teleost ray-finned fishes. *Cell*, 184(5), 1377-1391 e1314. <https://doi.org/10.1016/j.cell.2021.01.046>
- Bibikova, M., Carroll, D., Segal, D. J., Trautman, J. K., Smith, J., Kim, Y. G., & Chandrasegaran, S. (2001). Stimulation of homologous recombination through targeted cleavage by chimeric nucleases. *Mol Cell Biol*, 21(1), 289-297. <https://doi.org/10.1128/MCB.21.1.289-297.2001>

- Boisset, J. C., van Cappellen, W., Andrieu-Soler, C., Galjart, N., Dzierzak, E., & Robin, C. (2010). In vivo imaging of haematopoietic cells emerging from the mouse aortic endothelium. *Nature*, *464*(7285), 116-120. <https://doi.org/10.1038/nature08764>
- Bottiglione, F., Dee, C. T., Lea, R., Zeef, L. A. H., Badrock, A. P., Wane, M., Bugeon, L., Dallman, M. J., Allen, J. E., & Hurlstone, A. F. L. (2020). Zebrafish IL-4-like Cytokines and IL-10 Suppress Inflammation but Only IL-10 Is Essential for Gill Homeostasis. *J Immunol*, *205*(4), 994-1008. <https://doi.org/10.4049/jimmunol.2000372>
- Bresciani, E., Carrington, B., Wincovitch, S., Jones, M., Gore, A. V., Weinstein, B. M., Sood, R., & Liu, P. P. (2014). CBFbeta and RUNX1 are required at 2 different steps during the development of hematopoietic stem cells in zebrafish. *Blood*, *124*(1), 70-78. <https://doi.org/10.1182/blood-2013-10-531988>
- Brown, C., Gaspar, J., Pettit, A., Lee, R., Gu, X., Wang, H., Manning, C., Voland, C., Goldring, S. R., Goldring, M. B., Libermann, T. A., Gravallese, E. M., & Oettgen, P. (2004). ESE-1 is a novel transcriptional mediator of angiopoietin-1 expression in the setting of inflammation. *J Biol Chem*, *279*(13), 12794-12803. <https://doi.org/10.1074/jbc.M308593200>
- Brown, R. L., Sequeira, R. P., & Clarke, T. B. (2017). The microbiota protects against respiratory infection via GM-CSF signaling. *Nat Commun*, *8*(1), 1512. <https://doi.org/10.1038/s41467-017-01803-x>
- Brownlie, A., Hersey, C., Oates, A. C., Paw, B. H., Falick, A. M., Witkowska, H. E., Flint, J., Higgs, D., Jessen, J., Bahary, N., Zhu, H., Lin, S., & Zon, L. (2003). Characterization of embryonic globin genes of the zebrafish. *Dev Biol*, *255*(1), 48-61. [https://doi.org/10.1016/s0012-1606\(02\)00041-6](https://doi.org/10.1016/s0012-1606(02)00041-6)
- Buccitelli, C., & Selbach, M. (2020). mRNAs, proteins and the emerging principles of gene expression control. *Nat Rev Genet*, *21*(10), 630-644. <https://doi.org/10.1038/s41576-020-0258-4>
- Burns, A. R., & Guillemin, K. (2017). The scales of the zebrafish: host-microbiota interactions from proteins to populations. *Curr Opin Microbiol*, *38*, 137-141. <https://doi.org/10.1016/j.mib.2017.05.011>
- Burns, C. E., DeBlasio, T., Zhou, Y., Zhang, J., Zon, L., & Nimer, S. D. (2002). Isolation and characterization of runxa and runxb, zebrafish members of the runt family of transcriptional regulators. *Exp Hematol*, *30*(12), 1381-1389. [https://doi.org/10.1016/s0301-472x\(02\)00955-4](https://doi.org/10.1016/s0301-472x(02)00955-4)

- Byrd, A. L., Belkaid, Y., & Segre, J. A. (2018). The human skin microbiome. *Nat Rev Microbiol*, *16*(3), 143-155. <https://doi.org/10.1038/nrmicro.2017.157>
- Caballero-Flores, G., Pickard, J. M., & Nunez, G. (2023). Microbiota-mediated colonization resistance: mechanisms and regulation. *Nat Rev Microbiol*, *21*(6), 347-360. <https://doi.org/10.1038/s41579-022-00833-7>
- Camp, J. G., Frank, C. L., Lickwar, C. R., Guturu, H., Rube, T., Wenger, A. M., Chen, J., Bejerano, G., Crawford, G. E., & Rawls, J. F. (2014). Microbiota modulate transcription in the intestinal epithelium without remodeling the accessible chromatin landscape. *Genome Res*, *24*(9), 1504-1516. <https://doi.org/10.1101/gr.165845.113>
- Camp, J. G., Jazwa, A. L., Trent, C. M., & Rawls, J. F. (2012). Intronic cis-regulatory modules mediate tissue-specific and microbial control of *angptl4/fiaf* transcription. *PLoS Genet*, *8*(3), e1002585. <https://doi.org/10.1371/journal.pgen.1002585>
- Cass, A. N., Servetnick, M. D., & McCune, A. R. (2013). Expression of a lung developmental cassette in the adult and developing zebrafish swimbladder. *Evol Dev*, *15*(2), 119-132. <https://doi.org/10.1111/ede.12022>
- Chai, T., Shen, J., Sheng, Y., Huang, Y., Liang, W., Zhang, Z., Zhao, R., Shang, H., Cheng, W., Zhang, H., Chen, X., Huang, X., Zhang, Y., Liu, J., Yang, H., Wang, L., Pan, S., Chen, Y., Han, L.,...Fang, X. (2024). Effects of flora deficiency on the structure and function of the large intestine. *iScience*, *27*(2), 108941. <https://doi.org/10.1016/j.isci.2024.108941>
- Cheesman, S. E., Neal, J. T., Mittge, E., Seredick, B. M., & Guillemin, K. (2011). Epithelial cell proliferation in the developing zebrafish intestine is regulated by the Wnt pathway and microbial signaling via Myd88. *Proc Natl Acad Sci U S A*, *108* Suppl 1(Suppl 1), 4570-4577. <https://doi.org/10.1073/pnas.1000072107>
- Childers, L., Park, J., Wang, S., Liu, R., Barry, R., Watts, S. A., Rawls, J. F., & Bagnat, M. (2024). Protein absorption in the zebrafish gut is regulated by interactions between lysosome rich enterocytes and the microbiome. *bioRxiv*. <https://doi.org/10.1101/2024.06.07.597998>
- Choe, C. P., Choi, S. Y., Kee, Y., Kim, M. J., Kim, S. H., Lee, Y., Park, H. C., & Ro, H. (2021). Transgenic fluorescent zebrafish lines that have revolutionized biomedical research. *Lab Anim Res*, *37*(1), 26. <https://doi.org/10.1186/s42826-021-00103-2>
- Choi, H. M. T., Schwarzkopf, M., Fornace, M. E., Acharya, A., Artavanis, G., Stegmaier, J., Cunha, A., & Pierce, N. A. (2018). Third-generation in situ hybridization chain reaction:

multiplexed, quantitative, sensitive, versatile, robust. *Development*, 145(12).  
<https://doi.org/10.1242/dev.165753>

- Choi, S. G., Yi, Y., Kim, Y. S., Kato, M., Chang, J., Chung, H. W., Hahm, K. B., Yang, H. K., Rhee, H. H., Bang, Y. J., & Kim, S. J. (1998). A novel ets-related transcription factor, ERT/ESX/ESE-1, regulates expression of the transforming growth factor-beta type II receptor. *J Biol Chem*, 273(1), 110-117. <https://doi.org/10.1074/jbc.273.1.110>
- Christian, M., Cermak, T., Doyle, E. L., Schmidt, C., Zhang, F., Hummel, A., Bogdanove, A. J., & Voytas, D. F. (2010). Targeting DNA double-strand breaks with TAL effector nucleases. *Genetics*, 186(2), 757-761. <https://doi.org/10.1534/genetics.110.120717>
- Chun, C. K., Troll, J. V., Koroleva, I., Brown, B., Manzella, L., Snir, E., Almabrazi, H., Scheetz, T. E., Bonaldo Mde, F., Casavant, T. L., Soares, M. B., Ruby, E. G., & McFall-Ngai, M. J. (2008). Effects of colonization, luminescence, and autoinducer on host transcription during development of the squid-vibrio association. *Proc Natl Acad Sci U S A*, 105(32), 11323-11328. <https://doi.org/10.1073/pnas.0802369105>
- Clarke, T. B., Davis, K. M., Lysenko, E. S., Zhou, A. Y., Yu, Y., & Weiser, J. N. (2010). Recognition of peptidoglycan from the microbiota by Nod1 enhances systemic innate immunity. *Nat Med*, 16(2), 228-231. <https://doi.org/10.1038/nm.2087>
- Collins, J. T., Nguyen, A., & Badireddy, M. (2025). Anatomy, Abdomen and Pelvis, Small Intestine. In *StatPearls*. <https://www.ncbi.nlm.nih.gov/pubmed/29083773>
- Consortium, E. P. (2012). An integrated encyclopedia of DNA elements in the human genome. *Nature*, 489(7414), 57-74. <https://doi.org/10.1038/nature11247>
- Costa, M. M., Saraceni, P. R., Forn-Cuni, G., Dios, S., Romero, A., Figueras, A., & Novoa, B. (2013). IL-22 is a key player in the regulation of inflammation in fish and involves innate immune cells and PI3K signaling. *Dev Comp Immunol*, 41(4), 746-755. <https://doi.org/10.1016/j.dci.2013.08.021>
- Cronan, M. R., & Tobin, D. M. (2014). Fit for consumption: zebrafish as a model for tuberculosis. *Dis Model Mech*, 7(7), 777-784. <https://doi.org/10.1242/dmm.016089>
- Cronan, M. R., & Tobin, D. M. (2019). Endogenous Tagging at the *cdh1* Locus for Live Visualization of E-Cadherin Dynamics. *Zebrafish*, 16(3), 324-325. <https://doi.org/10.1089/zeb.2019.1746>

- Daniels, C. B., & Orgeig, S. (2001). The comparative biology of pulmonary surfactant: past, present and future. *Comp Biochem Physiol A Mol Integr Physiol*, 129(1), 9-36. [https://doi.org/10.1016/s1095-6433\(01\)00303-8](https://doi.org/10.1016/s1095-6433(01)00303-8)
- Davidson, A. J., & Zon, L. I. (2004). The 'definitive' (and 'primitive') guide to zebrafish hematopoiesis. *Oncogene*, 23(43), 7233-7246. <https://doi.org/10.1038/sj.onc.1207943>
- Davis, C. A., Hitz, B. C., Sloan, C. A., Chan, E. T., Davidson, J. M., Gabdank, I., Hilton, J. A., Jain, K., Baymuradov, U. K., Narayanan, A. K., Onate, K. C., Graham, K., Miyasato, S. R., Dreszer, T. R., Strattan, J. S., Jolanki, O., Tanaka, F. Y., & Cherry, J. M. (2018). The Encyclopedia of DNA elements (ENCODE): data portal update. *Nucleic Acids Res*, 46(D1), D794-D801. <https://doi.org/10.1093/nar/gkx1081>
- Davison, J. M., Lickwar, C. R., Song, L., Breton, G., Crawford, G. E., & Rawls, J. F. (2017). Microbiota regulate intestinal epithelial gene expression by suppressing the transcription factor Hepatocyte nuclear factor 4 alpha. *Genome Res*, 27(7), 1195-1206. <https://doi.org/10.1101/gr.220111.116>
- de Jong, J. L., & Zon, L. I. (2005). Use of the zebrafish system to study primitive and definitive hematopoiesis. *Annu Rev Genet*, 39, 481-501. <https://doi.org/10.1146/annurev.genet.39.073003.095931>
- Debaenst, S., Jarayseh, T., De Saffel, H., Bek, J. W., Boone, M., Josipovic, I., Kibleur, P., Kwon, R. Y., Coucke, P. J., & Willaert, A. (2025). Crispant analysis in zebrafish as a tool for rapid functional screening of disease-causing genes for bone fragility. *Elife*, 13. <https://doi.org/10.7554/eLife.100060>
- Degnan, B. M., Degnan, S. M., Naganuma, T., & Morse, D. E. (1993). The ets multigene family is conserved throughout the Metazoa. *Nucleic Acids Res*, 21(15), 3479-3484. <https://doi.org/10.1093/nar/21.15.3479>
- Deshmukh, H. S., Liu, Y., Menkiti, O. R., Mei, J., Dai, N., O'Leary, C. E., Oliver, P. M., Kolls, J. K., Weiser, J. N., & Worthen, G. S. (2014). The microbiota regulates neutrophil homeostasis and host resistance to Escherichia coli K1 sepsis in neonatal mice. *Nat Med*, 20(5), 524-530. <https://doi.org/10.1038/nm.3542>
- Detrich, H. W., 3rd, Kieran, M. W., Chan, F. Y., Barone, L. M., Yee, K., Rundstadler, J. A., Pratt, S., Ransom, D., & Zon, L. I. (1995). Intraembryonic hematopoietic cell migration during vertebrate development. *Proc Natl Acad Sci U S A*, 92(23), 10713-10717. <https://doi.org/10.1073/pnas.92.23.10713>

- Diaferia, G. R., Balestrieri, C., Prosperini, E., Nicoli, P., Spaggiari, P., Zerbi, A., & Natoli, G. (2016). Dissection of transcriptional and cis-regulatory control of differentiation in human pancreatic cancer. *EMBO J*, *35*(6), 595-617. <https://doi.org/10.15252/emboj.201592404>
- Dobin, A., Davis, C. A., Schlesinger, F., Drenkow, J., Zaleski, C., Jha, S., Batut, P., Chaisson, M., & Gingeras, T. R. (2013). STAR: ultrafast universal RNA-seq aligner. *Bioinformatics*, *29*(1), 15-21. <https://doi.org/10.1093/bioinformatics/bts635>
- Dobson, G. P., Letson, H. L., Biros, E., & Morris, J. (2019). Specific pathogen-free (SPF) animal status as a variable in biomedical research: Have we come full circle? *EBioMedicine*, *41*, 42-43. <https://doi.org/10.1016/j.ebiom.2019.02.038>
- Dong, D., Na, L., Zhou, K., Wang, Z., Sun, Y., Zheng, Q., Gao, J., Zhao, C., & Wang, W. (2021). FZD5 prevents epithelial-mesenchymal transition in gastric cancer. *Cell Commun Signal*, *19*(1), 21. <https://doi.org/10.1186/s12964-021-00708-z>
- Dong, Z., Yang, L., Lu, J., Guo, Y., Shen, S., Liang, J., & Guo, W. (2022). Downregulation of LINC00886 facilitates epithelial-mesenchymal transition through SIRT7/ELF3/miR-144 pathway in esophageal squamous cell carcinoma. *Clin Exp Metastasis*, *39*(4), 661-677. <https://doi.org/10.1007/s10585-022-10171-w>
- Dongre, A., & Weinberg, R. A. (2019). New insights into the mechanisms of epithelial-mesenchymal transition and implications for cancer. *Nat Rev Mol Cell Biol*, *20*(2), 69-84. <https://doi.org/10.1038/s41580-018-0080-4>
- Doyon, Y., McCammon, J. M., Miller, J. C., Faraji, F., Ngo, C., Katibah, G. E., Amora, R., Hocking, T. D., Zhang, L., Rebar, E. J., Gregory, P. D., Urnov, F. D., & Amacher, S. L. (2008). Heritable targeted gene disruption in zebrafish using designed zinc-finger nucleases. *Nat Biotechnol*, *26*(6), 702-708. <https://doi.org/10.1038/nbt1409>
- Dumas, A., Bernard, L., Poquet, Y., Lugo-Villarino, G., & Neyrolles, O. (2018). The role of the lung microbiota and the gut-lung axis in respiratory infectious diseases. *Cell Microbiol*, *20*(12), e12966. <https://doi.org/10.1111/cmi.12966>
- Dumbarton, T. C., Stoyek, M., Croll, R. P., & Smith, F. M. (2010). Adrenergic control of swimbladder deflation in the zebrafish (*Danio rerio*). *J Exp Biol*, *213*(Pt 14), 2536-2546. <https://doi.org/10.1242/jeb.039792>
- Dusing, M. R., Brickner, A. G., Lowe, S. Y., Cohen, M. B., & Wiginton, D. A. (2000). A duodenum-specific enhancer regulates expression along three axes in the small intestine.

*Am J Physiol Gastrointest Liver Physiol*, 279(5), G1080-1093.  
<https://doi.org/10.1152/ajpgi.2000.279.5.G1080>

- Dykova, I., Zak, J., Reichard, M., Souckova, K., Slaby, O., & Blazek, R. (2021). Swim bladder as a primary site of mycobacterial infection in *Nothobranchius* 'belly sliders'. *Dis Aquat Organ*, 145, 111-117. <https://doi.org/10.3354/dao03601>
- Eisen, J. S., & Smith, J. C. (2008). Controlling morpholino experiments: don't stop making antisense. *Development*, 135(10), 1735-1743. <https://doi.org/10.1242/dev.001115>
- El Aidy, S., Merrifield, C. A., Derrien, M., van Baarlen, P., Hooiveld, G., Levenez, F., Dore, J., Dekker, J., Holmes, E., Claus, S. P., Reijngoud, D. J., & Kleerebezem, M. (2013). The gut microbiota elicits a profound metabolic reorientation in the mouse jejunal mucosa during conventionalisation. *Gut*, 62(9), 1306-1314. <https://doi.org/10.1136/gutjnl-2011-301955>
- El-Brolosy, M. A., Kontarakis, Z., Rossi, A., Kuenne, C., Günther, S., Fukuda, N., Kikhi, K., Boezio, G. L. M., Takacs, C. M., Lai, S. L., Fukuda, R., Gerri, C., Giraldez, A. J., & Stainier, D. Y. R. (2019). Genetic compensation triggered by mutant mRNA degradation. *Nature*, 568(7751), 193-197. <https://doi.org/10.1038/s41586-019-1064-z>
- El-Brolosy, M. A., & Stainier, D. Y. R. (2017). Genetic compensation: A phenomenon in search of mechanisms. *PLoS Genet*, 13(7), e1006780. <https://doi.org/10.1371/journal.pgen.1006780>
- Ellett, F., Pase, L., Hayman, J. W., Andrianopoulos, A., & Lieschke, G. J. (2011). *mpeg1* promoter transgenes direct macrophage-lineage expression in zebrafish. *Blood*, 117(4), e49-56. <https://doi.org/10.1182/blood-2010-10-314120>
- Faure, S., & de Santa Barbara, P. (2011). Molecular embryology of the foregut. *J Pediatr Gastroenterol Nutr*, 52 Suppl 1(Suppl 1), S2-3. <https://doi.org/10.1097/MPG.0b013e3182105a1a>
- Feng, Y., Xue, H., Zhu, J., Yang, L., Zhang, F., Qian, R., Lin, W., & Wang, Y. (2016). ESE1 is Associated with Neuronal Apoptosis in Lipopolysaccharide Induced Neuroinflammation. *Neurochem Res*, 41(10), 2752-2762. <https://doi.org/10.1007/s11064-016-1990-1>
- Field, H. A., Ober, E. A., Roeser, T., & Stainier, D. Y. (2003). Formation of the digestive system in zebrafish. I. Liver morphogenesis. *Dev Biol*, 253(2), 279-290. [https://doi.org/10.1016/s0012-1606\(02\)00017-9](https://doi.org/10.1016/s0012-1606(02)00017-9)

- Fischer, K. R., Durrans, A., Lee, S., Sheng, J., Li, F., Wong, S. T., Choi, H., El Rayes, T., Ryu, S., Troeger, J., Schwabe, R. F., Vahdat, L. T., Altorki, N. K., Mittal, V., & Gao, D. (2015). Epithelial-to-mesenchymal transition is not required for lung metastasis but contributes to chemoresistance. *Nature*, *527*(7579), 472-476. <https://doi.org/10.1038/nature15748>
- Flemming, H. C., & Wuertz, S. (2019). Bacteria and archaea on Earth and their abundance in biofilms. *Nat Rev Microbiol*, *17*(4), 247-260. <https://doi.org/10.1038/s41579-019-0158-9>
- Flentjar, N., Chu, P. Y., Ng, A. Y., Johnstone, C. N., Heath, J. K., Ernst, M., Hertzog, P. J., & Pritchard, M. A. (2007). TGF-betaRII rescues development of small intestinal epithelial cells in Elf3-deficient mice. *Gastroenterology*, *132*(4), 1410-1419. <https://doi.org/10.1053/j.gastro.2007.02.054>
- Flores, E. M., Nguyen, A. T., Odem, M. A., Eisenhoffer, G. T., & Krachler, A. M. (2020). The zebrafish as a model for gastrointestinal tract-microbe interactions. *Cell Microbiol*, *22*(3), e13152. <https://doi.org/10.1111/cmi.13152>
- Fossum, S. L., Mutolo, M. J., Tugores, A., Ghosh, S., Randell, S. H., Jones, L. C., Leir, S. H., & Harris, A. (2017). Ets homologous factor (EHF) has critical roles in epithelial dysfunction in airway disease. *J Biol Chem*, *292*(26), 10938-10949. <https://doi.org/10.1074/jbc.M117.775304>
- Fu, Z. D., Selwyn, F. P., Cui, J. Y., & Klaassen, C. D. (2017). RNA-Seq Profiling of Intestinal Expression of Xenobiotic Processing Genes in Germ-Free Mice. *Drug Metab Dispos*, *45*(12), 1225-1238. <https://doi.org/10.1124/dmd.117.077313>
- Fung, K. Y., de Geus, E. D., Ying, L., Cumming, H., Bourke, N., Foster, S. C., & Hertzog, P. J. (2024). Expression of Interferon Epsilon in Mucosal Epithelium is Regulated by Elf3. *Mol Cell Biol*, *44*(8), 334-343. <https://doi.org/10.1080/10985549.2024.2366207>
- Galloway, J. L., Wingert, R. A., Thisse, C., Thisse, B., & Zon, L. I. (2005). Loss of gata1 but not gata2 converts erythropoiesis to myelopoiesis in zebrafish embryos. *Dev Cell*, *8*(1), 109-116. <https://doi.org/10.1016/j.devcel.2004.12.001>
- Galloway, J. L., & Zon, L. I. (2003). Ontogeny of hematopoiesis: examining the emergence of hematopoietic cells in the vertebrate embryo. *Curr Top Dev Biol*, *53*, 139-158. [https://doi.org/10.1016/s0070-2153\(03\)53004-6](https://doi.org/10.1016/s0070-2153(03)53004-6)
- Ganis, J. J., Hsia, N., Trompouki, E., de Jong, J. L., DiBiase, A., Lambert, J. S., Jia, Z., Sabo, P. J., Weaver, M., Sandstrom, R., Stamatoyannopoulos, J. A., Zhou, Y., & Zon, L. I. (2012).

Zebrafish globin switching occurs in two developmental stages and is controlled by the LCR. *Dev Biol*, 366(2), 185-194. <https://doi.org/10.1016/j.ydbio.2012.03.021>

Ge, R., Zhou, Y., Peng, R., Wang, R., Li, M., Zhang, Y., Zheng, C., & Wang, C. (2015). Conservation of the STING-Mediated Cytosolic DNA Sensing Pathway in Zebrafish. *J Virol*, 89(15), 7696-7706. <https://doi.org/10.1128/JVI.01049-15>

Ge, X., Ding, C., Zhao, W., Xu, L., Tian, H., Gong, J., Zhu, M., Li, J., & Li, N. (2017). Antibiotics-induced depletion of mice microbiota induces changes in host serotonin biosynthesis and intestinal motility. *J Transl Med*, 15(1), 13. <https://doi.org/10.1186/s12967-016-1105-4>

Glockner, F. O., Yilmaz, P., Quast, C., Gerken, J., Beccati, A., Ciuprina, A., Bruns, G., Yarza, P., Peplies, J., Westram, R., & Ludwig, W. (2017). 25 years of serving the community with ribosomal RNA gene reference databases and tools. *J Biotechnol*, 261, 169-176. <https://doi.org/10.1016/j.jbiotec.2017.06.1198>

Gordon, H. A. (1960). The germ-free animal. Its use in the study of "physiologic" effects of the normal microbial flora on the animal host. *Am J Dig Dis*, 5, 841-867. <https://doi.org/10.1007/BF02232187>

Gore, A. V., Pillay, L. M., Venero Galanternik, M., & Weinstein, B. M. (2018). The zebrafish: A fantastic model for hematopoietic development and disease. *Wiley Interdiscip Rev Dev Biol*, 7(3), e312. <https://doi.org/10.1002/wdev.312>

Grall, F., Gu, X., Tan, L., Cho, J. Y., Inan, M. S., Pettit, A. R., Thamrongsak, U., Choy, B. K., Manning, C., Akbarali, Y., Zerbini, L., Rudders, S., Goldring, S. R., Gravallesse, E. M., Oettgen, P., Goldring, M. B., & Libermann, T. A. (2003). Responses to the proinflammatory cytokines interleukin-1 and tumor necrosis factor alpha in cells derived from rheumatoid synovium and other joint tissues involve nuclear factor kappaB-mediated induction of the Ets transcription factor ESE-1. *Arthritis Rheum*, 48(5), 1249-1260. <https://doi.org/10.1002/art.10942>

Grall, F. T., Prall, W. C., Wei, W., Gu, X., Cho, J. Y., Choy, B. K., Zerbini, L. F., Inan, M. S., Goldring, S. R., Gravallesse, E. M., Goldring, M. B., Oettgen, P., & Libermann, T. A. (2005). The Ets transcription factor ESE-1 mediates induction of the COX-2 gene by LPS in monocytes. *FEBS J*, 272(7), 1676-1687. <https://doi.org/10.1111/j.1742-4658.2005.04592.x>

Gratacap, R. L., Bergeron, A. C., & Wheeler, R. T. (2014). Modeling mucosal candidiasis in larval zebrafish by swimbladder injection. *J Vis Exp*(93), e52182. <https://doi.org/10.3791/52182>

- Gratacap, R. L., Rawls, J. F., & Wheeler, R. T. (2013). Mucosal candidiasis elicits NF-kappaB activation, proinflammatory gene expression and localized neutrophilia in zebrafish. *Dis Model Mech*, 6(5), 1260-1270. <https://doi.org/10.1242/dmm.012039>
- Gratacap, R. L., Scherer, A. K., Seman, B. G., & Wheeler, R. T. (2017). Control of Mucosal Candidiasis in the Zebrafish Swim Bladder Depends on Neutrophils That Block Filament Invasion and Drive Extracellular-Trap Production. *Infect Immun*, 85(9). <https://doi.org/10.1128/IAI.00276-17>
- Gregorieff, A., Stange, D. E., Kujala, P., Begthel, H., van den Born, M., Korving, J., Peters, P. J., & Clevers, H. (2009). The ets-domain transcription factor Spdef promotes maturation of goblet and paneth cells in the intestinal epithelium. *Gastroenterology*, 137(4), 1333-1345 e1331-1333. <https://doi.org/10.1053/j.gastro.2009.06.044>
- Grunwald, D. J., & Eisen, J. S. (2002). Headwaters of the zebrafish -- emergence of a new model vertebrate. *Nat Rev Genet*, 3(9), 717-724. <https://doi.org/10.1038/nrg892>
- Guo, C., Ma, X., Gao, F., & Guo, Y. (2023). Off-target effects in CRISPR/Cas9 gene editing. *Front Bioeng Biotechnol*, 11, 1143157. <https://doi.org/10.3389/fbioe.2023.1143157>
- Gupta, R. M., & Musunuru, K. (2014). Expanding the genetic editing tool kit: ZFNs, TALENs, and CRISPR-Cas9. *J Clin Invest*, 124(10), 4154-4161. <https://doi.org/10.1172/JCI72992>
- Gutierrez-Hartmann, A., Duval, D. L., & Bradford, A. P. (2007). ETS transcription factors in endocrine systems. *Trends Endocrinol Metab*, 18(4), 150-158. <https://doi.org/10.1016/j.tem.2007.03.002>
- Haber, A. L., Biton, M., Rogel, N., Herbst, R. H., Shekhar, K., Smillie, C., Burgin, G., Delorey, T. M., Howitt, M. R., Katz, Y., Tirosh, I., Beyaz, S., Dionne, D., Zhang, M., Raychowdhury, R., Garrett, W. S., Rozenblatt-Rosen, O., Shi, H. N., Yilmaz, O.,...Regev, A. (2017). A single-cell survey of the small intestinal epithelium. *Nature*, 551(7680), 333-339. <https://doi.org/10.1038/nature24489>
- Han, M. K., Zhou, Y., Murray, S., Tayob, N., Noth, I., Lama, V. N., Moore, B. B., White, E. S., Flaherty, K. R., Huffnagle, G. B., Martinez, F. J., & Investigators, C. (2014). Lung microbiome and disease progression in idiopathic pulmonary fibrosis: an analysis of the COMET study. *Lancet Respir Med*, 2(7), 548-556. [https://doi.org/10.1016/S2213-2600\(14\)70069-4](https://doi.org/10.1016/S2213-2600(14)70069-4)
- Harvie, E. A., & Huttenlocher, A. (2015). Neutrophils in host defense: new insights from zebrafish. *J Leukoc Biol*, 98(4), 523-537. <https://doi.org/10.1189/jlb.4MR1114-524R>

- Heinz, S., Benner, C., Spann, N., Bertolino, E., Lin, Y. C., Laslo, P., Cheng, J. X., Murre, C., Singh, H., & Glass, C. K. (2010). Simple combinations of lineage-determining transcription factors prime cis-regulatory elements required for macrophage and B cell identities. *Mol Cell*, *38*(4), 576-589. <https://doi.org/10.1016/j.molcel.2010.05.004>
- Heppert, J. K., Davison, J. M., Kelly, C., Mercado, G. P., Lickwar, C. R., & Rawls, J. F. (2021). Transcriptional programmes underlying cellular identity and microbial responsiveness in the intestinal epithelium. *Nat Rev Gastroenterol Hepatol*, *18*(1), 7-23. <https://doi.org/10.1038/s41575-020-00357-6>
- Heppert, J. K., Lickwar, C. R., Tillman, M. C., Davis, B. R., Davison, J. M., Lu, H. Y., Chen, W., Busch-Nentwich, E. M., Corcoran, D. L., & Rawls, J. F. (2022). Conserved roles for Hnf4 family transcription factors in zebrafish development and intestinal function. *Genetics*, *222*(4). <https://doi.org/10.1093/genetics/iyac133>
- Herbomel, P., Thisse, B., & Thisse, C. (1999). Ontogeny and behaviour of early macrophages in the zebrafish embryo. *Development*, *126*(17), 3735-3745. <https://doi.org/10.1242/dev.126.17.3735>
- Hollenhorst, P. C., McIntosh, L. P., & Graves, B. J. (2011). Genomic and biochemical insights into the specificity of ETS transcription factors. *Annu Rev Biochem*, *80*, 437-471. <https://doi.org/10.1146/annurev.biochem.79.081507.103945>
- Hooper, L. V. (2015). Epithelial cell contributions to intestinal immunity. *Adv Immunol*, *126*, 129-172. <https://doi.org/10.1016/bs.ai.2014.11.003>
- Hooper, L. V., Wong, M. H., Thelin, A., Hansson, L., Falk, P. G., & Gordon, J. I. (2001). Molecular analysis of commensal host-microbial relationships in the intestine. *Science*, *291*(5505), 881-884. <https://doi.org/10.1126/science.291.5505.881>
- Hou, Y., Sheng, Z., Mao, X., Li, C., Chen, J., Zhang, J., Huang, H., Ruan, H., Luo, L., & Li, L. (2016). Systemic inoculation of *Escherichia coli* causes emergency myelopoiesis in zebrafish larval caudal hematopoietic tissue. *Sci Rep*, *6*, 36853. <https://doi.org/10.1038/srep36853>
- Husebye, E., Hellstrom, P. M., & Midtvedt, T. (1994). Intestinal microflora stimulates myoelectric activity of rat small intestine by promoting cyclic initiation and aboral propagation of migrating myoelectric complex. *Dig Dis Sci*, *39*(5), 946-956. <https://doi.org/10.1007/BF02087542>

- Hwang, B., Lee, J. H., & Bang, D. (2018). Single-cell RNA sequencing technologies and bioinformatics pipelines. *Exp Mol Med*, 50(8), 1-14. <https://doi.org/10.1038/s12276-018-0071-8>
- Isalan, M. (2011). Zinc-finger nucleases: how to play two good hands. *Nat Methods*, 9(1), 32-34. <https://doi.org/10.1038/nmeth.1805>
- Jagannathan-Bogdan, M., & Zon, L. I. (2013). Hematopoiesis. *Development*, 140(12), 2463-2467. <https://doi.org/10.1242/dev.083147>
- Jin, H., Huang, Z., Chi, Y., Wu, M., Zhou, R., Zhao, L., Xu, J., Zhen, F., Lan, Y., Li, L., Zhang, W., Wen, Z., & Zhang, Y. (2016). c-Myb acts in parallel and cooperatively with Cebp1 to regulate neutrophil maturation in zebrafish. *Blood*, 128(3), 415-426. <https://doi.org/10.1182/blood-2015-12-686147>
- Jin, H., Xu, J., & Wen, Z. (2007). Migratory path of definitive hematopoietic stem/progenitor cells during zebrafish development. *Blood*, 109(12), 5208-5214. <https://doi.org/10.1182/blood-2007-01-069005>
- Jinek, M., Chylinski, K., Fonfara, I., Hauer, M., Doudna, J. A., & Charpentier, E. (2012). A programmable dual-RNA-guided DNA endonuclease in adaptive bacterial immunity. *Science*, 337(6096), 816-821. <https://doi.org/10.1126/science.1225829>
- Jones, L. O., Willms, R. J., Xu, X., Graham, R. D. V., Eklund, M., Shin, M., & Foley, E. (2023). Single-cell resolution of the adult zebrafish intestine under conventional conditions and in response to an acute *Vibrio cholerae* infection. *Cell Rep*, 42(11), 113407. <https://doi.org/10.1016/j.celrep.2023.113407>
- Jordan, C. K. I., & Clarke, T. B. (2024). How does the microbiota control systemic innate immunity? *Trends Immunol*, 45(2), 94-102. <https://doi.org/10.1016/j.it.2023.12.002>
- Joung, J. K., & Sander, J. D. (2013). TALENs: a widely applicable technology for targeted genome editing. *Nat Rev Mol Cell Biol*, 14(1), 49-55. <https://doi.org/10.1038/nrm3486>
- Jovic, D., Liang, X., Zeng, H., Lin, L., Xu, F., & Luo, Y. (2022). Single-cell RNA sequencing technologies and applications: A brief overview. *Clin Transl Med*, 12(3), e694. <https://doi.org/10.1002/ctm2.694>
- Jungi, T. W., & McGregor, D. D. (1978). Impaired chemotactic responsiveness of macrophages from gnotobiotic rats. *Infect Immun*, 19(2), 553-561. <https://doi.org/10.1128/iai.19.2.553-561.1978>

- Kandori, H., Hirayama, K., Takeda, M., & Doi, K. (1996). Histochemical, lectin-histochemical and morphometrical characteristics of intestinal goblet cells of germfree and conventional mice. *Exp Anim*, 45(2), 155-160. <https://doi.org/10.1538/expanim.45.155>
- Kanther, M., & Rawls, J. F. (2010). Host-microbe interactions in the developing zebrafish. *Curr Opin Immunol*, 22(1), 10-19. <https://doi.org/10.1016/j.coi.2010.01.006>
- Kanther, M., Sun, X., Mühlbauer, M., Mackey, L. C., Flynn, E. J., Bagnat, M., Jobin, C., & Rawls, J. F. (2011). Microbial colonization induces dynamic temporal and spatial patterns of NF- $\kappa$ B activation in the zebrafish digestive tract. *Gastroenterology*, 141(1), 197-207. <https://doi.org/10.1053/j.gastro.2011.03.042>
- Kanther, M., Tomkovich, S., Xiaolun, S., Grosser, M. R., Koo, J., Flynn, E. J., 3rd, Jobin, C., & Rawls, J. F. (2014). Commensal microbiota stimulate systemic neutrophil migration through induction of serum amyloid A. *Cell Microbiol*, 16(7), 1053-1067. <https://doi.org/10.1111/cmi.12257>
- Karim, F. D., Urness, L. D., Thummel, C. S., Klemsz, M. J., McKercher, S. R., Celada, A., Van Beveren, C., Maki, R. A., Gunther, C. V., Nye, J. A., & et al. (1990). The ETS-domain: a new DNA-binding motif that recognizes a purine-rich core DNA sequence. *Genes Dev*, 4(9), 1451-1453. <https://doi.org/10.1101/gad.4.9.1451>
- Kas, K., Finger, E., Grall, F., Gu, X., Akbarali, Y., Boltax, J., Weiss, A., Oettgen, P., Kapeller, R., & Libermann, T. A. (2000). ESE-3, a novel member of an epithelium-specific ets transcription factor subfamily, demonstrates different target gene specificity from ESE-1. *J Biol Chem*, 275(4), 2986-2998. <https://doi.org/10.1074/jbc.275.4.2986>
- Kennedy, E. A., King, K. Y., & Baldrige, M. T. (2018). Mouse Microbiota Models: Comparing Germ-Free Mice and Antibiotics Treatment as Tools for Modifying Gut Bacteria. *Front Physiol*, 9, 1534. <https://doi.org/10.3389/fphys.2018.01534>
- Kent, M. L., Sanders, J. L., Spagnoli, S., Al-Samarrie, C. E., & Murray, K. N. (2020). Review of diseases and health management in zebrafish *Danio rerio* (Hamilton 1822) in research facilities. *J Fish Dis*, 43(6), 637-650. <https://doi.org/10.1111/jfd.13165>
- Kent, M. L., Whipps, C. M., Matthews, J. L., Florio, D., Watral, V., Bishop-Stewart, J. K., Poort, M., & Bermudez, L. (2004). Mycobacteriosis in zebrafish (*Danio rerio*) research facilities. *Comp Biochem Physiol C Toxicol Pharmacol*, 138(3), 383-390. <https://doi.org/10.1016/j.cca.2004.08.005>
- Kervestin, S., & Jacobson, A. (2012). NMD: a multifaceted response to premature translational termination. *Nat Rev Mol Cell Biol*, 13(11), 700-712. <https://doi.org/10.1038/nrm3454>

- Khosravi, A., Yanez, A., Price, J. G., Chow, A., Merad, M., Goodridge, H. S., & Mazmanian, S. K. (2014). Gut microbiota promote hematopoiesis to control bacterial infection. *Cell Host Microbe*, 15(3), 374-381. <https://doi.org/10.1016/j.chom.2014.02.006>
- Kim, M., Ashida, H., Ogawa, M., Yoshikawa, Y., Mimuro, H., & Sasakawa, C. (2010). Bacterial interactions with the host epithelium. *Cell Host Microbe*, 8(1), 20-35. <https://doi.org/10.1016/j.chom.2010.06.006>
- Kim, N., Kim, H. K., Lee, S., Seo, J. H., Choi, J. W., Park, J., Min, S., Yoon, S., Cho, S. R., & Kim, H. H. (2020). Prediction of the sequence-specific cleavage activity of Cas9 variants. *Nat Biotechnol*, 38(11), 1328-1336. <https://doi.org/10.1038/s41587-020-0537-9>
- Kim, Y. G., Cha, J., & Chandrasegaran, S. (1996). Hybrid restriction enzymes: zinc finger fusions to Fok I cleavage domain. *Proc Natl Acad Sci U S A*, 93(3), 1156-1160. <https://doi.org/10.1073/pnas.93.3.1156>
- Kimura, Y., Hisano, Y., Kawahara, A., & Higashijima, S. (2014). Efficient generation of knock-in transgenic zebrafish carrying reporter/driver genes by CRISPR/Cas9-mediated genome engineering. *Sci Rep*, 4, 6545. <https://doi.org/10.1038/srep06545>
- Kissa, K., & Herbomel, P. (2010). Blood stem cells emerge from aortic endothelium by a novel type of cell transition. *Nature*, 464(7285), 112-115. <https://doi.org/10.1038/nature08761>
- Klemm, S. L., Shipony, Z., & Greenleaf, W. J. (2019). Chromatin accessibility and the regulatory epigenome. *Nat Rev Genet*, 20(4), 207-220. <https://doi.org/10.1038/s41576-018-0089-8>
- Klug, A. (2010). The discovery of zinc fingers and their applications in gene regulation and genome manipulation. *Annu Rev Biochem*, 79, 213-231. <https://doi.org/10.1146/annurev-biochem-010909-095056>
- Knox, B. P., Deng, Q., Rood, M., Eickhoff, J. C., Keller, N. P., & Huttenlocher, A. (2014). Distinct innate immune phagocyte responses to *Aspergillus fumigatus* conidia and hyphae in zebrafish larvae. *Eukaryot Cell*, 13(10), 1266-1277. <https://doi.org/10.1128/EC.00080-14>
- Kobberup, S., Nyeng, P., Juhl, K., Hutton, J., & Jensen, J. (2007). ETS-family genes in pancreatic development. *Dev Dyn*, 236(11), 3100-3110. <https://doi.org/10.1002/dvdy.21292>
- Koch, B. E. V., Yang, S., Lamers, G., Stougaard, J., & Spaink, H. P. (2018). Intestinal microbiome adjusts the innate immune setpoint during colonization through negative

regulation of MyD88. *Nat Commun*, 9(1), 4099. <https://doi.org/10.1038/s41467-018-06658-4>

- Kohda, A., Yamazaki, S., & Sumimoto, H. (2016). The Nuclear Protein IkappaBzeta Forms a Transcriptionally Active Complex with Nuclear Factor-kappaB (NF-kappaB) p50 and the Lcn2 Promoter via the N- and C-terminal Ankyrin Repeat Motifs. *J Biol Chem*, 291(39), 20739-20752. <https://doi.org/10.1074/jbc.M116.719302>
- Kong, H. H., Oh, J., Deming, C., Conlan, S., Grice, E. A., Beatson, M. A., Nomicos, E., Polley, E. C., Komarow, H. D., Program, N. C. S., Murray, P. R., Turner, M. L., & Segre, J. A. (2012). Temporal shifts in the skin microbiome associated with disease flares and treatment in children with atopic dermatitis. *Genome Res*, 22(5), 850-859. <https://doi.org/10.1101/gr.131029.111>
- Kouri, V. P., Olkkonen, J., Nurmi, K., Peled, N., Ainola, M., Mandelin, J., Nordstrom, D. C., & Eklund, K. K. (2023). IL-17A and TNF synergistically drive expression of proinflammatory mediators in synovial fibroblasts via IkappaBzeta-dependent induction of ELF3. *Rheumatology (Oxford)*, 62(2), 872-885. <https://doi.org/10.1093/rheumatology/keac385>
- Koussounadis, A., Langdon, S. P., Um, I. H., Harrison, D. J., & Smith, V. A. (2015). Relationship between differentially expressed mRNA and mRNA-protein correlations in a xenograft model system. *Sci Rep*, 5, 10775. <https://doi.org/10.1038/srep10775>
- Kroll, F., Powell, G. T., Ghosh, M., Gestri, G., Antinucci, P., Hearn, T. J., Tunbak, H., Lim, S., Dennis, H. W., Fernandez, J. M., Whitmore, D., Dreosti, E., Wilson, S. W., Hoffman, E. J., & Rihel, J. (2021). A simple and effective F0 knockout method for rapid screening of behaviour and other complex phenotypes. *Elife*, 10. <https://doi.org/10.7554/eLife.59683>
- Kushwah, R., Oliver, J. R., Wu, J., Chang, Z., & Hu, J. (2011). Elf3 regulates allergic airway inflammation by controlling dendritic cell-driven T cell differentiation. *J Immunol*, 187(9), 4639-4653. <https://doi.org/10.4049/jimmunol.1101967>
- Kwon, M. C., Koo, B. K., Kim, Y. Y., Lee, S. H., Kim, N. S., Kim, J. H., & Kong, Y. Y. (2009). Essential role of CR6-interacting factor 1 (Crif1) in E74-like factor 3 (ELF3)-mediated intestinal development. *J Biol Chem*, 284(48), 33634-33641. <https://doi.org/10.1074/jbc.M109.059840>
- Lam, S. H., Chua, H. L., Gong, Z., Lam, T. J., & Sin, Y. M. (2004). Development and maturation of the immune system in zebrafish, *Danio rerio*: a gene expression profiling, in situ hybridization and immunological study. *Dev Comp Immunol*, 28(1), 9-28. [https://doi.org/10.1016/s0145-305x\(03\)00103-4](https://doi.org/10.1016/s0145-305x(03)00103-4)

- Laudet, V., Niel, C., Duterque-Coquillaud, M., Leprince, D., & Stehelin, D. (1993). Evolution of the ets gene family. *Biochem Biophys Res Commun*, *190*(1), 8-14. <https://doi.org/10.1006/bbrc.1993.1002>
- Lawson, N. D., Li, R., Shin, M., Grosse, A., Yukselen, O., Stone, O. A., Kucukural, A., & Zhu, L. (2020). An improved zebrafish transcriptome annotation for sensitive and comprehensive detection of cell type-specific genes. *Elife*, *9*. <https://doi.org/10.7554/eLife.55792>
- Lee, H. J., Chang, J. H., Kim, Y. S., Kim, S. J., & Yang, H. K. (2003). Effect of ets-related transcription factor (ERT) on transforming growth factor (TGF)-beta type II receptor gene expression in human cancer cell lines. *J Exp Clin Cancer Res*, *22*(3), 477-480. <https://www.ncbi.nlm.nih.gov/pubmed/14582709>
- Lee, T. K., Poon, R. T., Yuen, A. P., Ling, M. T., Kwok, W. K., Wang, X. H., Wong, Y. C., Guan, X. Y., Man, K., Chau, K. L., & Fan, S. T. (2006). Twist overexpression correlates with hepatocellular carcinoma metastasis through induction of epithelial-mesenchymal transition. *Clin Cancer Res*, *12*(18), 5369-5376. <https://doi.org/10.1158/1078-0432.CCR-05-2722>
- Letunic, I., & Bork, P. (2018). 20 years of the SMART protein domain annotation resource. *Nucleic Acids Res*, *46*(D1), D493-D496. <https://doi.org/10.1093/nar/gkx922>
- Letunic, I., Khedkar, S., & Bork, P. (2021). SMART: recent updates, new developments and status in 2020. *Nucleic Acids Res*, *49*(D1), D458-D460. <https://doi.org/10.1093/nar/gkaa937>
- Levic, D. S., Yamaguchi, N., Wang, S., Knaut, H., & Bagnat, M. (2021). Knock-in tagging in zebrafish facilitated by insertion into non-coding regions. *Development*, *148*(19). <https://doi.org/10.1242/dev.199994>
- Levraud, J. P., Jouneau, L., Briolat, V., Laghi, V., & Boudinot, P. (2019). IFN-Stimulated Genes in Zebrafish and Humans Define an Ancient Arsenal of Antiviral Immunity. *J Immunol*, *203*(12), 3361-3373. <https://doi.org/10.4049/jimmunol.1900804>
- Li, D., Cheng, P., Wang, J., Qiu, X., Zhang, X., Xu, L., Liu, Y., & Qin, S. (2019). IRF6 Is Directly Regulated by ZEB1 and ELF3, and Predicts a Favorable Prognosis in Gastric Cancer. *Front Oncol*, *9*, 220. <https://doi.org/10.3389/fonc.2019.00220>
- Li, D., & Wu, M. (2021). Pattern recognition receptors in health and diseases. *Signal Transduct Target Ther*, *6*(1), 291. <https://doi.org/10.1038/s41392-021-00687-0>

- Li, G., Sun, Y., Kwok, I., Yang, L., Wen, W., Huang, P., Wu, M., Li, J., Huang, Z., Liu, Z., He, S., Peng, W., Bei, J. X., Ginhoux, F., Ng, L. G., & Zhang, Y. (2024). *Cebp1* and *Cebpbeta* transcriptional axis controls eosinophilopoiesis in zebrafish. *Nat Commun*, *15*(1), 811. <https://doi.org/10.1038/s41467-024-45029-0>
- Li, L., Jin, H., Xu, J., Shi, Y., & Wen, Z. (2011). *Irf8* regulates macrophage versus neutrophil fate during zebrafish primitive myelopoiesis. *Blood*, *117*(4), 1359-1369. <https://doi.org/10.1182/blood-2010-06-290700>
- Li, L., Miao, X., Ni, R., Wang, L., Gu, X., Yan, L., Tang, Q., & Zhang, D. (2015). Epithelial-specific ETS-1 (ESE1/ELF3) regulates apoptosis of intestinal epithelial cells in ulcerative colitis via accelerating NF- $\kappa$ B activation. *Immunol Res*, *62*(2), 198-212. <https://doi.org/10.1007/s12026-015-8651-3>
- Li, M., Zhao, L., Page-McCaw, P. S., & Chen, W. (2016). Zebrafish Genome Engineering Using the CRISPR-Cas9 System. *Trends Genet*, *32*(12), 815-827. <https://doi.org/10.1016/j.tig.2016.10.005>
- Li, X., & Wang, C. Y. (2021). From bulk, single-cell to spatial RNA sequencing. *Int J Oral Sci*, *13*(1), 36. <https://doi.org/10.1038/s41368-021-00146-0>
- Liao, H., Wu, J., VanDusen, N. J., Li, Y., & Zheng, Y. (2024). CRISPR-Cas9-mediated homology-directed repair for precise gene editing. *Mol Ther Nucleic Acids*, *35*(4), 102344. <https://doi.org/10.1016/j.omtn.2024.102344>
- Liao, Y., Smyth, G. K., & Shi, W. (2014). featureCounts: an efficient general purpose program for assigning sequence reads to genomic features. *Bioinformatics*, *30*(7), 923-930. <https://doi.org/10.1093/bioinformatics/btt656>
- Lickwar, C. R., Camp, J. G., Weiser, M., Cocchiaro, J. L., Kingsley, D. M., Furey, T. S., Sheikh, S. Z., & Rawls, J. F. (2017). Genomic dissection of conserved transcriptional regulation in intestinal epithelial cells. *PLoS Biol*, *15*(8), e2002054. <https://doi.org/10.1371/journal.pbio.2002054>
- Lickwar, C. R., Davison, J. M., Kelly, C., Mercado, G. P., Wen, J., Davis, B. R., Tillman, M. C., Semova, I., Andres, S. F., Vale, G., McDonald, J. G., & Rawls, J. F. (2022). Transcriptional Integration of Distinct Microbial and Nutritional Signals by the Small Intestinal Epithelium. *Cell Mol Gastroenterol Hepatol*, *14*(2), 465-493. <https://doi.org/10.1016/j.jcmgh.2022.04.013>
- Lieschke, G. J., Oates, A. C., Crowhurst, M. O., Ward, A. C., & Layton, J. E. (2001). Morphologic and functional characterization of granulocytes and macrophages in

embryonic and adult zebrafish. *Blood*, 98(10), 3087-3096.  
<https://doi.org/10.1182/blood.v98.10.3087>

Lieschke, G. J., Oates, A. C., Paw, B. H., Thompson, M. A., Hall, N. E., Ward, A. C., Ho, R. K., Zon, L. I., & Layton, J. E. (2002). Zebrafish SPI-1 (PU.1) marks a site of myeloid development independent of primitive erythropoiesis: implications for axial patterning. *Dev Biol*, 246(2), 274-295. <https://doi.org/10.1006/dbio.2002.0657>

Lin, J., Hou, L., Zhao, X., Zhong, J., Lv, Y., Jiang, X., Ye, B., & Qiao, Y. (2024). Switch of ELF3 and ATF4 transcriptional axis programs the amino acid insufficiency-linked epithelial-to-mesenchymal transition. *Mol Ther*, 32(6), 1956-1969.  
<https://doi.org/10.1016/j.ymthe.2024.04.025>

Liu, D., Skomorovska, Y., Song, J., Bowler, E., Harris, R., Ravasz, M., Bai, S., Ayati, M., Tamai, K., Koyuturk, M., Yuan, X., Wang, Z., Wang, Y., & Ewing, R. M. (2019). ELF3 is an antagonist of oncogenic-signalling-induced expression of EMT-TF ZEB1. *Cancer Biol Ther*, 20(1), 90-100. <https://doi.org/10.1080/15384047.2018.1507256>

Liu, F., Walmsley, M., Rodaway, A., & Patient, R. (2008). Fli1 acts at the top of the transcriptional network driving blood and endothelial development. *Curr Biol*, 18(16), 1234-1240. <https://doi.org/10.1016/j.cub.2008.07.048>

Liu, L., Wang, H., Zhang, H., Chen, X., Zhang, Y., Wu, J., Zhao, L., Wang, D., Pu, J., Ji, P., & Xie, P. (2022). Toward a Deeper Understanding of Gut Microbiome in Depression: The Promise of Clinical Applicability. *Adv Sci (Weinh)*, 9(35), e2203707.  
<https://doi.org/10.1002/advs.202203707>

Liu, M. S., Gong, S., Yu, H. H., Jung, K., Johnson, K. A., & Taylor, D. W. (2020). Engineered CRISPR/Cas9 enzymes improve discrimination by slowing DNA cleavage to allow release of off-target DNA. *Nat Commun*, 11(1), 3576. <https://doi.org/10.1038/s41467-020-17411-1>

Long, Q., Meng, A., Wang, H., Jessen, J. R., Farrell, M. J., & Lin, S. (1997). GATA-1 expression pattern can be recapitulated in living transgenic zebrafish using GFP reporter gene. *Development*, 124(20), 4105-4111. <https://doi.org/10.1242/dev.124.20.4105>

Longo, S., Riccio, M., & McCune, A. R. (2013). Homology of lungs and gas bladders: insights from arterial vasculature. *J Morphol*, 274(6), 687-703.  
<https://doi.org/10.1002/jmor.20128>

Longoni, N., Sarti, M., Albino, D., Civenni, G., Malek, A., Orтели, E., Pinton, S., Mello-Grand, M., Ostano, P., D'Ambrosio, G., Sessa, F., Garcia-Escudero, R., Thalmann, G. N.,

- Chiorino, G., Catapano, C. V., & Carbone, G. M. (2013). ETS transcription factor ESE1/ELF3 orchestrates a positive feedback loop that constitutively activates NF- $\kappa$ B and drives prostate cancer progression. *Cancer Res*, *73*(14), 4533-4547. <https://doi.org/10.1158/0008-5472.CAN-12-4537>
- Lou, Z., Lee, B. S., Ha, T., Xu, Y., Kim, H. J., Kim, C. H., & Lee, S. H. (2018). ESE-1 suppresses the growth, invasion and migration of human NSCLC cells and tumor formation in vivo. *Oncol Rep*, *40*(3), 1734-1742. <https://doi.org/10.3892/or.2018.6560>
- Loughran, S. J., Kruse, E. A., Hacking, D. F., de Graaf, C. A., Hyland, C. D., Willson, T. A., Henley, K. J., Ellis, S., Voss, A. K., Metcalf, D., Hilton, D. J., Alexander, W. S., & Kile, B. T. (2008). The transcription factor Erg is essential for definitive hematopoiesis and the function of adult hematopoietic stem cells. *Nat Immunol*, *9*(7), 810-819. <https://doi.org/10.1038/ni.1617>
- Love, M. I., Huber, W., & Anders, S. (2014). Moderated estimation of fold change and dispersion for RNA-seq data with DESeq2. *Genome Biol*, *15*(12), 550. <https://doi.org/10.1186/s13059-014-0550-8>
- Lukoseviciute, M., Gavriouchkina, D., Williams, R. M., Hochgreb-Hagele, T., Senanayake, U., Chong-Morrison, V., Thongjuea, S., Repapi, E., Mead, A., & Sauka-Spengler, T. (2018). From Pioneer to Repressor: Bimodal foxd3 Activity Dynamically Remodels Neural Crest Regulatory Landscape In Vivo. *Dev Cell*, *47*(5), 608-628 e606. <https://doi.org/10.1016/j.devcel.2018.11.009>
- Lukoseviciute, M., Ling, I. T. C., Senanayake, U., Candido-Ferreira, I., Taylor, G., Williams, R. M., & Sauka-Spengler, T. (2020). Tissue-Specific In Vivo Biotin Chromatin Immunoprecipitation with Sequencing in Zebrafish and Chicken. *STAR Protoc*, *1*(2), 100066. <https://doi.org/10.1016/j.xpro.2020.100066>
- Marin, I. A., Goertz, J. E., Ren, T., Rich, S. S., Onengut-Gumuscu, S., Farber, E., Wu, M., Overall, C. C., Kipnis, J., & Gaultier, A. (2017). Microbiota alteration is associated with the development of stress-induced despair behavior. *Sci Rep*, *7*, 43859. <https://doi.org/10.1038/srep43859>
- Martinez-Guryn, K., Hubert, N., Frazier, K., Urlass, S., Musch, M. W., Ojeda, P., Pierre, J. F., Miyoshi, J., Sontag, T. J., Cham, C. M., Reardon, C. A., Leone, V., & Chang, E. B. (2018). Small Intestine Microbiota Regulate Host Digestive and Absorptive Adaptive Responses to Dietary Lipids. *Cell Host Microbe*, *23*(4), 458-469 e455. <https://doi.org/10.1016/j.chom.2018.03.011>
- Massaquoi, M. S., Kong, G. L., Chilin-Fuentes, D., Ngo, J. S., Horve, P. F., Melancon, E., Hamilton, M. K., Eisen, J. S., & Guillemin, K. (2023). Cell-type-specific responses to the

microbiota across all tissues of the larval zebrafish. *Cell Rep*, 42(2), 112095.  
<https://doi.org/10.1016/j.celrep.2023.112095>

Mavrothalassitis, G., Fisher, R. J., Smyth, F., Watson, D. K., & Papas, T. S. (1994). Structural inferences of the ETS1 DNA-binding domain determined by mutational analysis. *Oncogene*, 9(2), 425-435. <https://www.ncbi.nlm.nih.gov/pubmed/8290254>

Melancon, E., Gomez De La Torre Canny, S., Sichel, S., Kelly, M., Wiles, T. J., Rawls, J. F., Eisen, J. S., & Guillemin, K. (2017). Best practices for germ-free derivation and gnotobiotic zebrafish husbandry. *Methods Cell Biol*, 138, 61-100.  
<https://doi.org/10.1016/bs.mcb.2016.11.005>

Milligan-McClellan, K., Charette, J. R., Phennicie, R. T., Stephens, W. Z., Rawls, J. F., Guillemin, K., & Kim, C. H. (2011). Study of host-microbe interactions in zebrafish. *Methods Cell Biol*, 105, 87-116. <https://doi.org/10.1016/B978-0-12-381320-6.00004-7>

Mitsuyama, M., Ohara, R., Amako, K., Nomoto, K., Yokokura, T., & Nomoto, K. (1986). Ontogeny of macrophage function to release superoxide anion in conventional and germfree mice. *Infect Immun*, 52(1), 236-239. <https://doi.org/10.1128/iai.52.1.236-239.1986>

Molyneaux, P. L., Cox, M. J., Wells, A. U., Kim, H. C., Ji, W., Cookson, W. O., Moffatt, M. F., Kim, D. S., & Maher, T. M. (2017). Changes in the respiratory microbiome during acute exacerbations of idiopathic pulmonary fibrosis. *Respir Res*, 18(1), 29.  
<https://doi.org/10.1186/s12931-017-0511-3>

Molyneaux, P. L., Cox, M. J., Willis-Owen, S. A., Mallia, P., Russell, K. E., Russell, A. M., Murphy, E., Johnston, S. L., Schwartz, D. A., Wells, A. U., Cookson, W. O., Maher, T. M., & Moffatt, M. F. (2014). The role of bacteria in the pathogenesis and progression of idiopathic pulmonary fibrosis. *Am J Respir Crit Care Med*, 190(8), 906-913.  
<https://doi.org/10.1164/rccm.201403-0541OC>

Montfort, J., Hervas-Sotomayor, F., Le Cam, A., & Murat, F. (2024). FEVER: an interactive web-based resource for evolutionary transcriptomics across fishes. *Nucleic Acids Res*, 52(W1), W65-W69. <https://doi.org/10.1093/nar/gkae264>

Morcos, P. A. (2007). Achieving targeted and quantifiable alteration of mRNA splicing with Morpholino oligos. *Biochem Biophys Res Commun*, 358(2), 521-527.  
<https://doi.org/10.1016/j.bbrc.2007.04.172>

Morgun, A., Dzutsev, A., Dong, X., Greer, R. L., Sexton, D. J., Ravel, J., Schuster, M., Hsiao, W., Matzinger, P., & Shulzhenko, N. (2015). Uncovering effects of antibiotics on the

host and microbiota using transkingdom gene networks. *Gut*, 64(11), 1732-1743.  
<https://doi.org/10.1136/gutjnl-2014-308820>

Morland, B., Smievoll, A. I., & Midtvedt, T. (1979). Comparison of peritoneal macrophages from germfree and conventional mice. *Infect Immun*, 26(3), 1129-1136.  
<https://doi.org/10.1128/iai.26.3.1129-1136.1979>

Moscou, M. J., & Bogdanove, A. J. (2009). A simple cipher governs DNA recognition by TAL effectors. *Science*, 326(5959), 1501. <https://doi.org/10.1126/science.1178817>

Mucenski, M. L., McLain, K., Kier, A. B., Swerdlow, S. H., Schreiner, C. M., Miller, T. A., Pietryga, D. W., Scott, W. J., Jr., & Potter, S. S. (1991). A functional c-myb gene is required for normal murine fetal hepatic hematopoiesis. *Cell*, 65(4), 677-689.  
[https://doi.org/10.1016/0092-8674\(91\)90099-k](https://doi.org/10.1016/0092-8674(91)90099-k)

Munjal, A., Hannezo, E., Tsai, T. Y., Mitchison, T. J., & Megason, S. G. (2021). Extracellular hyaluronate pressure shaped by cellular tethers drives tissue morphogenesis. *Cell*, 184(26), 6313-6325 e6318. <https://doi.org/10.1016/j.cell.2021.11.025>

Murayama, E., Kissa, K., Zapata, A., Mordelet, E., Briolat, V., Lin, H. F., Handin, R. I., & Herbomel, P. (2006). Tracing hematopoietic precursor migration to successive hematopoietic organs during zebrafish development. *Immunity*, 25(6), 963-975.  
<https://doi.org/10.1016/j.immuni.2006.10.015>

Murdoch, C. C., Espenschied, S. T., Matty, M. A., Mueller, O., Tobin, D. M., & Rawls, J. F. (2019). Intestinal Serum amyloid A suppresses systemic neutrophil activation and bactericidal activity in response to microbiota colonization. *PLoS Pathog*, 15(3), e1007381. <https://doi.org/10.1371/journal.ppat.1007381>

Murdoch, C. C., & Rawls, J. F. (2019). Commensal Microbiota Regulate Vertebrate Innate Immunity-Insights From the Zebrafish. *Front Immunol*, 10, 2100.  
<https://doi.org/10.3389/fimmu.2019.02100>

Nasevicius, A., & Ekker, S. C. (2000). Effective targeted gene 'knockdown' in zebrafish. *Nat Genet*, 26(2), 216-220. <https://doi.org/10.1038/79951>

Newman, M. A., Sundelin, T., Nielsen, J. T., & Erbs, G. (2013). MAMP (microbe-associated molecular pattern) triggered immunity in plants. *Front Plant Sci*, 4, 139.  
<https://doi.org/10.3389/fpls.2013.00139>

- Ng, A. N., de Jong-Curtain, T. A., Mawdsley, D. J., White, S. J., Shin, J., Appel, B., Dong, P. D., Stainier, D. Y., & Heath, J. K. (2005). Formation of the digestive system in zebrafish: III. Intestinal epithelium morphogenesis. *Dev Biol*, 286(1), 114-135. <https://doi.org/10.1016/j.ydbio.2005.07.013>
- Ng, A. Y., Waring, P., Ristevski, S., Wang, C., Wilson, T., Pritchard, M., Hertzog, P., & Kola, I. (2002). Inactivation of the transcription factor Elf3 in mice results in dysmorphogenesis and altered differentiation of intestinal epithelium. *Gastroenterology*, 122(5), 1455-1466. <https://doi.org/10.1053/gast.2002.32990>
- Oettgen, P., Alani, R. M., Barcinski, M. A., Brown, L., Akbarali, Y., Boltax, J., Kunsch, C., Munger, K., & Libermann, T. A. (1997). Isolation and characterization of a novel epithelium-specific transcription factor, ESE-1, a member of the ets family. *Mol Cell Biol*, 17(8), 4419-4433. <https://doi.org/10.1128/MCB.17.8.4419>
- Oettgen, P., Kas, K., Dube, A., Gu, X., Grall, F., Thamrongsak, U., Akbarali, Y., Finger, E., Boltax, J., Endress, G., Munger, K., Kunsch, C., & Libermann, T. A. (1999). Characterization of ESE-2, a novel ESE-1-related Ets transcription factor that is restricted to glandular epithelium and differentiated keratinocytes. *J Biol Chem*, 274(41), 29439-29452. <https://doi.org/10.1074/jbc.274.41.29439>
- Ogobuiro, I., Gonzales, J., Shumway, K. R., & Tuma, F. (2025). Physiology, Gastrointestinal. In *StatPearls*. <https://www.ncbi.nlm.nih.gov/pubmed/30725788>
- Ohkubo, T., Tsuda, M., Suzuki, S., El Borai, N., & Yamamura, M. (1999). Peripheral blood neutrophils of germ-free rats modified by in vivo granulocyte-colony-stimulating factor and exposure to natural environment. *Scand J Immunol*, 49(1), 73-77. <https://doi.org/10.1046/j.1365-3083.1999.00456.x>
- Ohkubo, T., Tsuda, M., Tamura, M., & Yamamura, M. (1990). Impaired superoxide production in peripheral blood neutrophils of germ-free rats. *Scand J Immunol*, 32(6), 727-729. <https://doi.org/10.1111/j.1365-3083.1990.tb03216.x>
- Oikawa, T., & Yamada, T. (2003). Molecular biology of the Ets family of transcription factors. *Gene*, 303, 11-34. [https://doi.org/10.1016/s0378-1119\(02\)01156-3](https://doi.org/10.1016/s0378-1119(02)01156-3)
- Oliveira, M. R., Tafuri, W. L., Afonso, L. C., Oliveira, M. A., Nicoli, J. R., Vieira, E. C., Scott, P., Melo, M. N., & Vieira, L. Q. (2005). Germ-free mice produce high levels of interferon-gamma in response to infection with *Leishmania major* but fail to heal lesions. *Parasitology*, 131(Pt 4), 477-488. <https://doi.org/10.1017/S0031182005008073>

- Ong, S. L. M., de Vos, I., Meroshini, M., Poobalan, Y., & Dunn, N. R. (2020). Microfibril-associated glycoprotein 4 (Mfap4) regulates haematopoiesis in zebrafish. *Sci Rep*, *10*(1), 11801. <https://doi.org/10.1038/s41598-020-68792-8>
- Otero, M., Plumb, D. A., Tsuchimochi, K., Dragomir, C. L., Hashimoto, K., Peng, H., Olivotto, E., Bevilacqua, M., Tan, L., Yang, Z., Zhan, Y., Oettgen, P., Li, Y., Marcu, K. B., & Goldring, M. B. (2012). E74-like factor 3 (ELF3) impacts on matrix metalloproteinase 13 (MMP13) transcriptional control in articular chondrocytes under proinflammatory stress. *J Biol Chem*, *287*(5), 3559-3572. <https://doi.org/10.1074/jbc.M111.265744>
- Oyelakin, A., Nayak, K. B., Glathar, A. R., Gluck, C., Wrynn, T., Tugores, A., Romano, R. A., & Sinha, S. (2022). EHF is a novel regulator of cellular redox metabolism and predicts patient prognosis in HNSCC. *NAR Cancer*, *4*(2), zcac017. <https://doi.org/10.1093/narcan/zcac017>
- Paik, E. J., & Zon, L. I. (2010). Hematopoietic development in the zebrafish. *Int J Dev Biol*, *54*(6-7), 1127-1137. <https://doi.org/10.1387/ijdb.093042ep>
- Parichy, D. M. (2015). Advancing biology through a deeper understanding of zebrafish ecology and evolution. *Elife*, *4*. <https://doi.org/10.7554/eLife.05635>
- Park, P. J. (2009). ChIP-seq: advantages and challenges of a maturing technology. *Nat Rev Genet*, *10*(10), 669-680. <https://doi.org/10.1038/nrg2641>
- Patsali, P., Kleanthous, M., & Lederer, C. W. (2019). Disruptive Technology: CRISPR/Cas-Based Tools and Approaches. *Mol Diagn Ther*, *23*(2), 187-200. <https://doi.org/10.1007/s40291-019-00391-4>
- Pevny, L., Simon, M. C., Robertson, E., Klein, W. H., Tsai, S. F., D'Agati, V., Orkin, S. H., & Costantini, F. (1991). Erythroid differentiation in chimaeric mice blocked by a targeted mutation in the gene for transcription factor GATA-1. *Nature*, *349*(6306), 257-260. <https://doi.org/10.1038/349257a0>
- Pham, L. N., Kanther, M., Semova, I., & Rawls, J. F. (2008). Methods for generating and colonizing gnotobiotic zebrafish. *Nat Protoc*, *3*(12), 1862-1875. <https://doi.org/10.1038/nprot.2008.186>
- Pio, F., Kodandapani, R., Ni, C. Z., Shepard, W., Klemsz, M., McKercher, S. R., Maki, R. A., & Ely, K. R. (1996). New insights on DNA recognition by ets proteins from the crystal structure of the PU.1 ETS domain-DNA complex. *J Biol Chem*, *271*(38), 23329-23337. <https://doi.org/10.1074/jbc.271.38.23329>

- Piovesan, A., Pelleri, M. C., Antonaros, F., Strippoli, P., Caracausi, M., & Vitale, L. (2019). On the length, weight and GC content of the human genome. *BMC Res Notes*, *12*(1), 106. <https://doi.org/10.1186/s13104-019-4137-z>
- Pragman, A. A., Kim, H. B., Reilly, C. S., Wendt, C., & Isaacson, R. E. (2012). The lung microbiome in moderate and severe chronic obstructive pulmonary disease. *PLoS One*, *7*(10), e47305. <https://doi.org/10.1371/journal.pone.0047305>
- Prescott, J. D., Koto, K. S., Singh, M., & Gutierrez-Hartmann, A. (2004). The ETS transcription factor ESE-1 transforms MCF-12A human mammary epithelial cells via a novel cytoplasmic mechanism. *Mol Cell Biol*, *24*(12), 5548-5564. <https://doi.org/10.1128/MCB.24.12.5548-5564.2004>
- Pronobis, M. I., Zheng, S., Singh, S. P., Goldman, J. A., & Poss, K. D. (2021). In vivo proximity labeling identifies cardiomyocyte protein networks during zebrafish heart regeneration. *Elife*, *10*. <https://doi.org/10.7554/eLife.66079>
- Quast, C., Pruesse, E., Yilmaz, P., Gerken, J., Schweer, T., Yarza, P., Peplies, J., & Glockner, F. O. (2013). The SILVA ribosomal RNA gene database project: improved data processing and web-based tools. *Nucleic Acids Res*, *41*(Database issue), D590-596. <https://doi.org/10.1093/nar/gks1219>
- Ran, F. A., Hsu, P. D., Wright, J., Agarwala, V., Scott, D. A., & Zhang, F. (2013). Genome engineering using the CRISPR-Cas9 system. *Nat Protoc*, *8*(11), 2281-2308. <https://doi.org/10.1038/nprot.2013.143>
- Rawlins, E. L. (2011). The building blocks of mammalian lung development. *Dev Dyn*, *240*(3), 463-476. <https://doi.org/10.1002/dvdy.22482>
- Rawls, J. F., Samuel, B. S., & Gordon, J. I. (2004). Gnotobiotic zebrafish reveal evolutionarily conserved responses to the gut microbiota. *Proc Natl Acad Sci U S A*, *101*(13), 4596-4601. <https://doi.org/10.1073/pnas.0400706101>
- Reehorst, C. M., Nightingale, R., Luk, I. Y., Jenkins, L., Koentgen, F., Williams, D. S., Darido, C., Tan, F., Anderton, H., Chopin, M., Schoffer, K., Eissmann, M. F., Buchert, M., Mouradov, D., Sieber, O. M., Ernst, M., Dhillon, A. S., & Mariadason, J. M. (2021). EHF is essential for epidermal and colonic epithelial homeostasis, and suppresses Apc-initiated colonic tumorigenesis. *Development*, *148*(12). <https://doi.org/10.1242/dev.199542>
- Rehulka, J., Kubatova, A., & Hubka, V. (2018). Swim bladder mycosis in pretty tetra (*Hemigrammus pulcher*) caused by *Exophiala pisciphila* and *Phaeophleospora*

- hymenocallidicola, and experimental verification of pathogenicity. *J Fish Dis*, 41(3), 487-500. <https://doi.org/10.1111/jfd.12750>
- Rehulka, J., Kubatova, A., & Hubka, V. (2020). Swim bladder mycosis in farmed rainbow trout *Oncorhynchus mykiss* caused by *Phoma herbarum* and experimental verification of pathogenicity. *Dis Aquat Organ*, 138, 237-246. <https://doi.org/10.3354/dao03464>
- Rein, L. A. M., Yang, H., & Chao, N. J. (2018). Applications of Gene Editing Technologies to Cellular Therapies. *Biol Blood Marrow Transplant*, 24(8), 1537-1545. <https://doi.org/10.1016/j.bbmt.2018.03.021>
- Ribatti, D., Tamma, R., & Annesse, T. (2020). Epithelial-Mesenchymal Transition in Cancer: A Historical Overview. *Transl Oncol*, 13(6), 100773. <https://doi.org/10.1016/j.tranon.2020.100773>
- Robertson, G. N., Croll, R. P., & Smith, F. M. (2014). The structure of the caudal wall of the zebrafish (*Danio rerio*) swim bladder: evidence of localized lamellar body secretion and a proximate neural plexus. *J Morphol*, 275(8), 933-948. <https://doi.org/10.1002/jmor.20274>
- Robertson, G. N., Lindsey, B. W., Dumbarton, T. C., Croll, R. P., & Smith, F. M. (2008). The contribution of the swimbladder to buoyancy in the adult zebrafish (*Danio rerio*): a morphometric analysis. *J Morphol*, 269(6), 666-673. <https://doi.org/10.1002/jmor.10610>
- Rolig, A. S., Parthasarathy, R., Burns, A. R., Bohannon, B. J., & Guillemin, K. (2015). Individual Members of the Microbiota Disproportionately Modulate Host Innate Immune Responses. *Cell Host Microbe*, 18(5), 613-620. <https://doi.org/10.1016/j.chom.2015.10.009>
- Rosenfeld, M. E., & Campbell, L. A. (2011). Pathogens and atherosclerosis: update on the potential contribution of multiple infectious organisms to the pathogenesis of atherosclerosis. *Thromb Haemost*, 106(5), 858-867. <https://doi.org/10.1160/TH11-06-0392>
- Rosowski, E. E., Knox, B. P., Archambault, L. S., Huttenlocher, A., Keller, N. P., Wheeler, R. T., & Davis, J. M. (2018). The Zebrafish as a Model Host for Invasive Fungal Infections. *J Fungi (Basel)*, 4(4). <https://doi.org/10.3390/jof4040136>
- Roth, B., Jayaratna, I., Sundi, D., Cheng, T., Melquist, J., Choi, W., Porten, S., Nitti, G., Navai, N., Wszolek, M., Guo, C., Czerniak, B., McConkey, D., & Dinney, C. (2017). Employing an orthotopic model to study the role of epithelial-mesenchymal transition in bladder cancer metastasis. *Oncotarget*, 8(21), 34205-34222. <https://doi.org/10.18632/oncotarget.11009>

- Rudders, S., Gaspar, J., Madore, R., Volland, C., Grall, F., Patel, A., Pellacani, A., Perrella, M. A., Libermann, T. A., & Oettgen, P. (2001). ESE-1 is a novel transcriptional mediator of inflammation that interacts with NF-kappa B to regulate the inducible nitric-oxide synthase gene. *J Biol Chem*, *276*(5), 3302-3309. <https://doi.org/10.1074/jbc.M006507200>
- Sagai, T., Amano, T., Maeno, A., Kimura, T., Nakamoto, M., Takehana, Y., Naruse, K., Okada, N., Kiyonari, H., & Shiroishi, T. (2017). Evolution of Shh endoderm enhancers during morphological transition from ventral lungs to dorsal gas bladder. *Nat Commun*, *8*, 14300. <https://doi.org/10.1038/ncomms14300>
- Sarmah, S., Hawkins, M. R., Manikandan, P., Farrell, M., & Marrs, J. A. (2022). Elf3 deficiency during zebrafish development alters extracellular matrix organization and disrupts tissue morphogenesis. *PLoS One*, *17*(11), e0276255. <https://doi.org/10.1371/journal.pone.0276255>
- Sart, S., Tsai, A. C., Li, Y., & Ma, T. (2014). Three-dimensional aggregates of mesenchymal stem cells: cellular mechanisms, biological properties, and applications. *Tissue Eng Part B Rev*, *20*(5), 365-380. <https://doi.org/10.1089/ten.TEB.2013.0537>
- Savage, D. C., & Dubos, R. (1968). Alterations in the mouse cecum and its flora produced by antibacterial drugs. *J Exp Med*, *128*(1), 97-110. <https://doi.org/10.1084/jem.128.1.97>
- Savage, D. C., Siegel, J. E., Snellen, J. E., & Whitt, D. D. (1981). Transit time of epithelial cells in the small intestines of germfree mice and ex-germfree mice associated with indigenous microorganisms. *Appl Environ Microbiol*, *42*(6), 996-1001. <https://doi.org/10.1128/aem.42.6.996-1001.1981>
- Scott, E. W., Simon, M. C., Anastasi, J., & Singh, H. (1994). Requirement of transcription factor PU.1 in the development of multiple hematopoietic lineages. *Science*, *265*(5178), 1573-1577. <https://doi.org/10.1126/science.8079170>
- Segal, D. J., Dreier, B., Beerli, R. R., & Barbas, C. F., 3rd. (1999). Toward controlling gene expression at will: selection and design of zinc finger domains recognizing each of the 5'-GNN-3' DNA target sequences. *Proc Natl Acad Sci U S A*, *96*(6), 2758-2763. <https://doi.org/10.1073/pnas.96.6.2758>
- Semova, I., Carten, J. D., Stombaugh, J., Mackey, L. C., Knight, R., Farber, S. A., & Rawls, J. F. (2012). Microbiota regulate intestinal absorption and metabolism of fatty acids in the zebrafish. *Cell Host Microbe*, *12*(3), 277-288. <https://doi.org/10.1016/j.chom.2012.08.003>

- Sender, R., Fuchs, S., & Milo, R. (2016). Revised Estimates for the Number of Human and Bacteria Cells in the Body. *PLoS Biol*, *14*(8), e1002533. <https://doi.org/10.1371/journal.pbio.1002533>
- Sengez, B., Aygun, I., Shehwana, H., Toyran, N., Tercan Avci, S., Konu, O., Stemmler, M. P., & Alotaibi, H. (2019). The Transcription Factor Elf3 Is Essential for a Successful Mesenchymal to Epithelial Transition. *Cells*, *8*(8). <https://doi.org/10.3390/cells8080858>
- Sharrocks, A. D. (2001). The ETS-domain transcription factor family. *Nat Rev Mol Cell Biol*, *2*(11), 827-837. <https://doi.org/10.1038/35099076>
- Sinh, N. D., Endo, K., Miyazawa, K., & Saitoh, M. (2017). Ets1 and ESE1 reciprocally regulate expression of ZEB1/ZEB2, dependent on ERK1/2 activity, in breast cancer cells. *Cancer Sci*, *108*(5), 952-960. <https://doi.org/10.1111/cas.13214>
- Sirri, R., Mandrioli, L., Zamparo, S., Errani, F., Volpe, E., Tura, G., Barbe, T., & Ciulli, S. (2020). Swim Bladder Disorders in Koi Carp (*Cyprinus carpio*). *Animals (Basel)*, *10*(11). <https://doi.org/10.3390/ani10111974>
- Song, E. A. C., Smalley, K., Oyelakin, A., Horeth, E., Che, M., Wrynn, T., Osinski, J., Romano, R. A., & Sinha, S. (2023). Genetic Study of Elf5 and Ehf in the Mouse Salivary Gland. *J Dent Res*, *102*(3), 340-348. <https://doi.org/10.1177/00220345221130258>
- Song, H., Shin, U., Nam, U., & Lee, Y. (2024). Exploring hematopoiesis in zebrafish using forward genetic screening. *Exp Mol Med*, *56*(1), 51-58. <https://doi.org/10.1038/s12276-023-01138-2>
- Soza-Ried, C., Hess, I., Netuschil, N., Schorpp, M., & Boehm, T. (2010). Essential role of c-myb in definitive hematopoiesis is evolutionarily conserved. *Proc Natl Acad Sci U S A*, *107*(40), 17304-17308. <https://doi.org/10.1073/pnas.1004640107>
- Spyropoulos, D. D., Pharr, P. N., Lavenburg, K. R., Jackers, P., Papas, T. S., Ogawa, M., & Watson, D. K. (2000). Hemorrhage, impaired hematopoiesis, and lethality in mouse embryos carrying a targeted disruption of the Fli1 transcription factor. *Mol Cell Biol*, *20*(15), 5643-5652. <https://doi.org/10.1128/MCB.20.15.5643-5652.2000>
- Stainier, D. Y. R., Raz, E., Lawson, N. D., Ekker, S. C., Burdine, R. D., Eisen, J. S., Ingham, P. W., Schulte-Merker, S., Yelon, D., Weinstein, B. M., Mullins, M. C., Wilson, S. W., Ramakrishnan, L., Amacher, S. L., Neuhaus, S. C. F., Meng, A., Mochizuki, N., Panula, P., & Moens, C. B. (2017). Guidelines for morpholino use in zebrafish. *PLoS Genet*, *13*(10), e1007000. <https://doi.org/10.1371/journal.pgen.1007000>

- Stephens, D. N., Klein, R. H., Salmans, M. L., Gordon, W., Ho, H., & Andersen, B. (2013). The Ets transcription factor EHF as a regulator of cornea epithelial cell identity. *J Biol Chem*, 288(48), 34304-34324. <https://doi.org/10.1074/jbc.M113.504399>
- Stosik, M., Tokarz-Deptula, B., & Deptula, W. (2022). Haematopoiesis in Zebrafish (*Danio Rerio*). *Front Immunol*, 13, 902941. <https://doi.org/10.3389/fimmu.2022.902941>
- Stream, A., & Madigan, C. A. (2022). Zebrafish: an underutilized tool for discovery in host-microbe interactions. *Trends Immunol*, 43(6), 426-437. <https://doi.org/10.1016/j.it.2022.03.011>
- Sun, H. B., Shen, J., & Yokota, H. (2000). Size-dependent positioning of human chromosomes in interphase nuclei. *Biophys J*, 79(1), 184-190. [https://doi.org/10.1016/S0006-3495\(00\)76282-5](https://doi.org/10.1016/S0006-3495(00)76282-5)
- Sur, A., Wang, Y., Capar, P., Margolin, G., Prochaska, M. K., & Farrell, J. A. (2023). Single-cell analysis of shared signatures and transcriptional diversity during zebrafish development. *Dev Cell*, 58(24), 3028-3047 e3012. <https://doi.org/10.1016/j.devcel.2023.11.001>
- Suzuki, M., Saito-Adachi, M., Arai, Y., Fujiwara, Y., Takai, E., Shibata, S., Seki, M., Rokutan, H., Maeda, D., Horie, M., Suzuki, Y., Shibata, T., Kiyono, T., & Yachida, S. (2021). E74-Like Factor 3 Is a Key Regulator of Epithelial Integrity and Immune Response Genes in Biliary Tract Cancer. *Cancer Res*, 81(2), 489-500. <https://doi.org/10.1158/0008-5472.CAN-19-2988>
- Sze, M. A., Dimitriu, P. A., Hayashi, S., Elliott, W. M., McDonough, J. E., Gosselink, J. V., Cooper, J., Sin, D. D., Mohn, W. W., & Hogg, J. C. (2012). The lung tissue microbiome in chronic obstructive pulmonary disease. *Am J Respir Crit Care Med*, 185(10), 1073-1080. <https://doi.org/10.1164/rccm.201111-2075OC>
- Sztal, T. E., & Stainier, D. Y. R. (2020). Transcriptional adaptation: a mechanism underlying genetic robustness. *Development*, 147(15). <https://doi.org/10.1242/dev.186452>
- Takaki, K., Davis, J. M., Winglee, K., & Ramakrishnan, L. (2013). Evaluation of the pathogenesis and treatment of *Mycobacterium marinum* infection in zebrafish. *Nat Protoc*, 8(6), 1114-1124. <https://doi.org/10.1038/nprot.2013.068>
- Thackray, L. B., Handley, S. A., Gorman, M. J., Poddar, S., Bagadia, P., Briseno, C. G., Theisen, D. J., Tan, Q., Hykes, B. L., Jr., Lin, H., Lucas, T. M., Desai, C., Gordon, J. I., Murphy, K. M., Virgin, H. W., & Diamond, M. S. (2018). Oral Antibiotic Treatment of Mice Exacerbates the Disease Severity of Multiple Flavivirus Infections. *Cell Rep*, 22(13), 3440-3453 e3446. <https://doi.org/10.1016/j.celrep.2018.03.001>

- Theriot, C. M., Koenigsnecht, M. J., Carlson, P. E., Jr., Hatton, G. E., Nelson, A. M., Li, B., Huffnagle, G. B., J, Z. L., & Young, V. B. (2014). Antibiotic-induced shifts in the mouse gut microbiome and metabolome increase susceptibility to *Clostridium difficile* infection. *Nat Commun*, 5, 3114. <https://doi.org/10.1038/ncomms4114>
- Tiedke, J., Gerlach, F., Mitz, S. A., Hankeln, T., & Burmester, T. (2011). Ontogeny of globin expression in zebrafish (*Danio rerio*). *J Comp Physiol B*, 181(8), 1011-1021. <https://doi.org/10.1007/s00360-011-0588-9>
- Torraca, V., & Mostowy, S. (2018). Zebrafish Infection: From Pathogenesis to Cell Biology. *Trends Cell Biol*, 28(2), 143-156. <https://doi.org/10.1016/j.tcb.2017.10.002>
- Tymms, M. J., Ng, A. Y., Thomas, R. S., Schutte, B. C., Zhou, J., Eyre, H. J., Sutherland, G. R., Seth, A., Rosenberg, M., Papas, T., Debouck, C., & Kola, I. (1997). A novel epithelial-expressed ETS gene, ELF3: human and murine cDNA sequences, murine genomic organization, human mapping to 1q32.2 and expression in tissues and cancer. *Oncogene*, 15(20), 2449-2462. <https://doi.org/10.1038/sj.onc.1201427>
- Uddin, F., Rudin, C. M., & Sen, T. (2020). CRISPR Gene Therapy: Applications, Limitations, and Implications for the Future. *Front Oncol*, 10, 1387. <https://doi.org/10.3389/fonc.2020.01387>
- van der Sar, A. M., Stockhammer, O. W., van der Laan, C., Spaik, H. P., Bitter, W., & Meijer, A. H. (2006). MyD88 innate immune function in a zebrafish embryo infection model. *Infect Immun*, 74(4), 2436-2441. <https://doi.org/10.1128/IAI.74.4.2436-2441.2006>
- van der Vaart, M., van Soest, J. J., Spaik, H. P., & Meijer, A. H. (2013). Functional analysis of a zebrafish myd88 mutant identifies key transcriptional components of the innate immune system. *Dis Model Mech*, 6(3), 841-854. <https://doi.org/10.1242/dmm.010843>
- van Soest, J. J., Stockhammer, O. W., Ordas, A., Bloemberg, G. V., Spaik, H. P., & Meijer, A. H. (2011). Comparison of static immersion and intravenous injection systems for exposure of zebrafish embryos to the natural pathogen *Edwardsiella tarda*. *BMC Immunol*, 12, 58. <https://doi.org/10.1186/1471-2172-12-58>
- Villar, D., Berthelot, C., Aldridge, S., Rayner, T. F., Lukk, M., Pignatelli, M., Park, T. J., Deaville, R., Erichsen, J. T., Jasinska, A. J., Turner, J. M., Bertelsen, M. F., Murchison, E. P., Flicek, P., & Odom, D. T. (2015). Enhancer evolution across 20 mammalian species. *Cell*, 160(3), 554-566. <https://doi.org/10.1016/j.cell.2015.01.006>
- Villasante, A., Ramirez, C., Rodriguez, H., Catalan, N., Diaz, O., Rojas, R., Opazo, R., & Romero, J. (2019). In-depth analysis of swim bladder-associated microbiota in rainbow

- trout (*Oncorhynchus mykiss*). *Sci Rep*, 9(1), 8974. <https://doi.org/10.1038/s41598-019-45451-1>
- Volkman, H. E., Pozos, T. C., Zheng, J., Davis, J. M., Rawls, J. F., & Ramakrishnan, L. (2010). Tuberculous granuloma induction via interaction of a bacterial secreted protein with host epithelium. *Science*, 327(5964), 466-469. <https://doi.org/10.1126/science.1179663>
- Wallace, K. N., Akhter, S., Smith, E. M., Lorent, K., & Pack, M. (2005). Intestinal growth and differentiation in zebrafish. *Mech Dev*, 122(2), 157-173. <https://doi.org/10.1016/j.mod.2004.10.009>
- Wang, H., Fang, R., Cho, J. Y., Libermann, T. A., & Oettgen, P. (2004). Positive and negative modulation of the transcriptional activity of the ETS factor ESE-1 through interaction with p300, CREB-binding protein, and Ku 70/86. *J Biol Chem*, 279(24), 25241-25250. <https://doi.org/10.1074/jbc.M401356200>
- Wang, S., Gong, X., Xiao, F., & Yang, Y. (2024). Recent advances in host-focused molecular tools for investigating host-gut microbiome interactions. *Front Microbiol*, 15, 1335036. <https://doi.org/10.3389/fmicb.2024.1335036>
- Wang, Z., Du, J., Lam, S. H., Mathavan, S., Matsudaira, P., & Gong, Z. (2010). Morphological and molecular evidence for functional organization along the rostrocaudal axis of the adult zebrafish intestine. *BMC Genomics*, 11, 392. <https://doi.org/10.1186/1471-2164-11-392>
- Watral, V., & Kent, M. L. (2007). Pathogenesis of *Mycobacterium* spp. in zebrafish (*Danio rerio*) from research facilities. *Comp Biochem Physiol C Toxicol Pharmacol*, 145(1), 55-60. <https://doi.org/10.1016/j.cbpc.2006.06.004>
- Weisburg, W. G., Barns, S. M., Pelletier, D. A., & Lane, D. J. (1991). 16S ribosomal DNA amplification for phylogenetic study. *J Bacteriol*, 173(2), 697-703. <https://doi.org/10.1128/jb.173.2.697-703.1991>
- Wen, J., Mercado, G. P., Volland, A., Doden, H. L., Lickwar, C. R., Crooks, T., Kakiyama, G., Kelly, C., Cocchiario, J. L., Ridlon, J. M., & Rawls, J. F. (2021). Fxr signaling and microbial metabolism of bile salts in the zebrafish intestine. *Sci Adv*, 7(30). <https://doi.org/10.1126/sciadv.abg1371>
- Whipps, C. M., Lieggi, C., & Wagner, R. (2012). Mycobacteriosis in zebrafish colonies. *ILAR J*, 53(2), 95-105. <https://doi.org/10.1093/ilar.53.2.95>

- Whitsett, J. A., & Alenghat, T. (2015). Respiratory epithelial cells orchestrate pulmonary innate immunity. *Nat Immunol*, *16*(1), 27-35. <https://doi.org/10.1038/ni.3045>
- Whitsett, J. A., Wert, S. E., & Weaver, T. E. (2010). Alveolar surfactant homeostasis and the pathogenesis of pulmonary disease. *Annu Rev Med*, *61*, 105-119. <https://doi.org/10.1146/annurev.med.60.041807.123500>
- Wiedenheft, B., Sternberg, S. H., & Doudna, J. A. (2012). RNA-guided genetic silencing systems in bacteria and archaea. *Nature*, *482*(7385), 331-338. <https://doi.org/10.1038/nature10886>
- Wiles, T. J., Jemielita, M., Baker, R. P., Schlomann, B. H., Logan, S. L., Ganz, J., Melancon, E., Eisen, J. S., Guillemin, K., & Parthasarathy, R. (2016). Host Gut Motility Promotes Competitive Exclusion within a Model Intestinal Microbiota. *PLoS Biol*, *14*(7), e1002517. <https://doi.org/10.1371/journal.pbio.1002517>
- Wiles, T. J., Schlomann, B. H., Wall, E. S., Betancourt, R., Parthasarathy, R., & Guillemin, K. (2020). Swimming motility of a gut bacterial symbiont promotes resistance to intestinal expulsion and enhances inflammation. *PLoS Biol*, *18*(3), e3000661. <https://doi.org/10.1371/journal.pbio.3000661>
- Willett, C. E., Cortes, A., Zuasti, A., & Zapata, A. G. (1999). Early hematopoiesis and developing lymphoid organs in the zebrafish. *Dev Dyn*, *214*(4), 323-336. [https://doi.org/10.1002/\(SICI\)1097-0177\(199904\)214:4<323::AID-AJA5>3.0.CO;2-3](https://doi.org/10.1002/(SICI)1097-0177(199904)214:4<323::AID-AJA5>3.0.CO;2-3)
- Willett, C. E., Kawasaki, H., Amemiya, C. T., Lin, S., & Steiner, L. A. (2001). Ikaros expression as a marker for lymphoid progenitors during zebrafish development. *Dev Dyn*, *222*(4), 694-698. <https://doi.org/10.1002/dvdy.1223>
- Willms, R. J., Jones, L. O., Hocking, J. C., & Foley, E. (2022). A cell atlas of microbe-responsive processes in the zebrafish intestine. *Cell Rep*, *38*(5), 110311. <https://doi.org/10.1016/j.celrep.2022.110311>
- Wilson, M. H., Ekker, S. C., & Farber, S. A. (2021). Imaging cytoplasmic lipid droplets in vivo with fluorescent perilipin 2 and perilipin 3 knock-in zebrafish. *Elife*, *10*. <https://doi.org/10.7554/eLife.66393>
- Winata, C. L., Korzh, S., Kondrychyn, I., Zheng, W., Korzh, V., & Gong, Z. (2009). Development of zebrafish swimbladder: The requirement of Hedgehog signaling in specification and organization of the three tissue layers. *Dev Biol*, *331*(2), 222-236. <https://doi.org/10.1016/j.ydbio.2009.04.035>

- Winkler, E. S., Shrihari, S., Hykes, B. L., Jr., Handley, S. A., Andhey, P. S., Huang, Y. S., Swain, A., Droit, L., Chebrolu, K. K., Mack, M., Vanlandingham, D. L., Thackray, L. B., Cella, M., Colonna, M., Artyomov, M. N., Stappenbeck, T. S., & Diamond, M. S. (2020). The Intestinal Microbiome Restricts Alphavirus Infection and Dissemination through a Bile Acid-Type I IFN Signaling Axis. *Cell*, *182*(4), 901-918 e918. <https://doi.org/10.1016/j.cell.2020.06.029>
- Wondimu, E. B., Culley, K. L., Quinn, J., Chang, J., Dragomir, C. L., Plumb, D. A., Goldring, M. B., & Otero, M. (2018). Elf3 Contributes to Cartilage Degradation in vivo in a Surgical Model of Post-Traumatic Osteoarthritis. *Sci Rep*, *8*(1), 6438. <https://doi.org/10.1038/s41598-018-24695-3>
- Wu, J., Duan, R., Cao, H., Field, D., Newnham, C. M., Koehler, D. R., Zamel, N., Pritchard, M. A., Hertzog, P., Post, M., Tanswell, A. K., & Hu, J. (2008). Regulation of epithelium-specific Ets-like factors ESE-1 and ESE-3 in airway epithelial cells: potential roles in airway inflammation. *Cell Res*, *18*(6), 649-663. <https://doi.org/10.1038/cr.2008.57>
- Xia, H., Chen, H., Cheng, X., Yin, M., Yao, X., Ma, J., Huang, M., Chen, G., & Liu, H. (2022). Zebrafish: an efficient vertebrate model for understanding role of gut microbiota. *Mol Med*, *28*(1), 161. <https://doi.org/10.1186/s10020-022-00579-1>
- Xiong, Z., Lo, H. P., McMahon, K. A., Martel, N., Jones, A., Hill, M. M., Parton, R. G., & Hall, T. E. (2021). In vivo proteomic mapping through GFP-directed proximity-dependent biotin labelling in zebrafish. *Elife*, *10*. <https://doi.org/10.7554/eLife.64631>
- Xu, H. J., Bai, J., Tian, Y., Feng, X., Chen, A. P., Wang, J., Wu, J., Jin, X. R., Zhang, F., Quan, M. Y., Chen, C., Lee, K. Y., & Zhang, J. S. (2023). ESE1/AGR2 axis antagonizes TGF-beta-induced epithelial-mesenchymal transition in low-grade pancreatic cancer. *Cancer Med*, *12*(5), 5979-5993. <https://doi.org/10.1002/cam4.5397>
- Xu, Y., & Li, Z. (2020). CRISPR-Cas systems: Overview, innovations and applications in human disease research and gene therapy. *Comput Struct Biotechnol J*, *18*, 2401-2415. <https://doi.org/10.1016/j.csbj.2020.08.031>
- Yachida, S., Wood, L. D., Suzuki, M., Takai, E., Totoki, Y., Kato, M., Luchini, C., Arai, Y., Nakamura, H., Hama, N., Elzawahry, A., Hosoda, F., Shirota, T., Morimoto, N., Hori, K., Funazaki, J., Tanaka, H., Morizane, C., Okusaka, T.,...Shibata, T. (2016). Genomic Sequencing Identifies ELF3 as a Driver of Ampullary Carcinoma. *Cancer Cell*, *29*(2), 229-240. <https://doi.org/10.1016/j.ccell.2015.12.012>
- Yamamoto, M., Yamazaki, S., Uematsu, S., Sato, S., Hemmi, H., Hoshino, K., Kaisho, T., Kuwata, H., Takeuchi, O., Takeshige, K., Saitoh, T., Yamaoka, S., Yamamoto, N., Yamamoto, S., Muta, T., Takeda, K., & Akira, S. (2004). Regulation of Toll/IL-1-

receptor-mediated gene expression by the inducible nuclear protein IkappaBzeta. *Nature*, 430(6996), 218-222. <https://doi.org/10.1038/nature02738>

Yang, H., Luan, Y., Liu, T., Lee, H. J., Fang, L., Wang, Y., Wang, X., Zhang, B., Jin, Q., Ang, K. C., Xing, X., Wang, J., Xu, J., Song, F., Sriranga, I., Khunsriraksakul, C., Salameh, T., Li, D., Choudhary, M. N. K.,...Yue, F. (2020). A map of cis-regulatory elements and 3D genome structures in zebrafish. *Nature*, 588(7837), 337-343. <https://doi.org/10.1038/s41586-020-2962-9>

Yang, H., Zhou, Y., Gu, J., Xie, S., Xu, Y., Zhu, G., Wang, L., Huang, J., Ma, H., & Yao, J. (2013). Deep mRNA sequencing analysis to capture the transcriptome landscape of zebrafish embryos and larvae. *PLoS One*, 8(5), e64058. <https://doi.org/10.1371/journal.pone.0064058>

Ye, L., Bae, M., Cassilly, C. D., Jabba, S. V., Thorpe, D. W., Martin, A. M., Lu, H. Y., Wang, J., Thompson, J. D., Lickwar, C. R., Poss, K. D., Keating, D. J., Jordt, S. E., Clardy, J., Liddle, R. A., & Rawls, J. F. (2021). Enteroendocrine cells sense bacterial tryptophan catabolites to activate enteric and vagal neuronal pathways. *Cell Host Microbe*, 29(2), 179-196 e179. <https://doi.org/10.1016/j.chom.2020.11.011>

Yeung, T. L., Leung, C. S., Wong, K. K., Gutierrez-Hartmann, A., Kwong, J., Gershenson, D. M., & Mok, S. C. (2017). ELF3 is a negative regulator of epithelial-mesenchymal transition in ovarian cancer cells. *Oncotarget*, 8(10), 16951-16963. <https://doi.org/10.18632/oncotarget.15208>

Yilmaz, P., Parfrey, L. W., Yarza, P., Gerken, J., Pruesse, E., Quast, C., Schweer, T., Peplies, J., Ludwig, W., & Glockner, F. O. (2014). The SILVA and "All-species Living Tree Project (LTP)" taxonomic frameworks. *Nucleic Acids Res*, 42(Database issue), D643-648. <https://doi.org/10.1093/nar/gkt1209>

Yoshida, N., Yoshida, S., Araie, M., Handa, H., & Nabeshima, Y. (2000). Ets family transcription factor ESE-1 is expressed in corneal epithelial cells and is involved in their differentiation. *Mech Dev*, 97(1-2), 27-34. [https://doi.org/10.1016/s0925-4773\(00\)00419-6](https://doi.org/10.1016/s0925-4773(00)00419-6)

Zakrzewska, A., Cui, C., Stockhammer, O. W., Benard, E. L., Spaink, H. P., & Meijer, A. H. (2010). Macrophage-specific gene functions in Spi1-directed innate immunity. *Blood*, 116(3), e1-11. <https://doi.org/10.1182/blood-2010-01-262873>

Zarrinpar, A., Chaix, A., Xu, Z. Z., Chang, M. W., Marotz, C. A., Saghatelian, A., Knight, R., & Panda, S. (2018). Antibiotic-induced microbiome depletion alters metabolic homeostasis by affecting gut signaling and colonic metabolism. *Nat Commun*, 9(1), 2872. <https://doi.org/10.1038/s41467-018-05336-9>

- Zhang, X., Zhang, R., Wang, Y., Li, L., & Zhong, Z. (2024). CDK5 Upregulated by ELF3 Transcription Promotes IL-1beta-induced Inflammation and Extracellular Matrix Degradation in Human Chondrocytes. *Cell Biochem Biophys*, 82(4), 3333-3344. <https://doi.org/10.1007/s12013-024-01415-5>
- Zhang, Y., Jin, H., Li, L., Qin, F. X., & Wen, Z. (2011). cMyb regulates hematopoietic stem/progenitor cell mobilization during zebrafish hematopoiesis. *Blood*, 118(15), 4093-4101. <https://doi.org/10.1182/blood-2011-03-342501>
- Zhang, Y., Liu, H., Yao, J., Huang, Y., Qin, S., Sun, Z., Xu, Y., Wan, S., Cheng, H., Li, C., Zhang, X., & Ke, Y. (2016). Manipulating the air-filled zebrafish swim bladder as a neutrophilic inflammation model for acute lung injury. *Cell Death Dis*, 7(11), e2470. <https://doi.org/10.1038/cddis.2016.365>
- Zheng, L., Xu, M., Xu, J., Wu, K., Fang, Q., Liang, Y., Zhou, S., Cen, D., Ji, L., Han, W., & Cai, X. (2018). ELF3 promotes epithelial-mesenchymal transition by protecting ZEB1 from miR-141-3p-mediated silencing in hepatocellular carcinoma. *Cell Death Dis*, 9(3), 387. <https://doi.org/10.1038/s41419-018-0399-y>
- Zheng, W., Wang, Z., Collins, J. E., Andrews, R. M., Stemple, D., & Gong, Z. (2011). Comparative transcriptome analyses indicate molecular homology of zebrafish swimbladder and mammalian lung. *PLoS One*, 6(8), e24019. <https://doi.org/10.1371/journal.pone.0024019>
- Zheng, X., Carstens, J. L., Kim, J., Scheible, M., Kaye, J., Sugimoto, H., Wu, C. C., LeBleu, V. S., & Kalluri, R. (2015). Epithelial-to-mesenchymal transition is dispensable for metastasis but induces chemoresistance in pancreatic cancer. *Nature*, 527(7579), 525-530. <https://doi.org/10.1038/nature16064>
- Zhou, J., Chehab, R., Tkalcevic, J., Naylor, M. J., Harris, J., Wilson, T. J., Tsao, S., Tellis, I., Zavarsek, S., Xu, D., Lapinskas, E. J., Visvader, J., Lindeman, G. J., Thomas, R., Ormandy, C. J., Hertzog, P. J., Kola, I., & Pritchard, M. A. (2005). Elf5 is essential for early embryogenesis and mammary gland development during pregnancy and lactation. *EMBO J*, 24(3), 635-644. <https://doi.org/10.1038/sj.emboj.7600538>
- Zhou, Y., Zhou, B., Pache, L., Chang, M., Khodabakhshi, A. H., Tanaseichuk, O., Benner, C., & Chanda, S. K. (2019). Metascape provides a biologist-oriented resource for the analysis of systems-level datasets. *Nat Commun*, 10(1), 1523. <https://doi.org/10.1038/s41467-019-09234-6>
- Zorn, A. M., & Wells, J. M. (2009). Vertebrate endoderm development and organ formation. *Annu Rev Cell Dev Biol*, 25, 221-251. <https://doi.org/10.1146/annurev.cellbio.042308.113344>

Zwick, R. K., Kasparek, P., Palikuqi, B., Viragova, S., Weichselbaum, L., McGinnis, C. S., McKinley, K. L., Rathnayake, A., Vaka, D., Nguyen, V., Trentesaux, C., Reyes, E., Gupta, A. R., Gartner, Z. J., Locksley, R. M., Gardner, J. M., Itzkovitz, S., Boffelli, D., & Klein, O. D. (2024). Epithelial zonation along the mouse and human small intestine defines five discrete metabolic domains. *Nat Cell Biol*, 26(2), 250-262.  
<https://doi.org/10.1038/s41556-023-01337-z>